OPEN ACCESS

University of BRISTOL

This electronic thesis or dissertation has been downloaded from Explore Bristol Research, http://research-information.bristol.ac.uk

Author:
Stan, Georgiana F

Title:
The dynamic regulation of PICK1 BAR domain dimerisation during synaptic plasticity

General rights
Access to the thesis is subject to the Creative Commons Attribution - NonCommercial-No Derivatives 4.0 International Public License. A copy of this may be found at https://creativecommons.org/licenses/by-nc-nd/4.0/legalcode This license sets out your rights and the restrictions that apply to your access to the thesis so it is important you read this before proceeding.

Take down policy
Some pages of this thesis may have been removed for copyright restrictions prior to having it been deposited in Explore Bristol Research. However, if you have discovered material within the thesis that you consider to be unlawful e.g. breaches of copyright (either yours or that of a third party) or any other law, including but not limited to those relating to patent, trademark, confidentiality, data protection, obscenity, defamation, libel, then please contact collections-metadata@bristol.ac.uk and include the following information in your message:

• Your contact details
• Bibliographic details for the item, including a URL
• An outline nature of the complaint

Your claim will be investigated and, where appropriate, the item in question will be removed from public view as soon as possible.

The dynamic regulation of PICK1 BAR domain dimerisation during synaptic plasticity

Georgiana F. Stan

A dissertation submitted to the University of Bristol in accordance with the requirements for award of the degree of Doctor of Philosophy in the School of Biochemistry, Faculty of Life Sciences

March 2021

Word count: 37,687

Abstract

PICK1 is a uniquely structured protein because it contains both a BAR domain and a PDZ domain. The PDZ domain mediates a plethora of protein-protein interactions, including with the GluA2 subunit of AMPA receptors. Through the BAR domain, PICK1 is capable of recognising and binding lipid membranes, although there is no evidence indicating a curvature induction mechanism for this protein. PICK1 has been shown to readily assemble into dimers and higher order oligomers in solution, but investigations looking at PICK1 dimerisation in a cellular environment are limited. PICK1 is mainly expressed in neurons and has been shown to participate in the internalisation of GluA2-containing AMPARs in response to synaptic plasticity. Additionally, PICK1 has been defined as a calcium-binding protein. In this study, I aim to investigate how PICK1 dimerisation is regulated in response to calcium and the potential consequences this has for PICK1 function.

I present novel findings in support of a membrane tubulating mechanism for PICK1. This is the first demonstration of a role for PICK1 in the active generation of membrane curvature, as well as the first evidence showing stimulus-induced dimerisation of BAR domains. PICK1 dimerisation is increased by approximately two-fold in the presence of calcium when overexpressed in HEK293 cells and using purified protein. Furthermore, this is a biphasic effect which suggests that calcium-induced PICK1 dimerisation is a direct regulatory mechanism for PICK1 function, mediated through acidic regions within its structure. Additionally, FLIM-FRET imaging of neurons showed that PICK1 dimerisation was upregulated immediately after LTD only. Cryo-EM imaging and COS-7 tubulation assays demonstrated that PICK1 can form tubules only in the presence of calcium. By replacing the ^{271}DDDE^{274} region with alanine which abolishes this calcium binding pocket, I was able to generate a mutant that shows impaired dimerisation in response to calcium. When tested in the COS-7 tubulation assay, this mutant was severely impaired in its ability to produce tubules. Taken together, these results provide a potential mechanism for PICK1 function where calcium stimulation during synaptic plasticity promotes PICK1 dimerisation which in turn leads to membrane remodelling and the potential internalisation of GluA2-containing AMPA receptors.

Author’s declaration

I declare that the work in this dissertation was carried out in accordance with the requirements of the University's *Regulations and Code of Practice for Research Degree Programmes* and that it has not been submitted for any other academic award. Except where indicated by specific reference in the text, the work is the candidate's own work. Work done in collaboration with, or with the assistance of, others, is indicated as such. Any views expressed in the dissertation are those of the author.

SIGNED: .....Georgiana Stan..... DATE:.....01.04.2021.....

Acknowledgements

First and foremost, I would like to thank my supervisor, Prof Jonathan Hanley, for all the support over the course of the years, but particularly during my second and final years. I am grateful for the opportunity to have learnt from you and I appreciate all the ideas and encouragement to pursue them that you have given me. I look forward to continuing our collaboration and am incredibly motivated to get this published!

Secondly, I would like to thank Prof Catherine Nobes and Prof Pete Cullen, who were my progression panel members. I always found our panel meetings incredibly beneficial, not only for the opportunity to discuss strategies for navigating my project, but also for the general advice on how to be a scientist. I hope that you will recognise how much I've progressed since nervously shaking in Kate's office during our first panel meeting and this is in part due to your guidance.

A special thank you must reach Dr Dominic Alibhai for teaching me how to do FLIM-FRET imaging, which was my favourite part of the project.

I would also like to thank everyone in the Hanley/Henley bubble, with Kev and Suko receiving special mentions as the post-docs who hold the lab together. We are all so lucky to have you there at all hours of the day and night! One day, I hope to simultaneously be as organised as Suko and as laid-back as Kev. To everyone else, working together has always been a pleasure and I can't wait until we can all go to the pub again.

I am also grateful for the friends I have made along the way, including Jacob, Hope and Siobhan – my #1 … Our Wednesday drinks helped me through a difficult period and perhaps I would not be writing this if it weren't for you.

My final and most heartfelt thank you goes to my parents, without whom none of this would have been made possible. Thank you for always believing in me, for always supporting me even from such a long distance away. I hope to always make you proud.

List of abbreviations

ABP/GRIP	Androgen-Binding Protein/Glutamate Receptor-Interacting Protein
AMPA	α-Amino-3-hydroxy-5-Methyl-4-isoxazolePropionic Acid
AMPAR	α-Amino-3-hydroxy-5-Methyl-4-isoxazolePropionic Acid Receptor
ANOVA	ANalysis Of VAriance
AP2	Adaptor Protein 2
BAR	Bin/Amphiphysin/Rvs
BDNF	Brain-Derived Neurotrophic Factor
CaMKII	Ca2+/calModulin-dependent protein Kinase II
CAR	C-terminal Acidic Region
CIP4	CDC42 (Cell Division Control Protein 42) Interacting Protein 4
CME	Clathrin-Mediated Endocytosis
DAT	Dopamine Transporter
DMEM	Dulbecco's Modified Eagle Medium
dNTP	deoxyriboNucleotide TriPhosphate
DSS	DiSuccinimidyl Suberate
EDTA	EthyleneDiamine Tetraacetic Acid
FCHo	Fes/CIP4 homology
FIJI	Fiji Is Just ImageJ
FLIM	Fluorescence Lifetime Imaging Microscopy
FRET	Forster’s Radiative Energy Transfer
GABA	Gamma AminoButyric Acid
GFP	Green Fluorescent Protein
HBS	HEPES Buffered Solution

HBSS	Hanks' Buffered Salt Solution
HEK293	Human Embryonic Kidney293
HEPES	N-2-HydroxyEthylPiperazine-N-EthaneSulfonic acid
ICA69	Islet Cell Autoantigen69
KO	KnockOut
LTD	Long-Term Depression
LTP	Long-Term Potentiation
MAP2	Microtubule-Associated Protein 2
MARCK	Myristoylated Alanine-Rich protein C Kinase substrate
MBP	Mannose Binding Protein
NAR	N-terminal Acidic Region
NMDA	N-Methyl-D-Aspartate
NMDAR	N-Methyl-D-Aspartate Receptor
NT	N-Terminus
PACSIN	Protein kinase C And Casein kinase Substrate In Neurons protein 2
PBS	Phosphate Buffered Solution
PBS-T	Phosphate Buffered Solution + 0.1% Tween
PCR	Polymerase Chain Reaction
PDZ	Post synaptic density protein (PSD95), Drosophila disc large tumor suppressor (Dlg1), and Zonula occludens-1 protein (zo-1).
PFA	ParaFormAldehyde
PICK1	Protein Interacting with C Kinase1
PKC	Protein Kinase C
PSD95	PostSynaptic Density95
PVDF	PolyVinyliDene Fluoride

RFP	Red Fluorescent Protein
SAP97	Synapse-Associated Protein-97
SAXS	Small Angle X-ray Scattering
SDS-PAGE	Sodium Dodecyl Sulfate PolyAcrylamide Gel Electrophoresis
SEM	Standard Error of the Mean
SNX	Sorting NeXin
synGAP	synaptic Ras GTPase Activating Protein
TCSPC	Time-Correlated Single Photon Counting
WT	Wild-Type
YFP	Yellow Fluorescent Protein

List of figures

List of tables

Table of contents

Chapter 1

General Introduction

1.1. Neuronal communication in the context of learning and memory

Without a doubt, the human brain can be regarded as the most complex mammalian organ with much about brain function yet to be discovered. Composed of billions of neurons which assemble into vast networks where each neuron could be forming up to a thousand connections with its neighbours, it is unsurprising that it has taken decades of research to uncover some of the many pathways that underlie higher brain function. In essence, the role of the brain is to learn and adapt by collecting all available sensory information, analysing and storing important environmental cues in the form of memories and prompting behavioural responses that are favourable for the individual's survival. Although functional specificity of the brain architecture remains a point of debate between neuroscientists (Kanwisher, 2010), it has become accepted over the years that certain brain regions are preferentially involved in specific tasks such as the sensory cortices, located within corresponding lobes, Broca's area for speech or the hippocampus for memory formation (Figure 1.1.). Nevertheless, there is a considerable amount of information constantly being exchanged between different areas of the brain and the regulation of neuronal communication is paramount to normal brain function.

1.1.1. Hebbian plasticity

One of the biggest questions still being addressed in the field of neuroscience is how memories are encoded, stored and retrieved at the cellular and molecular level. Indeed, evidence collected over the course of the last century has led to the concept of the engram – the neuronal 'trace' of a memory (Josselyn & Tonegawa, 2020). It is hypothesised that populations of neurons within all areas of the brain are primed and ready to accept new connections at any given time and it is their simultaneous activation in response to an experience or stimulus that results in enduring changes in connectivity such that the encoded memory can be evoked at a later time by the re-activation of the engram. This is in agreement with one of the oldest fundamental theories for neuronal communication termed Hebbian plasticity which has been famously shortened to the phrase 'Neurons that fire together, wire together' (Hebb, 1949). Interestingly, it was years later that physiological evidence in support of Hebb's

mnemonic postulate started emerging, when the clinical study describing the famous H. M. patient who had severe hippocampal lesions was published (Scoville & Milner, 1957). Because H. M. had lost the ability to retain any new memories, despite his long-term memory remaining unaffected, it was proposed that the hippocampus is essential for new memory acquisition. Researchers were later able to demonstrate experimentally that high frequency stimulation of hippocampal slice neurons resulted in increased potentiation of neurotransmission which was maintained hours after the initial stimulus (Bliss & Lomo, 1973).

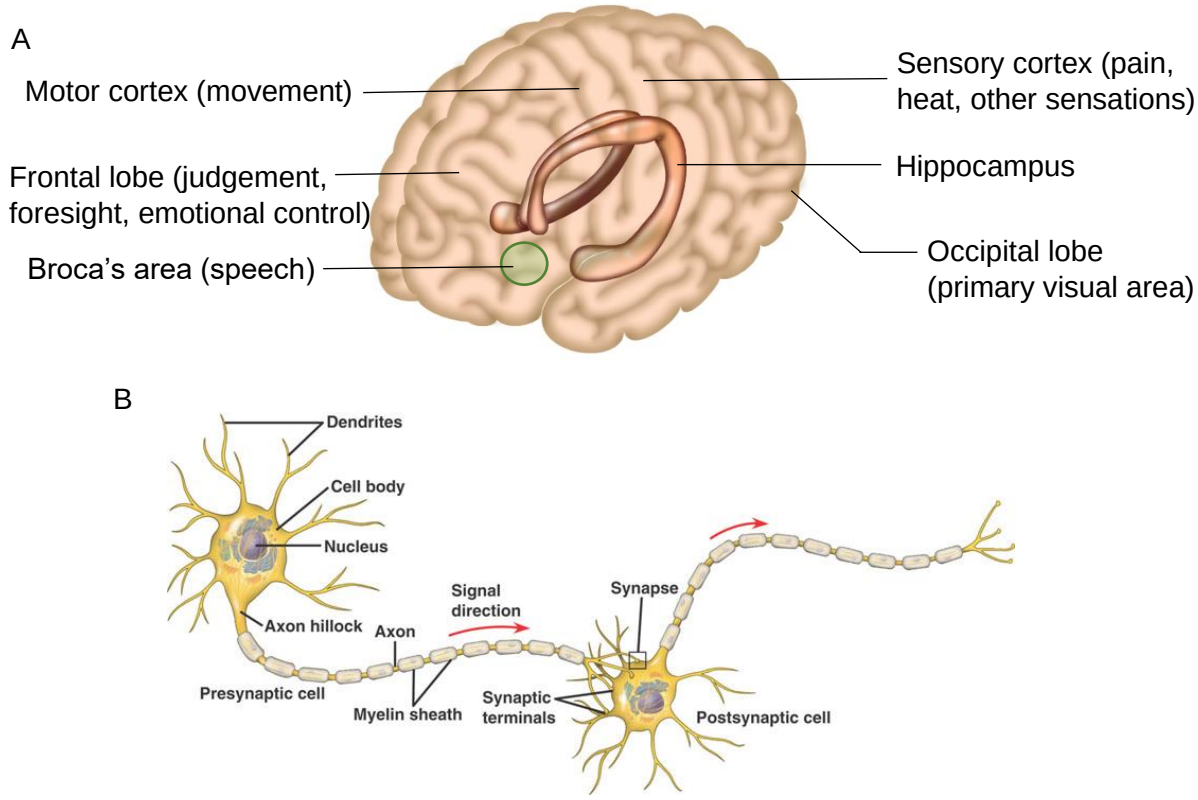

Figure 1.1.: The functional anatomy of the brain and the typical neuronal synapse. (A) The human brain is structured into two symmetrical hemispheres and contains five different lobes with specialised functions. Although structurally symmetrical, the left and right hemispheres have different functions such as motor control of the contralateral side of the body or the Broca/Wernicke areas which control speech production/understanding and are only present on the left side of the brain. The hippocampus is a C-shaped formation located deep within the medial temporal lobe and is important for the acquisition of new memories. Image courtesy of Salk Institute. (B) The synapse is the junction between two nerve cells which allows for the propagation of an action potential through the release of neurotransmitter from a presynaptic neuron which then diffuses into the synaptic cleft and activates receptors on the dendritic spines of a postsynaptic neuron. Image courtesy of PMG Biology.

1.1.2. Activity-dependent synaptic plasticity

This newly described property of activity-dependent synaptic strengthening was named long-term potentiation (LTP) and shortly after its discovery, an opposing effect called long-term depression (LTD) was observed after the activation of hippocampal neurons in response to a low frequency train of stimuli (Dunwiddie & Lynch, 1978). Moreover, the finding that LTP and LTD are reversible and inducible within the same synapse *in vivo* solidified the potential that synaptic plasticity has to bidirectionally regulate memory (Heynen *et al.*, 1996). In addition to long lasting enhancement of synaptic transmission, properties such as input specificity, associativity and cooperativity point to the possibility that LTP is sufficient for learning. Indeed, the correlation between memory acquisition in an inhibitory avoidance paradigm and the expression of LTP *in vivo* offers such evidence (Whitlock *et al.*, 2006), and more recently scientists have been able to optogenetically inactivate and reactivate fear conditioning (Nabavi *et al.*, 2014). However, the matter is complicated by the existence of multiple types of memories depending on the information that is encoded, for example declarative memory involves remembering facts (semantic memory) and events (episodic memory), while procedural memory is the memory for skills. In spatial object recognition experiments where rodents are attracted by the introduction of a novel stimulus, it has been found that both LTP and LTD are involved at different stages (Kemp & Manahan-Vaughan, 2004; Clarke *et al.*, 2010). Interestingly, LTD seems to be more relevant in the context of some psychological disorders and ageing, with studies showing that memory impairment associated with stress or ageing correlates with the induction of long term depotentiation (Foster & Kumar, 2007; Wong *et al.*, 2007).

1.1.3. Other theories for the expression of synaptic plasticity

While research into the electrophysiology of synapses contributes to the synaptic plasticity and memory hypothesis (Takeuchi *et al.*, 2014), there are some other aspects to consider. Prior experience can result in neuronal plasticity that does not necessarily encode a particular memory, such that the same dendritic spines formed in adaptation to monocular deprivation are re-potentiated when a second monocular deprivation is induced following a recovery period (Hofer *et al.*, 2009). More recently,

alternative theories have been proposed in which learning is facilitated through changes in excitability induced by epigenetic modifications or exosome-mediated interneuronal non-coding RNA exchange (Abraham *et al.*, 2019). For example, neuronal excitability could be intrinsically regulated through the modification of DNA methylation patterns which were shown to be altered following hippocampal dependent fear conditioning in mice and rats (Halder *et al.*, 2016; Duke *et al.*, 2017). Furthermore, injecting a naïve group of *Aplysia* snails with RNA extracted from trained animals resulted in the induction of long-term sensitisation which is a form of learning in this species and this provides evidence in support of RNA-mediated learning mechanisms (Bedecarrats *et al.*, 2018). While some propose an integrated function for both synaptic plasticity and intrinsic neuronal excitability (Lisman *et al.*, 2018), others have gone as far as to question the validity of synaptic plasticity as the mechanism of learning due to the difficulty of demonstrating direct causality *in vivo*. This can be at least in part explained by the limitations of electrophysiology as a methodology for LTP and LTD detection because memories are likely encoded in sparse synapses which are impossible to pinpoint and homeostatic plasticity could also potentially interfere with field recordings. As a consequence, a significant amount of research has been dedicated to the characterisation of the molecular mechanisms that coordinate the expression of synaptic plasticity and these will be discussed in detail throughout this chapter.

1.2. Synaptic plasticity: a molecular perspective

In order to understand how neurons are capable of bidirectional adaptation in response to different levels of activity, it is important to take a closer look at the molecular composition of the synapse. As mentioned earlier (Figure 1.1.B), there are two component parts to a synapse, namely a pre-synaptic terminal represented by the axonal projection of one neuron and a post-synaptic compartment of another called a dendritic spine. It is known that synaptic plasticity induces changes in both participating neurons, such as regulating neurotransmitter release from the axon or altering protein surface expression in the postsynaptic neuron. For the purpose of this thesis I will be focusing on the adaptations that relate to the post-synaptic neuron and

in response to LTD, although the multiple forms and mechanisms of synaptic plasticity have been reviewed here (Citri & Malenka, 2008).

1.2.1. Glutamate receptors mediate neuronal transmission through intracellular ion influx

Excitatory neurotransmission is mediated by the activation of ligand-gated ion channels that are expressed at the level of the dendritic spine, in response to glutamate and other excitatory neurotransmitters. Glutamate is the ligand for different types of receptors, including ionotropic receptors that form a pore which allows ion influx into the cell and metabotropic receptors which initiate signal transduction cascades. Of the ionotropic receptors, two classes are of particular relevance to synaptic plasticity, namely the α-amino-3-hydroxy-5-methyl-4-isoxazolepropionic acid receptors (AMPARs) and N-methyl-D-aspartate receptors (NMDARs). When glutamate is released from the intracellular pool of vesicles maintained within the presynaptic neuron, it binds to both AMPA and NMDA receptors. AMPARs are regarded as quick responders to glutamate stimulation, with fast activation that allows positively charged Na^+ to enter the neuron. As the membrane potential becomes reversed, the cell is depolarised which alleviates NMDA channel blockade by an extracellular Mg^{2+} ion and allows calcium influx through the channel pore (Traynelis *et al.*, 2010). This provides an elegant mechanism through which NMDARs can act as coincidence detectors for synaptic activity, which is an important requirement for plasticity where both the pre-synaptic and post-synaptic neurons must be activated at the same time. Indeed, the essential role of NMDARs for hippocampal synaptic plasticity and memory is reflected in studies in which NMDAR subunits are knocked-out or overexpressed (Tsien *et al.*, 1996; Tang *et al.*, 1999), as well as papers that use pharmacological inhibition of NMDARs (Dudek & Bear, 1992; Thiels *et al.*, 1996; Babiec *et al.*, 2014). In these studies, overexpression of NMDAR subunit 2B resulted in enhanced memory and learning during behavioural tasks, whereas pharmacological inhibition and NMDAR gene deletion led to severe impairment of spatial learning abilities in mice.

1.2.2. Calcium is an essential small signalling factor involved in LTP and LTD

The similarities that LTP and LTD share in terms of electrophysiological induction are mirrored in their molecular mechanism as they both require AMPAR and NMDAR activation, and one plausible way for regulating the direction in which plasticity occurs is through calcium signalling. Calcium is one of the main signalling factors in all cells, but it is especially important for highly compartmentalised neurons where it can directly interact with a large number of calcium sensors, calcium-dependent kinases or phosphatases, scaffold proteins and cytoskeleton components. It has been suggested that the differential effect of calcium for the expression of plasticity can be attributed to the duration of calcium influx through the open NMDARs and/or the concentration of calcium within the microenvironment of the synapse (Hansel *et al.*, 1997; Harney *et al.*, 2006; Taniike *et al.*, 2008).

Furthermore, the importance of regulating calcium dynamics at the level of the dendritic spine of postsynaptic neurons has been highlighted in recent years following the development of highly sensitive calcium-binding fluorescent dyes such as Green-BAPTA, Fluo-4 and X-Rhod (Higley & Sabatini, 2012). Following early indications that calcium concentration within dendritic spines is uncoupled from changes in calcium recorded from the dendritic shaft (Guthrie *et al.*, 1991), others have shown how calcium dynamics that are specific to dendritic spines are tied to their location on the dendrite. For example, distal spines are smaller and less prone to potentiation in spite of increased NMDAR-mediated calcium signalling (Walker *et al.*, 2017), while proximal spines show reduced calcium decay kinetics which favour the expression of LTD (Holthoff *et al.*, 2002). In addition, individual spines show different calcium dynamics depending on their surface-to-volume ratios, buffering capacity and molecular composition which can affect the source as well as the magnitude of calcium influx (Cornelisse *et al.*, 2007; Bell *et al.*, 2019). In brief, there are three main sources of calcium influx into the synapse in response to excitation: ionotropic glutamate receptors, voltage-gated calcium channels and internal stores (Higley & Sabatini, 2012). NMDARs mediate the highest proportion of intracellular calcium influx and although the effect differs greatly between spines of different sizes, it can be blocked by using subunit specific antagonists which suggests the composition of the receptor has more influence than the size of the spine (Sobczyk *et al.*, 2005). In resting neurons,

the concentration of calcium has been recorded at approximately 80nM in both spines and dendrites (Guthrie *et al.*, 1991; Sabatini *et al.*, 2002). A single action potential can cause a rise in calcium concentration up to 500nM in dendritic spines which returns to basal levels within 12ms. Calculations suggest that NMDAR-mediated calcium influx can reach local concentrations of up to 12μM, however calcium is quickly bound by buffering proteins leading to free calcium concentrations of 1μM (Sabatini *et al.*, 2002). During synaptic plasticity, an acute rise in intracellular calcium concentration (>10μM for a few seconds) was favourable for LTP, whereas a more modest yet sustained calcium increase (800nM for >1 minute) correlated with LTD (Yang *et al.*, 1999). Studies have shown that repeated calcium spikes resulted in a cumulative transient calcium concentration, and when the neurons were active during calcium spiking this resulted in synaptic potentiation, whereas when the neurons were active more than 5 seconds prior to calcium spiking, the result was depotentiation (Grienberger *et al.*, 2014; Cichon & Gan, 2015). This suggests that multiple aspects of calcium dynamics regulate the direction of synaptic plasticity, including the source of calcium, calcium concentration, calcium spike frequency and calcium decay through buffering, as well as the activity status of the neuron.

Traditionally, the consensus has been that low calcium levels during LTD expression are sufficient to activate phosphatases such as calcineurin and protein phosphatase1, while kinases which have a much lower affinity for calcium require a larger increase in concentration as seen during LTP (Figure 1.2., Luscher & Malenka, 2012). Nevertheless, it has been shown that CaMKII, a neuronally enriched kinase whose activity is influenced by calcium either directly or through the calcium sensing protein calmodulin, can control the expression of LTD in Purkinje cells by decoding the frequency of calcium pulses into corresponding levels of kinase activity. In addition, another calcium-binding kinase named PKC was found to also exhibit sensitivity to the calcium pulses used to evoke LTD (Zamora Chimal & De Schutter, 2018). After activation, CaMKII and PKC go on to phosphorylate a large number of synaptically expressed proteins, including scaffolding proteins such as SAP97, cytoskeleton proteins such as MAP2, tau and MARCKS, signalling molecules such as SynGAP and Tiam, as well as ion channels including NMDARs and AMPARs (Shonesy *et al.*, 2014; Callender & Newton, 2017). Interestingly, CaMKII activity has been associated with both LTP and LTD, but with a different AMPAR subunit substrate preference

depending on the type of plasticity evoked (Coultrap *et al.*, 2014). As such, it is more likely that the switch between LTP and LTD involves the integration of calcium dynamics with other signalling pathways in a cooperative manner, for example with BDNF signalling or metabotropic glutamate receptors (Nevian & Saksmann, 2006; Colgan *et al.*, 2018).

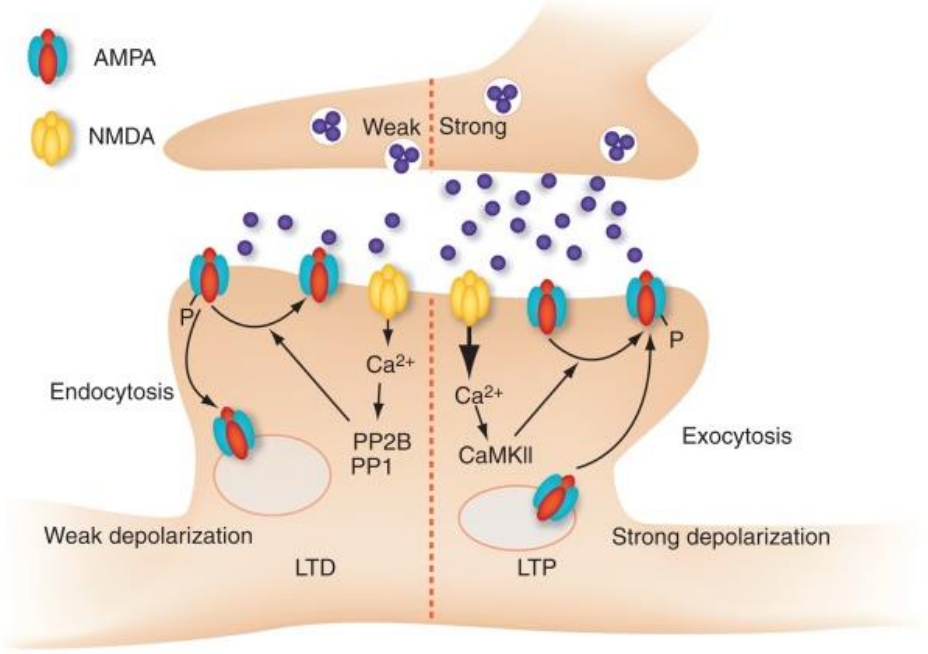

Figure 1.2.: The molecular mechanisms of bidirectional synaptic plasticity. Under basal conditions, the postsynaptic dendritic spine expresses AMPARs and NMDARs, and the presynaptic neuron contains neurotransmitters packed within a pool of exocytotic vesicles that are ready to be released. Following neuronal stimulation, glutamate crosses the synaptic cleft and activates both receptor types although with different kinetics such that AMPARs are initial responders followed by the less sensitive NMDARs which have lower affinity. Stronger synaptic stimulation necessary for LTP results in increased glutamate release causing strong AMPAR activation that promotes fast cellular depolarisation. This alleviates Mg^{2+} blockage of the NMDAR channels, allowing calcium to enter through the open pore. As intracellular calcium concentration rises, kinases such as CaMKII are activated and phosphorylate GluA1 subunits promoting an increase in their conductibility, but also retention at the synapse. At the same time, pathways which promote AMPAR exocytosis are initiated and lead to increased surface expression of GluA1-containing AMPARs. During LTD, a weaker initial stimulus again activates AMPA and NMDARs, but results in a lower intracellular calcium concentration that only reaches the threshold for phosphatase activation. Dephosphorylation of the GluA1 AMPAR subunit then leads to their subsequent internalisation through endocytosis. Figure from (Luscher & Malenka, 2012).

1.2.3. NMDA receptors: structure and function

Both AMPA and NMDA receptors are large, transmembrane glutamate-gated ion channels that are heteromeric assemblies of different subunits. NMDARs are heterotetramers composed of combinations of three subfamilies of NMDAR subunits classified based on sequence homology: GluN1, four distinct subtypes of GluN2 (GluN2A, GluN2B, GluN2C and GluN2D) and two GluN3 subtypes (GluN3A and GluN3B). The most common NMDAR subtype found in the postsynapse of the adult forebrain are di-heteromeric GluN1/GluN2A and tri-heteromeric GluN1/GluN2A/GluN2B, with the expression of the other subtypes depending on developmental stage, brain region and subcellular localisation (Paoletti *et al.*, 2013). The subunit composition of NMDARs dictates properties such as channel conductance, calcium permeability, desensitisation, trafficking and downstream signalling. Some have suggested that different NMDAR subtypes are involved in different forms of plasticity because selective inhibition of GluN2A-containing NMDARs prevents LTP without affecting LTD and blocking GluN2B-contaning receptors abolishes LTD without affecting LTP (Liu *et al.*, 2004). Importantly, NMDARs are subject to activity-induced changes in their current conductivity and synaptic availability (Hunt & Castillo, 2012), however this is considerably less dynamic than AMPAR plasticity triggered through NMDAR activation.

1.2.4. AMPA receptors: structure and function

AMPARs are tetrameric homo- or heterodimers composed of GluA1-4 subunits that are divided into two classes depending on the length of their cytoplasmic tail: GluA1, GluA4 and a splicing variant of GluA2 containing long C-terminal domains, and GluA2, GluA3 and a spliced variant of GluA4 featuring shorter tail ends. The main AMPAR subtypes found at hippocampal synapses are GluA1/GluA2 and GluA2/GluA3 di-heteromers, with a small homomeric population of GluA1 only receptors. The importance of the different C-terminal domains for appropriate receptor expression, trafficking, protein-protein interactions and synaptic plasticity is the topic of a number of reviews (Diering & Huganir, 2018; Zhou *et al.*, 2018; Bissen *et al.*, 2019). The GluA2 subunit is particularly interesting because it undergoes mRNA editing, converting a conserved glutamine into arginine at residue 607 which falls within the channel pore.

This single amino acid substitution changes the permeability of GluA2-containing AMPARs, rendering them impermeable to calcium ions such that these receptors present with a linear current-voltage relationship, as opposed to GluA2-lacking AMPARs that show an inward-rectifying current (Burnashev *et al.*, 1992). GluA2 editing appears to be an essential step in the quality control of AMPAR expression because the subunits which fail to contain the substituted residue are retained at the endoplasmic reticulum (Greger *et al.*, 2002) and while GluA1 AMPARs are recruited to the synapse in activity-dependent manner, GluA2-containing AMPAR membrane insertion is mainly constitutive (Araki & Huganir, 2010). Indeed, AMPAR trafficking is one of the main regulatory mechanisms through which synaptic plasticity is achieved, with surface expression of and calcium influx through GluA1 channels promoting GluA2/GluA3 exocytosis during LTP and inversely, GluA2-containing AMPARs internalisation during LTD (Henley & Wilkinson, 2013). In order to support this process, a pool of endocytic AMPARs is maintained in the proximity of synapses and undergoes constant recycling to and from the surface (Petrini *et al.*, 2009). The activity-dependent activation of kinases and phosphatases discussed above is of relevance here because phosphorylation represents one of the molecular switches between AMPAR internalisation/surface expression, as is the case for GluA2 subunit phosphorylation at the PKC site S880 which leads to receptor endocytosis (Xia *et al.*, 2000). Evidence suggests that this is facilitated by a small cytoplasmic protein called PICK1 which binds both PKC and the tail of GluA2 acting as a scaffold to bring these two proteins together (Perez *et al.*, 2001).

1.2.5. AMPAR-interacting proteins at the synapse

The appropriate synaptic expression and trafficking of AMPARs is supported by a number of structurally unrelated AMPAR auxiliary proteins. The vast extent of AMPAR function in terms of neuronal signalling is highlighted by proteomics analysis of AMPAR distribution across all brain regions and during development. Studies have shown that AMPAR subunit composition varies significantly according to brain region and developmental stage, and this also translates to the differential co-expression of a variety of AMPAR interacting proteins (Schwenk *et al.*, 2012; Schwenk *et al.*, 2014). As such, AMPARs are expressed at the level of the synapse together with a core of

proteins such as the transmembrane AMPAR regulatory proteins (TARPs) (Ben-Yaacov *et al.*, 2017), the cornichon homologs 2 or 3 (CNIH2 or 3) (Shanks *et al.*, 2014) and protein GSG1L (Twomey *et al.*, 2018). Additionally, the periphery of AMPARs contains even more accessory proteins such as CKAMPs 44 and 52, the MAGUK family of proteins, Noelin and PRRTs 1 and 2 (Schwenk *et al.*, 2012). These proteins either interact directly with the AMPARs subunits or indirectly through the assembly of the core, resulting in consequences for the signalling properties and pharmacology of the AMPAR as a channel which in turn modulates its function during neuronal plasticity (Kato *et al.*, 2010; von Engelhardt *et al.*, 2010; Miguez-Cabello *et al.*, 2020).

With regards to AMPAR trafficking, the role of the different auxiliary proteins varies. In the case of stargazin, which is the best characterised member of the TARPs, studies have been able to show that the interaction with AMPARs is required for the appropriate surface expression of the receptor (Chen *et al.*, 2000). Furthermore, activity-dependent phosphorylation by PKA, PKC and CaMKII can lead to increased synaptic clustering of stargazin which underlies LTP, whereas phosphorylation by MAPK and dephosphorylation by PP1 leads to depotentiation (Tomita *et al.*, 2005; Stein & Chetkovich, 2010). Indeed, during NMDA-mediated LTD, the interaction between stargazin and AP2 regulates the removal of AMPARs from the synapse to early endosomes, followed by the interaction between stargazin and AP3A that promotes further trafficking to the late endosome/lysosome (Matsuda *et al.*, 2013). In the case of CNIH2 and 3, there is some evidence which suggests that these proteins function in the anterograde transport of GluA1 and GluA2 subunits from the endoplasmic reticulum to the cell surface of neurons (Harmel *et al.*, 2012). Interestingly, GSG1L has been shown to promote the opposite in hippocampal neurons, where overexpression favoured an increase in AMPAR endocytosis and also had an inhibitory effect on the strength of synaptic transmission (Gu *et al.*, 2016).

Some of the AMPAR-interacting proteins found at the level of the synapse have been grouped together because they contain at least one PDZ domain which can interact with the cytoplasmic tails of AMPAR subunits. This broad category of proteins includes GRIP, PICK1 and members of the MAGUK family such as PSD-95/PSD-93, SAP97/SAP102 and MPP2 (Bissen *et al.*, 2019). First, the MAGUK family of proteins function as scaffolds which maintain the synaptic anchoring of AMPARs as well as NMDARs at the level of the post-synaptic density (Chen *et al.*, 2015). However, they

also have distinct roles such that SAP102 was shown to function primarily in the surface expression of AMPARs and NMDARs during synaptogenesis, whereas PSD-95 increases the number of surface AMPARs during synaptic maturation (Elias *et al.*, 2008). Furthermore, super-resolution imaging studies have been able to demonstrate that AMPARs form clustered nanodomains together with PSD-95 in glutamatergic synapses (Nair *et al.*, 2013). Indeed, it has been hypothesised that PDS-95 can capture and sequester AMPARs that are diffusely expressed at newly developed synapses (Mondin *et al.*, 2011). GRIP1/2 or ABP, a shorter splice variant, contains several PDZ domains and serves a similar purpose for the anchoring of AMPARs at the synapse but uses different binding sites than PSD-95 (Srivastava *et al.*, 1998). Interestingly, mutations that abolish the PDZ-mediated interaction between GluA2 and GRIP resulted in a reduced accumulation of AMPARs at the synapse over time, and this was mimicked by a single point mutation at S880A within the GluA2 sequence (Osten *et al.*, 2000). This mutation blocked the interaction with ABP/GRIP, but not with PICK1. Moreover, the phosphorylation of S880 in GluA2 results in reduced ABP/GRIP association, increased PICK1 binding and subsequent AMPAR internalisation (Chung *et al.*, 2000). Indeed, PICK1 has been shown to function in the removal of GluA2-contaning AMPARs from the synapse in response to LTD (Lin & Huganir, 2007; Anggono *et al.*, 2013; Fiuza *et al.*, 2017).

1.3. PICK1 – a neuronally expressed scaffold protein

PICK1, named after the acronym for protein interacting with C kinase 1, was first discovered in a yeast two-hybrid screening study aimed to uncover novel PKCα interactions (Figure 1.3.) (Staudinger *et al.*, 1995). Shortly after, the newly identified 55 kDa protein was found to contain a N-terminal PDZ domain which dictated its specificity to the PKCα isoform (Staudinger *et al.*, 1997). A role for PICK1 in neurotransmission began being outlined when studies showed that it is primarily expressed in the brain and colocalises with GluA2 subunits at excitatory synapses (Xia *et al.*, 1999). A breadth of research followed looking to further characterise the PICK1 PDZ domain specificity and it soon became apparent that PICK1 was a promiscuous protein, capable of interacting with several classes of PDZ ligands (Xu & Xia, 2006). The initial list of over 40 proteins, mainly transmembrane receptors but also structural

proteins and signal transducers, has been expanded to include over 60 interactors of various affinities more recently (Bolia *et al.*, 2012). Even though initial studies predicted a coiled-coil motif downstream of the PDZ domain, it was the publication of the crystal structure of the amphiphysin BAR domain (Peter *et al.*, 2004) together with the high degree of sequence homology between PICK1 and arfaptin2 that consolidated PICK1 as a BAR domain-containing protein (Figure 1.3.). The newly described property of binding lipid membranes was integral to the cellular performance of PICK1 in facilitating AMPAR trafficking and the expression of LTD (Jin *et al.*, 2006). In addition, the BAR domain sequence was mapped approximately between residues 148-356 and this overlapped with the region found to facilitate PICK1 dimerisation in early studies (Staudinger *et al.*, 1997).

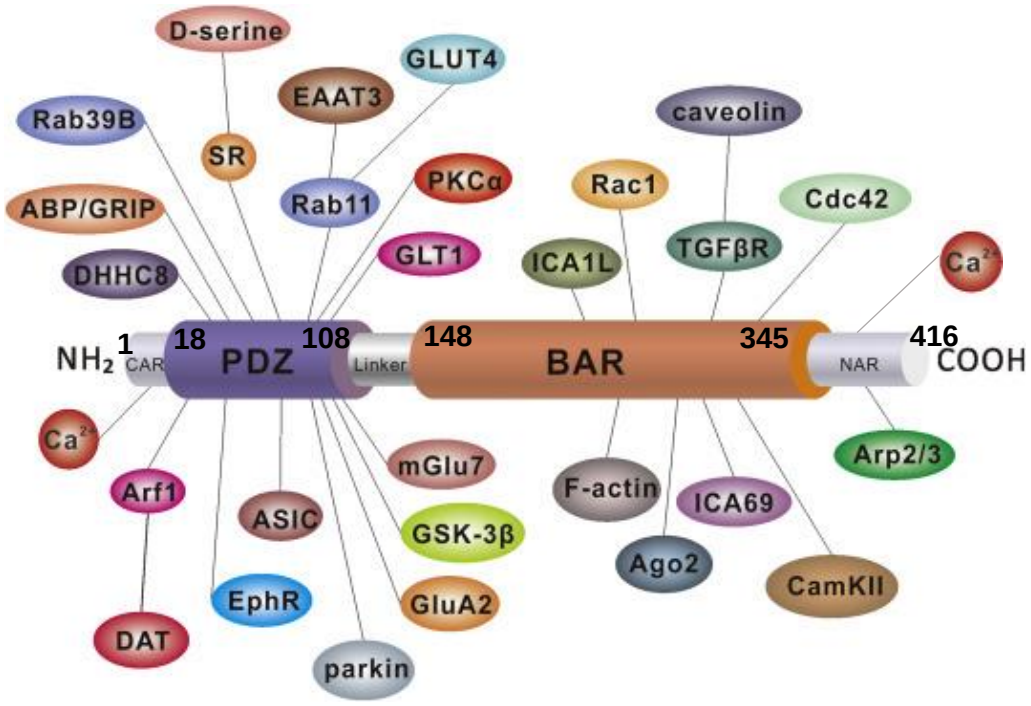

Figure 1.3.: Schematic representation of the PICK1 structural domains and the multitude of protein-protein interactions that they mediate. PICK1 is the only protein identified so far which contains both a PDZ and BAR domain. The unstructured regions at the N- and C-terminus contain several acidic residues which allow them to bind calcium ions. The PDZ and BAR domain are connected by a flexible, unstructured linker. The PDZ mediates many interactions with proteins which contain a C-terminal PDZ motif, such as GluA2, DAT, ABP/GRIP, PKCα. The BAR domain can mediate PICK1 heterodimerisation with ICA1L and ICA69, as well as several protein-protein interactions such as Ago2, CaMKII, Rac1 and Cdc42. Figure adapted with permission from (Li *et al.*, 2016).

Finally, three other unstructured areas of interest have been identified within the PICK1 sequence: a flexible linker between the PDZ and BAR domains and two regions rich in negatively charged amino acids, namely the N-terminal acidic region (NAR) and the C-terminal acidic region (CAR). While these regions do not form secondary structures, they are most likely involved in the regulation of PICK1 function. For example the degree of flexibility in the linker could determine the positioning of the PDZ domains in relation to the BAR domain interface in the dimer, whereas the CAR has been proposed to associate with the PDZ-BAR domains of the partnering molecule, thus contributing to the autoinhibition of the lipid-binding BAR domain (Jin *et al.*, 2006; Madasu *et al.*, 2015).

1.3.1. PICK1 as a calcium binding protein

The terminal acidic regions have also been shown to participate in the functional regulation of the protein in a calcium-dependent manner. Studies were able to demonstrate how the deletion of the 4-12 amino acid stretch of PICK1 NAR rendered the protein insensitive to calcium-induced increases of the GluA2-PICK1 interaction (Hanley & Henley, 2005). Furthermore, there is evidence to support that calcium binding to the NAR results in conformational changes within the PICK1 molecule and that mutations in this region blocked LTD and disrupted AMPAR trafficking (Citri *et al.*, 2010). Calcium binding is also necessary for the intracellular retention of internalised GluA2 following NMDAR activation and in response to LTD (Sossa *et al.*, 2006). A similar calcium-dependent effect has been observed with the CAR such that PICK1 interactions with Argonaute2, a component of the RNA-induced silencing complex, are disrupted following calcium binding of the CAR during chemical LTD induction (Rajgor *et al.*, 2017).

1.3.2. The expression and regulation of PICK1

In addition to the brain, PICK1 can also be found in a variety of tissues, including heart, liver, lung and muscle and it is evolutionarily conserved from *C. elegans* to humans (Staudinger *et al.*, 1995). Although such broad expression suggests an essential cellular function for the protein, PICK1 knockout mice are viable (Gardner *et al.*, 2005;

Steinberg *et al.*, 2006). However, chromaffin cells extracted from them are significantly impaired in their vesicle size and number, supporting a role for PICK1 in vesicle biogenesis (Pinheiro *et al.*, 2014). During the development of the brain, the expression of PICK1 can be detected as early as embryonic day 15 after which it gradually increases until after postnatal day 14 (Xia *et al.*, 1999). Interestingly, results showed that PICK1 KO mice are impaired in their hippocampal expression of LTD and LTP as well as in learning during adulthood but not as juveniles, indicating a developmental role for the expression of PICK1 in the brain (Volk *et al.*, 2010). In addition, a role for PICK1 in synapse maturation has been highlighted more recently by the discovery that PICK1 mediates AMPAR targeting to the synapse in response to neurexin, a neurodevelopmental signalling protein (Xu *et al.*, 2014). The expression of PICK1 is mainly cytosolic in a variety of cell types, while in neurons that form excitatory synapses it can be detected both pre- and postsynaptically (Haglerod *et al.*, 2009). It has been shown that PICK1 is targeted to the axonal synapse through its interaction with syntabulin (Xu *et al.*, 2016), while heterodimeric associations with ICA69, another BAR domain-containing protein, have been hypothesised to sequester PICK1 at the dendritic level away from spines (Cao *et al.*, 2007). From looking at the information provided so far about PICK1 and its mechanism of action during synaptic plasticity, it becomes apparent that PICK1-mediated AMPAR trafficking is highly regulated in response to neuronal depolarisation and subsequent calcium influx. However, other aspects of PICK1 function also rely on neuronal activation, such as the interaction between PICK1 and the Arp2/3 complex which mediates changes in dendritic spine morphology (Rocca *et al.*, 2008; Nakamura *et al.*, 2011), as well as the interaction with Argonaute2 which regulates miRNA function and represses expression of certain cellular targets (Antoniou *et al.*, 2014).

1.3.3. PICK1 in health and disease

Due to its involvement in so many cellular processes, it comes as no surprise that PICK1 has been implicated in a variety of neurological disorders. For example, a link between specific single nucleotide polymorphisms in the PICK1 gene and the risk of developing Alzheimer's disease has recently been shown in addition to evidence that supports a prospective therapeutic role for the inhibition of PICK1 in

neurodegeneration (Lin *et al.*, 2018; Xu *et al.*, 2018). Researchers found that small molecule inhibitors of the PICK1-GluA2 interactions stabilised GluA2 surface expression and blocked LTD in Aβ-induced neurodegeneration. In Parkinson's disease, it has been hypothesised that blocking the interaction between PICK1 and parkin offers neuroprotective benefits as a potential therapy by reducing the levels of Parkin-mediated mitophagy and subsequent neuronal degradation, as well as conferring resistance to MBTB-induced toxicity in PICK1 knockout mice (He *et al.*, 2018). Genetic variation of PICK1 has also been found to correlate with drug-induced psychosis (Matsuzawa *et al.*, 2007), while PICK1-PDZ domain inhibitors attenuate drug seeking behaviours in mice (Turner *et al.*, 2020). Lastly, PICK1 has been classed as a schizophrenia susceptibility gene and is possibly involved in the pathway of the disease through its interaction with serine racemase which synthesises D-serine (Fujii *et al.*, 2006). Therefore, PICK1 emerges as a robust protein at the forefront of a number of cellular trafficking processes and further understanding of its mechanism of action shows great potential for deciphering the basic function of learning and memory in addition to its value as a target for therapeutical intervention in neurological disorders. As such, the rest of this chapter will address in more detail how the two main functional domains of PICK1 support the role of the only protein known to contain both domains within its structure.

1.3.4. PICK1 PDZ domain mediated interactions

PDZ domains are protein interaction modules of approximately 90 amino acids in length which assemble into a core of six β-sheets 'sandwiched' between two α-helices. The name derives from the initial identification of the domain in three separate proteins, namely the PSD-95/SAP90, the Drosophila septate junction protein Discs-large, and the epithelial tight junction protein ZO-1 (PDZ). Although there is limited primary sequence conservation between PDZ domains, the evolutionary maintenance of the structural core together with the large variety of PDZ-binding motifs certifies the role of PDZ domain-containing proteins as essential scaffolds which mainly function in bringing together and maintaining the co-localisation of important binding partners. This is particularly relevant in the context of neuronal communication where the timing of the subcellular localisation of proteins is of significant relevance for the appropriate

functioning of the synapse. As such, it is unsurprising that the postsynaptic density hosts several PDZ-domain proteins with the most abundant being PSD-95 but also GRIP/ABP, Shank and PICK1 (Kim & Sheng, 2004).

The PICK1 PDZ domain was the first of its structural components to be identified and confirmed. The single PDZ domain was mapped between residues 18-108 and was experimentally shown to mediate the association between PICK1 and PKCα through the ^{669}QSAV^{672} terminal sequence of PKCα (Staudinger *et al.*, 1997). The PDZ domain participates in protein-protein interactions by recognising the PDZ-binding motif consensus ((S/T)XV) located at the COOH-terminus of binding partners. In order to facilitate this interaction, the PDZ binding pocket contains a carboxylate-binding loop with the highly conserved sequence R/K-XXX-G-Φ-G-Φ, where X is any amino acid and Φ is any hydrophobic residue. The binding specificity of the PDZ domain to its ligand is dictated by C-terminal residue of the PDZ-domain protein and the -2 position of the target peptide. Furthermore, PDZ domains have been classified depending on the sequence of their respective ligands: class I PDZ domains recognise the sequence Ser/Thr-X-Φ-COOH, class II bind the Φ-X-Φ-COOH motif and class III recognise Asp/Glu-X-Φ-COOH as their preferred ligand (Lee & Zheng, 2010). Interestingly, PICK1 has been shown to bind not only to class I specific motifs such as the PKCα sequence previously mentioned, but also class II binding motifs such as the tails of the GluA2, GluA3 and GluA4C AMPAR subtypes which all end in the -SVKI terminal sequence (Xia *et al.*, 1999). Furthermore, the specificity of the interactions with the different classes of ligands is so strong that a single mutation within the carboxylate-binding loop (K27E) abolishes the interaction between PICK1 and GluA2 but not with PKCα (Dev *et al.*, 2004). Indeed, it has been hypothesised that the ability of PICK1 to bind to both classes is influenced by Lys83 in the αB1 position of the PDZ domain. Studies looking into the binding affinities of PICK1 and its ligands have been able to show a 15-fold preference for the class I type of ligands such as the dopamine transporter as compared to class II binding partners such as PKC. In addition, mutating Lys83 to mimic a canonical type I binding pocket (K->H) increased the affinity for PKCα by 60-fold (Madsen *et al.*, 2005). In fact, it is probable that the promiscuity of PICK1 evolved through a combination of increased tolerance for the canonical binding mechanisms and acceptance of additional non-canonical binding motifs (Erlendsson *et al.*, 2014).

As previously mentioned, PICK1 can interact with a large number of PDZ binding partners. Of noteworthy mention are the proteins involved in the regulation of neuronal function, namely the ephrin signalling family of proteins, several important neurotransmitter transporters (dopamine transporter, noradrenaline transporter, glutamate transporter, serotonin transporter), proteins relevant for neurodevelopment (neuroligin), in addition to the previously mentioned AMPAR subtypes. A recent study was able rank the PDZ-mediated interactions of PICK1 in order of their binding affinities (Bolia *et al.*, 2012). This provides an interesting insight into the preferred PDZ interactions of PICK1 and could offer potential explanations for the coordination of the many protein-protein interactions facilitated through PICK1. It is possible that the changes in the subcellular localisation of PICK1 mediated through the membrane-affinity of the BAR domain in conjunction with the different binding affinities of the PDZ domain result in the subsequent exchange of binding partners. Indeed, it is necessary to first explore the function of the BAR domain in order to understand the full mechanism of action of PICK1.

1.4. The BAR domain family and membrane remodelling

Membranes are cellular components essential not only for the structural delimitation of the cell from its environment, but also for the appropriate compartmentalisation within the cytoplasm of the various organelles including the Golgi apparatus, endoplasmic reticulum and mitochondria. Additionally, membranes are constantly being transported between the cell surface and other internal compartments such as endosomes and transport vesicles in both directions in order to support the expression and turnover of transmembrane proteins. Of course, depending on the type of compartment from which they originate, membranes are composed of different lipids including various phospholipids, glycerolipids and sphingolipids which are assembled in a double bilayer according to well-defined ratios (Casares *et al.*, 2019). The availability of such variety of lipids allows for specific interactions to take place between many membrane-associated and membrane-recognising proteins which function integrally to coordinate processes relating to membrane dynamics. Besides lipids, the membrane contains many transmembrane proteins, as well as peripheral membrane proteins localised on its internal side. Interestingly, the integration of

proteins into the lipid bilayer provides the characteristics of a ‘fluid matrix’ to the membrane: at a microscopic level, it retains its molecular properties including lipid and protein diffusion, while at a macroscopic level it behaves as a highly elastic barrier.

The BAR domain family comprises a vast array of thousands of proteins mainly involved in the cellular trafficking of cargo and membrane reshaping. The elucidation of the crystal structure of the amphiphysin BAR domain was essential for establishing how the three α-helices contained within its sequence assemble into a curved domain (Peter *et al.*, 2004). The intrinsic properties of the BAR domain are recognising and binding lipid membranes of particular curvature as well as functioning as dimerisation modules to facilitate self-association. Indeed, in the case of amphiphysin it was shown that two molecules are assembled in the form of an elongated banana-shaped dimer. The two strands interact in an antiparallel fashion that results in a six-helix bundle in the middle of the dimer which represents a hydrophobic interface between monomers. The degree of curvature is dictated by how the monomers intersect and by any kinks contained within the α-helices. Interestingly, the concave surface of the dimer contained several positively charged regions which were shown to facilitate binding to negatively-charged lipid heads within the membrane (Peter *et al.*, 2004).

From a physics point of view, the forces governing membrane deformation are bending energies that are influenced by membrane stiffness and stretching energies that depend on surface tension. When BAR domain proteins associate with a membrane, they alter the energy equilibrium by causing a mismatch between the local curvature and the intrinsic curvature of the protein, in addition to introducing protein-lipid mixing entropies (Simunovic *et al.*, 2015). While highly diverse in terms of length, charge and magnitude of curvature, several classes of BAR domain-containing proteins have been differentiated based on their curvature induction mechanism. Firstly, the classical and N-BAR domain family contains the highest degree of curvature within its structure which leads to preferential binding to smaller liposomes of approximately 10-40nm diameter (Qualmann *et al.*, 2011). Examples of proteins belonging to this category are arfaptin, PICK1, members of the sorting nexins family (SNX), amphiphysin and endophilin. The latter two are canonical members of the N-BAR subfamily because they contain a short amphipathic helix immediately prior to their BAR domain which has been shown to participate in curvature sensing through its insertion into the lipid bilayer, not only in their case but also more recently for PICK1 (Peter *et al.*, 2004; Mim

et al., 2012; Herlo *et al.*, 2018). A second class of BAR domains shares the common property of inward invagination with classical BARs and these are called the F-BARs. Representative members of this family are the FCHo proteins and CIP4 which preferentially interact with larger liposomes of over 40nm due to the lower curvature of their BAR interface (Frost *et al.*, 2008). Finally, a third category of BAR domain proteins refers to members of the I-BAR family which are inverted in their structure and as such they contribute to negative curvature for the formation of protruding cellular extensions such as filopodia (Breuer *et al.*, 2019).

1.4.1 BAR domains during clathrin-mediated endocytosis

As indicated by their complex membrane remodelling properties, it is unsurprising that BAR domain-containing proteins are involved in the regulation of vesicle trafficking. The process of membrane internalisation is called endocytosis and not only does it affect the external surface area and internal compartmentalisation of the cell, but it also controls the expression of surface proteins, extracellular signalling pathways and nutrient uptake. In this section, I briefly discuss the mechanisms of clathrin-mediated endocytosis and how various BAR domains are sequentially recruited during this process in order to put into perspective the downstream effects of BAR domain function. CME is a continually occurring and highly regulated form of endocytosis present in most eukaryotic cells because of its relevance for the internalisation of extracellular and transmembrane cargo. When the subcellular environment is favourable for endocytosis, for example following the activation of a receptor by its ligand, a scaffold of proteins is recruited to the plasma membrane from the cytosol. The first responding proteins are assembled into lattices which cover up what is quickly becoming a clathrin-coated pit. The recruitment of adaptor proteins leads to the concentration of cargo at the site of the emerging vesicle in preparation for internalisation. Next, we see a series of BAR domain-containing proteins being targeted to the membrane and participating in the tubulation and constriction of the neck prior to its scission and intracellular release. The remodelling of the actin cytoskeleton also contributes to the remodelling of the membrane, and after internalisation the clathrin coat is disassembled and endocytic vesicles are further

trafficked towards degradation or back towards surface recycling (Kaksonen & Roux, 2018) (Figure 1.4.).

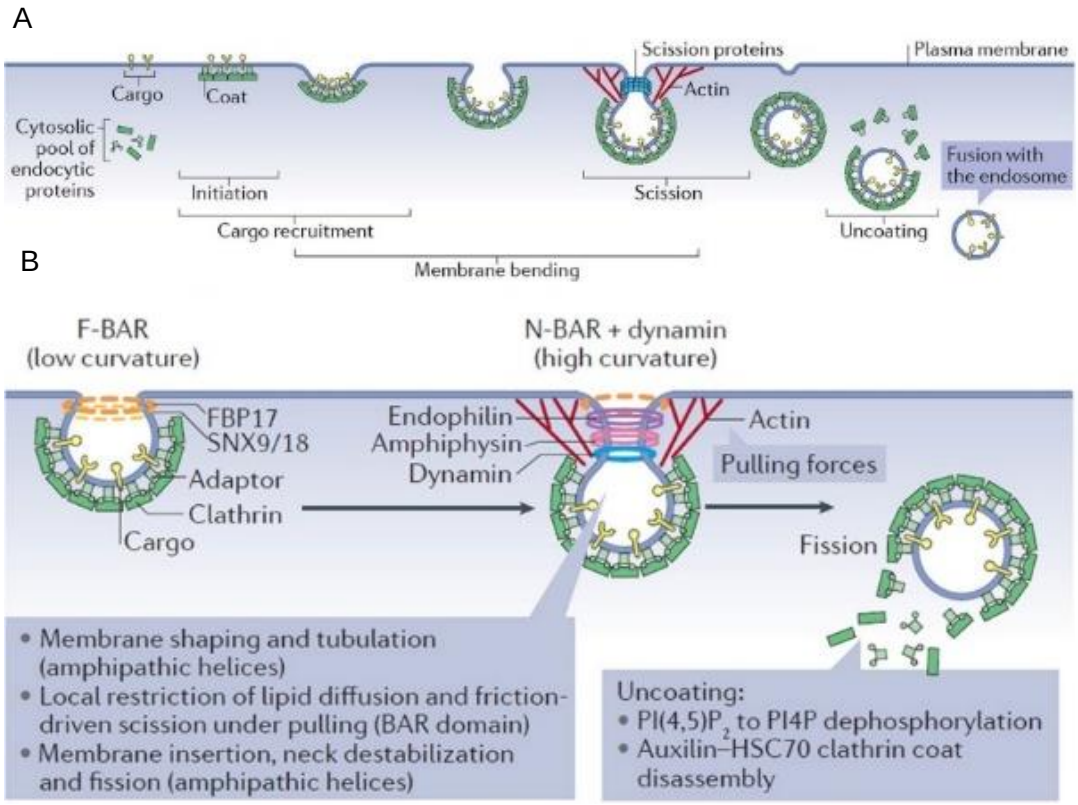

Figure 1.4.: Mechanisms of clathrin-mediated endocytosis. (A) Clathrin-mediated endocytosis is a highly regulated cellular mechanism used to control the levels of transmembrane receptors and membrane-associated proteins at the cellular surface. As such, several steps are involved with different classes of proteins being recruited sequentially to the plasma membrane. During initiation, adaptor proteins such as AP2 recognise and bind the appropriate cargo and this is followed by the assembly of the clathrin coat. Once cargo recruitment is complete, several BAR domain proteins are targeted to the emerging vesicle due to their ability to sense curvature. In addition, BAR domains also show membrane bending capacity and promote further constriction of the vesicle which is eventually released intracellularly after scission by GTPases such as dynamin. Once internalised, the uncoating of the endocytic vesicle takes places which allows it to enter the endocytic pathway. (B) BAR domain proteins involved in clathrin-mediated endocytosis and their mechanism of action. Initially, BAR domains belonging to the F-BAR family of proteins such as FBP17 and SNX9/18 are recruited due to their preference for low membrane curvature. These proteins will participate in the further constriction of the emerging tubule neck which then becomes accessible to N-BAR domain-containing proteins such as endophilin and amphiphysin which have a much higher level of tubulation activity. Finally, dynamin is recruited in order to promote the scission and internalisation of the endocytic vesicle. Figure is adapted with permission from (Kaksonen & Roux, 2018).

Due to the large number of molecules involved in the coordination of CME, it is justified to only touch on some of the key proteins and how they contribute to the internalisation of vesicles. In addition, we are particularly interested in the regulation of CME in a neuronal context because of the importance of synaptic membrane trafficking as one of the underlying mechanisms for synaptic plasticity (Hanley, 2018; Hiester *et al.*, 2018). Indeed, early studies were able to show how internalised GluA2 colocalised with clathrin-coated structures and how interfering with CME abolished the expression of LTD in hippocampal and cerebellar neurons (Man *et al.*, 2000; Wang & Linden, 2000). Moreover, the discovery that essential components of the endocytic machinery such as clathrin, AP2 and dynamin were localised in the lateral proximity of the post-synaptic density suggested that CME takes place in a precise spatial and temporal manner away from the main pool of surface receptors (Racz *et al.*, 2004). The fact that coated structures extracted from brains are smaller in size than those from epithelial cells, as well as the existence of some brain specific isoforms of clathrin and dynamin provides further indication that neuronal CME could have evolved to support the particularities of neurotransmitter release and receptor surface expression (Kirchhausen *et al.*, 2014). For example, AP180 is a neuronally enriched adaptor protein which promotes the assembly of clathrin at synapses following acute depolarisation (Wu *et al.*, 2010). In the case of AMPARs, GluA2 subunits are recruited to clathrin-coated pits through a direct interaction between the C-terminal tail of the receptor and the μ2 subunit of the adaptor protein AP2 in response to NMDA stimulation (Lee *et al.*, 2002; Kastning *et al.*, 2007). Activity-regulated gene expression of candidate plasticity gene 2 (CPG2) has been linked with activity dependent endocytosis of AMPARs through its direct interaction with the actin cytoskeleton but also by the recruitment of endophilin to the site of actin polymerisation to promote membrane remodelling (Loebrich *et al.*, 2013; Loebrich *et al.*, 2016). Amphiphysin is a BAR domain protein with great potential for the coordination of vesicle internalisation due to its interactions with clathrin and AP2, in addition to its recruitment of dynamin which is a GTPase required for the vesicle neck scission which occurs during the late stages of CME (Slepnev *et al.*, 2000; Brett *et al.*, 2002). Interestingly, PICK1 shares similarities with amphiphysin in terms of its curvature and binds the α-appendage of AP2 through the same FxDxF motif (Fiuza *et al.*, 2017). As discussed throughout this chapter, PICK1 has been shown to bind not only the GluA2 cargo itself, but also actin and the Arp2/3 complex, as well as dynamin2. This points towards a central role for

PICK1 in the regulation of CME with potential implications starting from the early stages of cargo selection and clustering with adaptor proteins all the way through the late stages of vesicle scission and internalisation.

1.4.2. The main mechanisms involved in BAR domain-mediated curvature generation

Two main mechanisms have been proposed to explain how BAR domains function in the sensing and induction of membrane curvature (Figure 1.5.). The distinction between the two processes has been difficult to investigate due to challenges in obtaining sufficient temporal resolution of these events: is the BAR domain initially attracted by favourable lipid-protein interactions and then after binding and activation, the BAR domain can proceed to alter membrane shape or is the BAR domain preferentially recruited to membranes already displaying curvature? Whereas some BAR domain proteins such as centaurin and oligophrenin preferred binding to smaller liposomes, amphiphysin indiscriminately associated with vesicles of various sizes and subsequent curvature. The deletion of the N-terminal amphipathic helix from the N-BAR domain of amphiphysin was able to introduce a preference for vesicles of up to 100nm which suggests that the BAR domain alone can function as a curvature sensing module (Peter *et al.*, 2004). Indeed, further investigation into this mechanism revealed that the ability of the endophilin BAR domain to sense liposome curvature is dictated by the N-BAR amphipathic helix (Bhatia *et al.*, 2009). On the other hand, molecular dynamics simulations indicated that BAR domains could introduce membrane curvature as a direct consequence of the intrinsic curvature shown by the crescent-shaped dimer during the scaffolding that occurs following lipid membrane binding (Blood & Voth, 2006; Mahmood *et al.*, 2019).

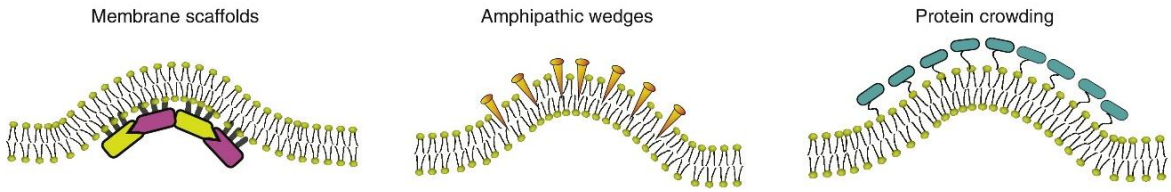

Figure 1.5.: The three mechanisms of membrane curvature induction adopted by BAR domain proteins. BAR domains are capable of disrupting membrane tension and inducing particular curvatures through three mechanisms: membrane scaffolding, the insertion of amphipathic wedges or protein crowding. During membrane scaffolding, BAR domain proteins assemble in helical oligomeric structures which surround the membrane and force it to adopt the intrinsic curvature of the BAR domain. The insertion of amphipathic wedges or helices which are characteristic of N-BAR domain proteins disrupt membrane tension therefore promoting membrane bending. Protein crowding is the most recently identified mechanism and refers to the tension generated through steric hindrance forces of the accumulating BAR domains which eventually lead to membrane bending. Figure adapted with permission from (Rossy *et al.*, 2014).

Nevertheless, the evidence which supports a role for the BAR domain in the active generation of curvature is overwhelming. For example, the incubation of endophilin with 200 or 400nm liposomes results in the formation of highly curved tubules of about 35-50nm diameter at low protein concentrations which are further constricted into similarly sized round vesicles with higher concentrations (Gallop *et al.*, 2006). Similarly, amphiphysin has been shown to initially bind and deform vesicles due to weak interactions with the N-BAR helix at low concentrations followed by a more pronounced insertion of the amphipathic helix which leads to tubulation in the presence of higher oligomeric states of protein (Isas *et al.*, 2015). A concentration dependency for the switch between membrane association and tubulation has also been demonstrated for endophilin such that it acts as curvature sensor at low concentrations and a curvature generator at higher concentrations (Zhu *et al.*, 2012). Taken together, these findings suggest that BAR domains operate a multimodal mechanism for membrane sensing, stabilising and bending which integrates the recognition of membrane composition and curvature with the active insertion of the amphipathic helix and concentration-dependent protein scaffolding in order to support membrane remodelling on a seconds-to-minutes timescale (Poudel *et al.*, 2016). Interestingly, a third mechanism for membrane tubulation has been emerging more recently and takes into account the forces generated by protein crowding in the proximity of membranes (Figure 1.5.). In this model, it is hypothesised that large intrinsically disordered domains within full-length BAR domain proteins act

synergistically with the BAR domain itself to introduce steric hinderance forces which contribute to both membrane curvature sensing and generation (Zeno *et al.*, 2018; Snead *et al.*, 2019; Zeno *et al.*, 2019).

1.4.3. BAR domain dimerisation is essential for appropriate membrane remodelling

In terms of dimerisation, BAR domain proteins are well established as readily self-associated proteins. Resolving the crystal structures for a variety of BAR domain family members resulted in the currently accepted homodimeric model of the BAR domain interface for amphiphysin (Peter *et al.*, 2004), FCHo2 (Henne *et al.*, 2007), SNX1 (van Weering *et al.*, 2012) and endophilin (Weissenhorn, 2005). Furthermore, some family members are able to form heterodimers with closely related proteins, such as the heterodimerisation between APPL1 and APPL2 (Chial *et al.*, 2008) or the association between SNX4 with SNX7 or with SNX30 (van Weering *et al.*, 2012). In the case of endophilin, cryo-electron microscopy studies revealed how the dimerised protein surrounds tubular membranes and assembles further into oligomeric lattices by the help of tail-to-tail and lateral interactions depending on the diameter of the tubule (Mizuno *et al.*, 2010; Mim *et al.*, 2012). Further investigations focusing on the binding kinetics of BAR domain dimerisation found that relatively high affinities dictated the dimerisation of endophilin in solution and that the overall conformation of the dimer was maintained upon membrane binding with the exception of the amphipathic helix. Not only were the dimers stable in solution for hours to days, they also showed slow membrane uncoupling kinetics which supports a propensity for oligomerisation based scaffolding (Capraro *et al.*, 2013). Moreover, it has been suggested that the rigidity of the BAR domain dimer interface is crucial for appropriate tubulation of membranes (Masuda *et al.*, 2006). The importance of the integrity of the BAR domain dimer is highlighted by additional studies which show that single point mutations within the BAR domain can disrupt the curvature of the endophilin dimer resulting in impaired membrane association and deformation (Gortat *et al.*, 2012; Poudel *et al.*, 2016). Indeed, these findings are further solidified by observations of endophilin dimers within the cytoplasm of cells during heterologous expression of the protein (Ross *et al.*, 2011), as well as directly extracted from rat brain homogenates (Ringstad *et al.*, 2001).

1.4.4. PICK1 BAR domain-mediated dimerisation

The PICK1 BAR domain was identified due to its structural homology with the amphiphysin BAR domain and shares many of its properties. The coiled-coil motif was mapped between residues 148-356 and was initially characterised with regards to facilitating PICK1 self-association (Staudinger *et al.*, 1997). While NMR crystallography is efficient for determining the structure of singular domains, unfortunately it cannot resolve structures which contain several potentially flexible domains. For this reason, two separate groups set out to decipher the structure of full length PICK1 using small-angle X-ray scattering (SAXS) (Figure 1.6.). Interestingly, both groups agreed that PICK1 readily self-associates in solution to form dimers and higher order oligomers, although they disagreed about where the PDZ domains are located relative to the BAR domain scaffold and therefore about the source of PICK1 autoinhibition. Madasu and colleagues found that the PDZ domains are tightly packed in a rigid manner at the end of the concave surface with the binding pocket oriented in the same direction as the BAR domain membrane interface (Madasu *et al.*, 2015). On the other hand, Karlsen and his team were able to show that the PDZ domains are flexible in relation to the BAR domain by means of the unstructured linker region connecting the two domains (Karlsen *et al.*, 2015). In this conformation, the PDZ domains cover up the concave surface of the BAR domain therefore participating in the autoinhibition of PICK1 membrane binding. This is mediated by hydrophobic interactions between the PDZ and BAR domain as suggested by molecular dynamics simulations (He *et al.*, 2011). The differences behind the conformations obtained by SAXS could stem from how the purified protein samples were prepared prior to SAXS data acquisition in an effort to limit concentration-dependent protein aggregation. While Madasu et al. decided to stabilise the structure of the dimer by fusing a maltose-binding protein to the PICK1 N-terminus, Karlsen and his group chose to substitute the final three C-terminal amino acids with LKV, the minimal binding sequence of the PICK1 PDZ domain. Nevertheless, both groups agreed on the dimeric nature of the protein, with the Karlsen group going further and also modelling PICK1 oligomerisation which showed that tetramers are most likely to associate in an offset manner, similar to the scaffolding observed with the F-BAR proteins CIP4 and FBP17 (Frost *et al.*, 2008).

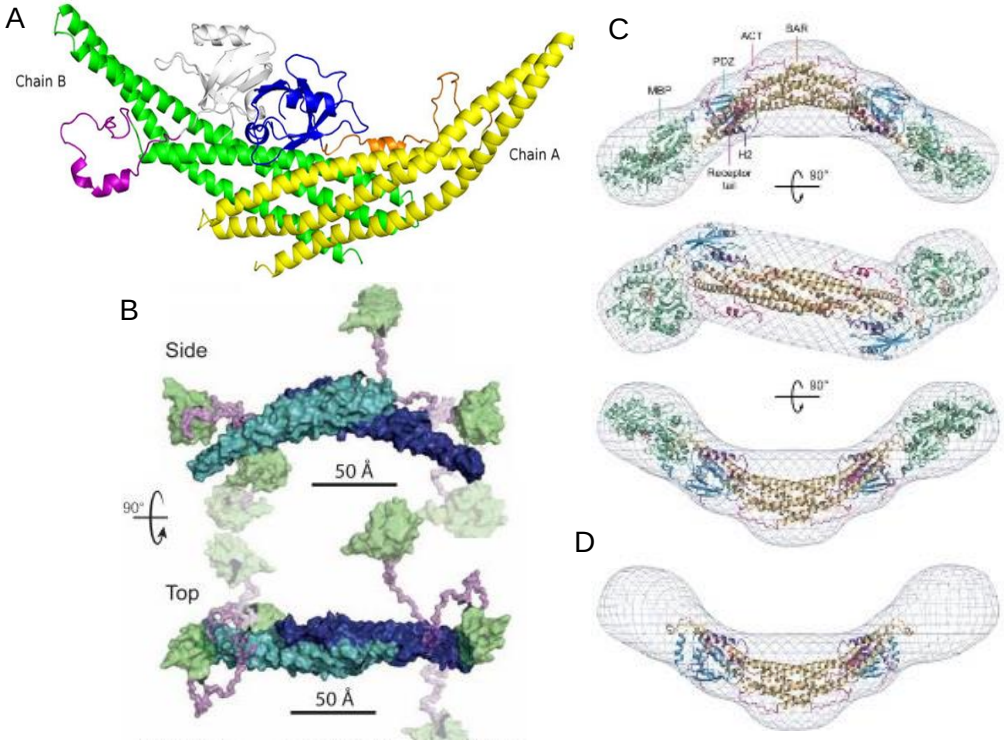

Figure 1.6.: The three structural models of PICK1 dimerisation available in the literature. (A) A PICK1 dimer complex was developed with protein-protein docking tools using the crystal structure of the PICK1 PDZ domain and a homology-based model of the BAR domain. In this simulation, the PDZ domains block the lipid binding surface of PICK1 due to their inward folding onto the concave surface of the BAR domain dimer interface. This model is consistent with experimental evidence which shows that the PDZ domain has an inhibitory effect on PICK1 BAR domain function (Perez *et al.*, 2001). BAR domains are represented in green and yellow, while PDZ domains are in blue and white. The linkers are in pink and orange. Figure obtained from (Han & Weinstein, 2008) with permission. (B) PICK1 dimer modelled by small angle X-ray scattering using the PICK1^{LKV} mutant. The mutation represents the substitution of the last three amino acids at the C-terminus (CDS) with LKV which is the minimal binding sequence of the PICK1 PDZ domain. The mutant was generated in order to favour and stabilise the assembly of dimeric PICK1 as opposed to higher order oligomers for the appropriate detection of the dimer structure. In this model, the PDZ domains remain highly flexible in relation to the BAR domain, which allows PICK1 to perform long-range scaffolding of membrane associated proteins. Figure obtained from (Karlsen *et al.*, 2015). (C) PICK1 dimer model obtained by small angle X-ray scattering using MBP-PICK1. In this study, a fusion between PICK1 and MBP was used in order to stabilise the PICK1 dimer for data collection. Although the model was generated using the same technique as the previous one, the predictions were different and could be explained by the different strategies used for the stabilisation of the PICK1 dimer. In this model, the PDZ domains were rigid in terms of their location at the tip of the BAR domain crescent, but their orientation remained flexible. Additionally, the amphipathic helix (H2) and C-terminal acidic region are also included in this model. (D) PICK1 dimer model excluding the MBP cap. Figure obtained from (Madasu *et al.*, 2015) with permission.

1.4.5. The PICK1 BAR domain can also participate in heterodimerisation with ICA69

In addition to mediating self-assembly, the PICK1 BAR domain has also been shown to participate in heterodimerisation with ICA69, another BAR-domain containing protein which together with PICK1 can regulate vesicle biogenesis, affecting metabolic homeostasis and insulin secretion (Cao *et al.*, 2013; Holst *et al.*, 2013). Moreover, the BAR domain-mediated interaction between PICK1 and ICA69 has been shown to disrupt GluA2 receptor trafficking and surface expression. Interestingly, over three quarters of available PICK and ICA69 are associated with each other in the brain, while at a subcellular level, ICA69 colocalises with PICK1 in dendrites but is absent from synapses (Cao *et al.*, 2007). This provides an elegant regulatory mechanism for PICK1 in which the protein is maintained away from dendritic spines through its interaction with ICA69 and opens up a potential requirement for PICK1 activation in response to stimuli to allow its homodimerisation and subsequent redistribution to the synapse. The inhibitory nature of the ICA69-PICK1 heterodimerisation is reflected in the fact that it occludes the expression of cerebellar LTD and prevents synapse maturation (Wang *et al.*, 2013; Xu *et al.*, 2014).

1.4.6. PICK1 BAR domain binding to lipid membranes is essential for its function

Another essential function for the PICK1 BAR domain is to recognise and bind lipid membranes. One study in particular was central for the characterisation of the membrane-binding properties of PICK1 and answers many questions regarding the specificities of the interaction. Jin and colleagues were the first to show how PICK1 is present mainly in the pellet fraction following incubation with liposomal mixtures, and further investigation showed how PICK1 has a preferential affinity for the phosphoinositides PtdIns(3)P, PtdIns(4)P, and PtdIns(5)P (Jin *et al.*, 2006). PtdIns(4)P is usually found on Golgi-derived vesicles, PtdIns(3)P are enriched at the early endosome and PtdIns(5)P is localised at the nucleus (Shewan *et al.*, 2011). Furthermore, the interaction is mediated through three positively charged residues in the centre of the concave surface of the BAR domain, lysines 251, 252 and 257 (3KE mutant), as well as two residues located at the end of the crescent dimer, lysines 266

and 268 (2KE mutant). Mutating these amino acids to glutamate abolished the appropriate synaptic targeting of PICK1, as well as its ability to cluster and regulate the surface expression of AMPARs and occluded LTD in hippocampal and cerebellar neurons (Jin *et al.*, 2006; Steinberg *et al.*, 2006). Some have proposed that the clustering of PDZ ligands by PICK1 relies on the activation of its BAR domain through direct interaction with the lipid membrane because artificial membrane targeting induced by myristoylation resulted in reduced numbers of 2KE-PICK1 clusters (Madsen *et al.*, 2008). In addition, others have attributed a potential regulatory role to the direct binding of membranes such that phosphorylation of S77 within the PDZ domain is increased by 10-fold in the presence of liposomes (Ammendrup-Johnsen *et al.*, 2012). Because the phosphomimic mutant S77D has reduced clustering capacity, this points towards a plausible negative feedback loop in which PICK1 phosphorylation by PKCα ensures appropriate levels of clustering are maintained.

1.4.7. The regulation of PICK1 BAR domain-mediated membrane binding

An interesting perspective that emerges asks whether the other domains of PICK1 participate in the regulation of its membrane binding dynamics. To this extent, it has been shown that the C-terminal tail negatively affects the ability of PICK1 to bind to lipid bilayers due to its negatively charged amino acid stretch which potentially folds onto the positively charged BAR domain surface inhibiting it. Intriguingly, the role of the PDZ domain proved more evasive to decipher, as initially studies reported that lacking the PDZ domain results in impaired lipid association (Jin *et al.*, 2006), however this claim was later disputed. Indeed, other groups were able to demonstrate that deletion of the PDZ domain still resulted in large clustering of PICK1 which was then abolished by the introduction of the 2KE and 3KE mutations (Madsen *et al.*, 2008). Moreover, others have speculated that the PDZ domain is itself capable of recognising and binding membranes in a manner which could be essential for the proper function of PICK1. The PICK1 PDZ domain showed different phospholipid binding compared to the PICK1 BAR domain such that the following preference occurs: PtdIns(3,4,5)P > PtdIns(4,5)P ≥ PtdIns3P. Because the double and triple phosphorylated lipids are more common at the plasma membrane and on internalised vesicles, this suggests that the PDZ domain is required for appropriate membrane targeting during

endocytosis (Shewan *et al.*, 2011). Investigations revealed that PDZ-mediated lipid binding occurs through two distinct binding motifs: a positively charged region on the opposite side of the PDZ binding groove and a flexible loop between two β-sheets which contains a conserved CPC motif (Erlendsson & Madsen, 2015). Indeed, mutations replacing these cysteine residues with glycine (CC-GG mutant) abolished the ability of PICK1 to associate with membranes and to direct AMPARs to the surface, while maintaining its ability to bind GluA2 which suggests that the membrane- and lipid-binding properties of the PDZ are not mutually exclusive (Pan *et al.*, 2007).

In addition, deleting the PDZ together with the V121E, L125E mutation nearly abolished fractional binding of liposomes which was not seen independently with each mutation (Herlo *et al.*, 2018). This seems to solidify the importance of the PDZ domain for membrane binding, along with evidence supporting a role for the region immediately N-terminal to the BAR domain. Part of the unstructured ~100 amino acid linker connecting the PDZ and BAR domains in PICK1, residues 113-130 have been shown through modelling to be capable of assembling into an amphipathic helix which is involved in membrane curvature sensing. The distinction between curvature sensing and curvature induction has been difficult to determine from a mechanistic point of view, however this study has been able to show that the V121E, L125E mutation in the amphipathic helix results in reduced binding of small 75nm liposomes, while larger 500nm liposomes remain unaffected. Together with evidence that PICK1 shows a significantly higher absolute density on smaller liposomes, this suggests two potential membrane-binding motifs are involved (Herlo *et al.*, 2018). Therefore, the dynamics of PICK1 membrane binding are complex and dictated by several factors, including not only the intrinsic properties of the BAR domain itself such as phospholipid affinity, but also on the adjacent structural components which serve an additional role.

1.4.8. PICK1 BAR domain-mediated protein-protein interactions

Finally, the BAR domain itself has been directly implicated in a number of protein-protein interactions relevant for its role in AMPAR trafficking and synaptic plasticity. For example, it has been shown that when PICK1 participates in the transfer of GluA2 from being synaptically anchored by ABP/GRIP to becoming internalised, this is a consequence of a direct interaction between the two scaffold proteins achieved by the

BAR domain of PICK1 and the linker II region of ABP/GRIP. Disrupting this interaction has significant impact on the function of PICK1 because it impedes all aspects of GluA2 trafficking, including constitutive recycling, NMDA-induced internalisation, and surface recycling (Lu & Ziff, 2005). Furthermore, the BAR domain has also been shown to facilitate interaction with actin, a globular protein which polymerises into microfilaments that are assembled and disassembled to accommodate dendritic spine growth or shrinkage in response to synaptic plasticity. Together with evidence that PICK1 also directly interacts with and inhibits the Arp2/3 complex, this supports a role for PICK1 in the regulation of dendritic spine morphology and during AMPAR endocytosis (Rocca *et al.*, 2008; Nakamura *et al.*, 2011). One of the known functions of BAR domain proteins is binding and recruiting members of the small GTPase family to the plasma membrane where they can interact with their effectors. Indeed, PICK1 has also been shown to directly associate with Cdc42 and Rac1 in a BAR-domain dependent manner therefore solidifying its involvement in actin dynamics (Rocca & Hanley, 2015). More recently, investigations have revealed that PICK1 is also able to bind two important proteins that coordinate the internalisation of vesicles through a highly regulated process called clathrin-mediated endocytosis (CME). Via the FxDxF and DxF motifs within the BAR domain, PICK1 binds to the α-appendage of AP2, one of the earlier proteins to be recruited during CME, followed later by a direct association between the BAR domain and the GTPase domain of dynamin2 which is responsible for the scission of the newly formed vesicle (Fiuza *et al.*, 2017).

All in all, PICK1 is a scaffold and membrane remodelling protein with unique functional characteristics dictated by its two major structural domains, the BAR and PDZ domains. By bringing together a large number of PDZ-motif containing proteins in the proximity of membranes, PICK1 has evolved to be essential for the appropriate maintenance of AMPAR surface expression through trafficking. Specific interactions with numerous components of the endocytic machinery allow for the tightly regulated spatial and temporal clustering of relevant proteins which precedes CME. Additionally, its accessory structural features bestow a calcium-sensing ability for the activity-dependent regulation of PICK1 which supports its role in the expression of synaptic plasticity.

1.5. The role of PICK1 in the coordination of AMPAR trafficking

The first indication that PICK1 could be involved in the regulation of neuronal transmission was discovered when researchers looked at the expression of PICK1 and found that it was enriched at synapses where it colocalised and interacts with GluA2-contanining AMPARs (Xia *et al.*, 1999). Its ability to cluster AMPARs during co-expression in heterologous cells, as well as removal of GluA2-containing AMPARs from the synapse following PKC activation suggested that PICK1 function is related to AMPAR trafficking in an activity-dependent manner (Perez *et al.*, 2001). Nevertheless, other studies were able to demonstrate a role for PICK1 in the differential surface expression of GluA2- and GluA1-containing AMPARs under basal conditions, where overexpression of PICK1 resulted in increased GluA2 internalisation without affecting GluA1 surface levels (Terashima *et al.*, 2004). The binding of PICK1 to the GluA2 subunit is mediated through the cytoplasmic tail of the subunit and is regulated through the phosphorylation of residue S880 in response to PKC activity, such that an increase in phosphoS880 leads to increased PICK1 interactions while simultaneously disrupting AMPAR synaptic anchoring (Matsuda *et al.*, 1999; Chung *et al.*, 2000; Lin & Huganir, 2007). Interestingly, one group proposes the formation of a triple complex between PICK1, PKC and the synaptic scaffold protein GRIP, where PICK1 bound to activated PKC is targeted to the post-synaptic density, recognising and directly binding GRIP thus facilitating the phosphorylation of GluA2 S880 which causes the subsequent release of GRIP and binding of PICK1 to GluA2 (Lu & Ziff, 2005). Other studies provided further evidence that PKC activation and the resulting PICK1-mediated GluA2-containing AMPAR internalisation could be correlated to electrophysiological and chemical induction of LTD in neurons (Iwakura *et al.*, 2001; Kim *et al.*, 2001). Together, these findings have contributed to the proposed mechanism for PICK1 function in supporting GluA2-containing AMPAR endocytosis in response to LTD (Figure 1.7.).

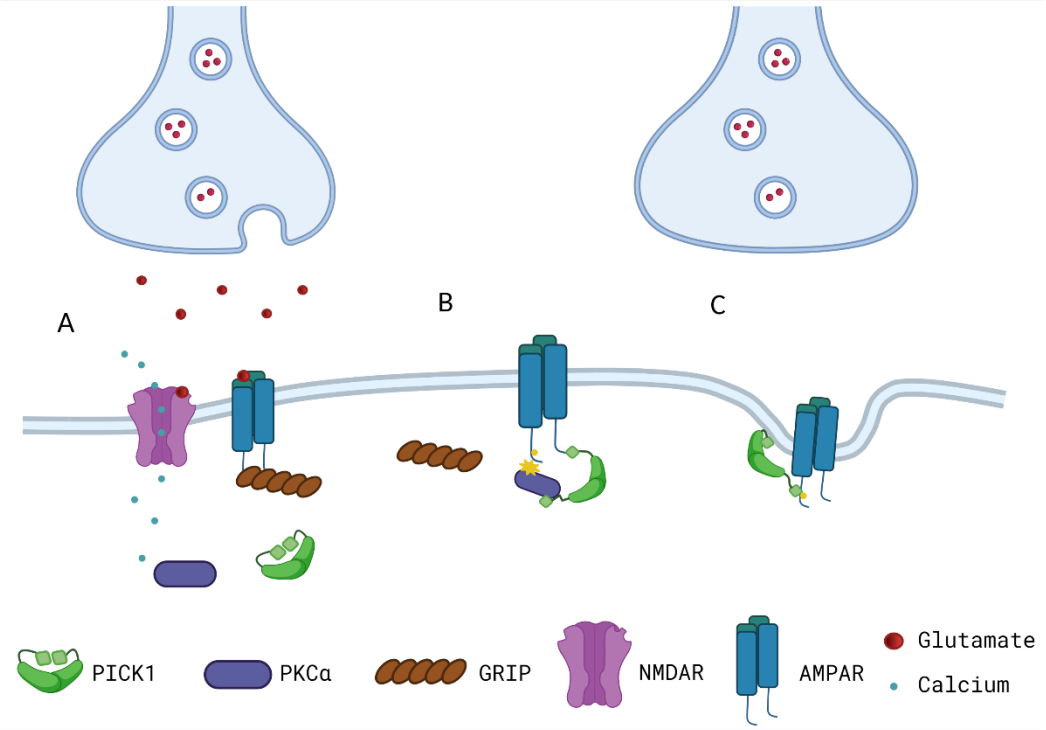

Figure 1.7.: Mechanism of PICK1-mediated AMPAR endocytosis during NMDAR-mediated LTD. (A) AMPARs are maintained within the post-synaptic density by directly associating with PDZ-containing synaptic anchoring proteins such as GRIP/ABP. Neuronal activity and presynaptic glutamate release activates AMPARs and NMDARs on the postsynaptic neuron. (B) Once intracellular calcium concentration reaches a certain threshold, PKCα becomes activated and interacts with PICK1 via its PDZ domain in order to redistribute to AMPAR clusters where PKCα can phosphorylate GluA2 at Ser880. (C) Phosphorylated GluA2 dissociates from GRIP/ABP, but PICK1 remains associated and promotes endocytosis through BAR-domain mediated membrane binding (Perez *et al.*, 2001). Image generated with BioRender.com.

1.5.1. PICK1 is involved throughout all stages of clathrin-mediated endocytosis of AMPARs

In addition to the interaction with AMPARs, PICK1 has also been shown to directly bind proteins that orchestrate the endocytic machinery itself (Fiuza *et al.*, 2017). In brief, the main mechanism for AMPAR internalisation is clathrin-mediated endocytosis which can be separated into three stages: cargo recognition and clathrin coated pit formation, curvature induction and coat growth and finally vesicle scission (Chapter 1.4.). A variety of proteins are sequentially involved at different stages and PICK1 has been associated with interactors that are recruited throughout the process. In the initial

phase, PICK1 recognises and binds the α appendage of the adaptor protein AP2 in an activity-dependent manner, mediated through the calcium-sensing phosphatase calcineurin. Because blocking the PICK1-AP2 interaction disrupts NMDAR-induced GluA2 clustering at clathrin coated pits, it has been suggested that PICK1 is involved in the removal of AMPARs from the post-synaptic density towards the endocytic zone (Fiuza *et al.*, 2017). The next step of endocytosis features the recruitment of proteins from the BAR domain family which are well characterised as membrane curvature sensors due to their ability to recognise and bind lipid bilayers. PACSIN is an F-BAR domain-containing protein which is highly expressed in neurons and essential for NMDAR-mediated AMPAR trafficking. In order to perform its cellular function, PACSIN associates with GluA2 via PICK1 and disrupting the interaction between PICK1 and PACSIN results in reduced levels of internalised AMPARs following NMDA stimulation (Anggono *et al.*, 2013). Finally, PICK1 has been shown to directly interact with the GTPase domain of dynamin which is recruited to the neck of the newly internalised vesicle in order to facilitate scission and intracellular release, however the functional consequences of this interaction remain unknown (Fiuza *et al.*, 2017).

1.5.2. The role of PICK1 in the coordination of the endocytic pathway

It is worth briefly discussing here the cellular trafficking events that typically occur following endocytosis and how PICK1 is involved in their coordination. Firstly, internalised vesicles which contain AMPARs as their cargo can follow three prospective routes: a). they can be maintained as an intracellular pool of available AMPARs in case of further synaptic potentiation; b). they can be quickly returned to the surface as part of a constitutive recycling pathway or c). they can be further internalised and targeted for lysosomal degradation (Ehlers, 2000; Shepherd & Huganir, 2007; Parkinson, 2018). The precise molecular mechanisms regulating AMPAR endosomal sorting are yet to be uncovered, however the evidence available so far suggests that PICK1 is most likely involved in AMPAR surface recycling. While a number of studies highlight a role for PICK1 in hippocampal intracellular retention of synaptic GluA2 (Kim *et al.*, 2001; Lin & Huganir, 2007; Citri *et al.*, 2010), others have shown that disrupting PICK1-GluA2 interactions with small interfering peptides results in a reduction in extrasynaptic GluA2 in cerebellar stellate cells (Gardner *et al.*, 2005).

This points towards a dual role for PICK1 not only in the internalisation and intracellular retention of AMPARs, but also in their synaptic incorporation via the extrasynaptic regions, although further work is required to address the origin of resurfaced GluA2. It has been suggested that NSF, an ATPase involved in exocytosis, functions in the removal of PICK1 from being associated with the intracellular/extrasynaptic pool of endocytic GluA2 thus promoting AMPAR re-insertion under basal conditions through constitutive recycling, as well as following the expression of synaptic plasticity (Hanley *et al.*, 2002; Steinberg *et al.*, 2004; Gardner *et al.*, 2005). Furthermore, it has been shown that the interaction between PICK1 and PACSIN is required for the appropriate recycling of AMPARs to the plasma membrane (Widagdo *et al.*, 2016). Recent studies have also indicated a role for PICK1 in the trafficking of newly synthesised GluA2 by regulating endoplasmic reticulum exit in collaboration with CaMKII and in response to calcium (Lu *et al.*, 2014). Together, these findings suggest a complex role for PICK1 in the coordination of AMPAR trafficking, most likely determined through the integration of several neuronal signalling pathways which is made possible by the large number of potential PICK1 binding partners.

Taken together, the information presented so far highlights PICK1 as a modulator of neuronal communication. PICK1 controls several aspects of AMPAR trafficking, including basal surface expression and recycling, spine morphology and activity-induced removal of GluA2-containing AMPARs and in response to NMDA stimulation through clathrin-mediated endocytosis. Uniquely structured, the protein contains both a PDZ and BAR domain which function together to allow PICK1 to bind a large variety of ligands, while the BAR domain not only functions in membrane binding and subcellular localisation but also serves as a dimerisation domain. This is how PICK1 brings together many different proteins and coordinates many cellular functions. PICK1 dimerisation is worth further investigation due to its potentially significant implications for the appropriate function of the protein, as BAR domains require at least two monomers coming together to form the right curvature.

1.6. Aims and objectives

In this study, I am interested in exploring the consequences of calcium stimulation for the appropriate function of the PICK1 BAR domain. In particular, I will be investigating how PICK1 BAR domain-mediated dimerisation responds to external calcium manipulations in a reduced system, as well as in heterologous cells and neuronal environments. The aim is to uncover any potential effects that a novel mechanism for activity-dependent BAR domain dimerisation could have on the membrane remodelling capacity of PICK1. Specifically, the objectives can be divided into three main categories:

- Biochemical investigations using the cell-permeable irreversible crosslinker DSS in order to:
    - Assess how the dimerisation of PICK1 compares to other BAR domain proteins;
    - Determine whether PICK1 BAR domain-mediated dimerisation can be upregulated in response to calcium stimulation;
    - Discover which regions within the PICK1 structure are involved in the regulation of calcium-sensitive PICK1 dimerisation.
- Establishing a FLIM-FRET imaging protocol that can reliably detect PICK1-PICK1 interactions in neurons following chemical induction of LTD in order to assess whether PICK1 dimerisation is upregulated during synaptic plasticity.
- Investigations into the membrane remodelling capacity of PICK1 by:
    - Designing a mutant that is impaired in its overall dimerisation and also blocks the effect of calcium;
    - Testing the mutant in a COS-7 tubulation assay in order to determine whether calcium-sensitive PICK1 dimerisation is relevant for membrane tubulation.

Chapter 2

Methods and materials

2.1. Materials

All reagents were purchased from Sigma-Aldrich unless otherwise stated.

2.1.1. Plasticware and glassware

- Pipette tips (10-1000µl) were purchased from StarLab. Plastic pipettes (5-25ml) were purchased from CellStar.
- 1.5ml microcentrifuge tubes were from Eppendorf and 0.5ml PCR grade tubes were from StarLabs.
- 15ml and 50ml conical Falcon tubes, 30-100mm cell culture dishes, glass-bottom imaging dishes and T75 flasks were purchased from Greiner and CellStar.
- Spectrophotometer cuvettes were from Fisher Scientific.

2.1.2. Electronic equipment

The laminar hoods used for sterile cell cultures were from Holten LaminAir and incubators were from RS Biotech. Bacterial shaking incubator was manufactured by Brunswick Scientific. Thermal cycler PCR machine was manufactured by MJ Research PTC-2000. Benchtop centrifuges were from Eppendorf and Biofuge. The large low speed centrifuges were from Jouan. Bacterial cells were sonicated using the Microson Ultrasonic Cell Disrupter. The electrophoresis system including powerpack, boxes and cassettes were from Bio-Rad Laboratories. X-Ray film developer was purchased from Konica. Dissection microscope as well as the FLIM-FRET microscope, including lenses, pulsed laser and photon detector was manufactured by Leica.

2.2. Molecular biology techniques

2.2.1. Plasmid preparation

Many of the plasmids used in this study were already available or were generated in our laboratory except for mGFP-10-sREACh-N3 which was designed by Dr Ryohei Yasuda and purchased from Addgene (plasmid #21947), amphiphysin2-GFP was a gift from Dr Emmanuel Boucrot and GFP-endophilin was a gift from Dr Ira Milosevic, GFP-SNX1 was a gift from Dr Pete Cullen. Plasmids were amplified by bacterial transformation of DH5α competent *E. coli* cells which were cultured overnight at 37°C/220rpm in the shaking incubator in 50ml Luria Bertani (LB) medium supplemented with ampicillin (100µg/ml) or kanamycin (30µg/ml). Plasmid purification was carried out using the GeneJET Midiprep kit from Thermo Scientific.

2.2.2. PCR cloning and site-directed mutagenesis

PCR cloning of mGFP, sREACh and PICK1 into pcDNA3.1 was carried out using primers purchased from Eurofins Genomics (Table 1). KOD HotStart polymerase kit (Merck) was used according to instructions:

10x buffer - 5µl
dNTPs - 5µl
$MgSO_4$ - 3µl
Forward primer (10µM) – 1.5µl
Reverse primer (10µM) – 1.5µl
Template DNA (1ng/µl) - 10µl
dH_2O – 20.5µl
KOD polymerase - 1µl

The standard PCR reaction used throughout this study followed this programme:

1. Denaturation for 20s at 95°C;
2. Annealing for 10s at 55°C;
3. Elongation for 30s at 70°C;
4. Repeat cycle 20 times.

Mutations were generated by site-directed mutagenesis using primers purchased from Sigma (Table 1). Mutagenesis PCR reactions differed in the length of the elongation step depending on the size of the plasmid (25s/kb) and the number of cycles was increased to 23. The PCR reactions were set up using the KOD HotStart polymerase kit (Merck) according to the instructions above with additional 5% DMSO. Once the PCR reaction was completed, the PCR template was digested with DpnI (NEB) for 2h at 37°C.

Table 1: Primer sequences used for molecular subcloning and site-directed mutagenesis

Primers for subcloning (Eurofins Genomics)	
mGFP NT forward	5'- ATATATA GCTAGC CCACC ATGGTGAGCAAGGGCGAGGA
mGFP NT reverse	5'- TATATAT AAGCTT CGCCGAGAGTGATCCCGGCGGC
sReach NT forward	5'- ATATATA GCTAGC CCACC ATGGTGAGCAAGGGCGAGG
sReach NT reverse	5'- TATATAT AAGCTT CTTGTACAGCTCGTCCATGCC
PICK1 forward	5'- ATATAT AAGCTT CCATGTTTGCAGACTTAGACTAT
PICK1 reverse	5'- ATATAT GGATCC TTAGGAGTCACACCAGCTTCCGCC
Primers for site-directed mutagenesis (Sigma)	
F187K PICK1 forward	5'- CTGTCACAGACTCACCGGGCTAAAGGGGACGTGTTCTCTGTGATT
F187K PICK1 reverse	5'- AATCACAGAGAACACGTCCCCTTTAGCCCGGTGAGTCTGTGACAG
F210K PICK1 forward	5'- GCAAGTGAAGCATTTGTGAAGAAAGCTGACGCACACCGCAGCATT
F210K PICK1 reverse	5'- AATGCTGCGGTGTGCGTCAGCTTTCTTCACAAATGCTTCACTTGC
F337K PICK1 forward	5'- ATCGTGTTCCAGCTGCAGCGCAAAGTGTCTACCATGTCCAAGTAC
F337K PICK1 reverse	5'- GTACTTGGACATGGTAGACACTTTGCGCTGCAGCTGGAACACGAT
4A PICK1 forward	5'-CTGAAGGTGAAGGAGATGGCAGCAGCAGCATACAGCTGCATTGCCCTAGGA
4A PICK1 reverse	5'- TCCTAGGGCAATGCAGCTGTATGCTGCTGCTGCCATCTCCTTCACCTTCAG

2.2.3. Purification of PCR product and restriction enzyme digestion

The PCR product was purified using the GeneJET PCR Purification Kit from Thermo Scientific according to the manufacturer's instructions. Binding buffer was added at 5:1 ratio before being vortexed and added to the purification column. After 1min centrifugation using a benchtop centrifuge, flow-through was discarded and two washing steps were performed using the wash buffer. DNA was eluted in 25µl dH_2O. 5µl was mixed with 6X Loading buffer (NEB) and run on a 1.5% agarose gel for 25min at 135 V. The gel was visualised with a UV transilluminator to assess the quality and quantity of DNA present.

Restriction digestion reaction were followed according to the protocol for the PCR product:

CutSmart buffer - 10µl
Restriction enzyme 1 - 2µl
Restriction enzyme 2 - 2µl
PCR product - 20µl
dH_2O - up to 50µl

The vector was also cut via restriction digestion using the following protocol:

CutSmart buffer - 10µl
Restriction enzyme 1 - 2µl
Restriction enzyme 2 - 2µl
CIP - 2µl
Vector - 2µl
dH_2O - up to 50µl

The restriction enzymes used were NheI and HindIII for cloning mGFP and sREACh into pcDNA3.1 and HindIII and BamHI for cloning PICK1 in pcDNA3.1. The reaction was carried out at 37°C on a shaking incubator. After completion of digestion, the DNA was purified again using GeneJET PCR Purification Kit.

2.2.4. Ligation and transformation

Ligation of digested vector and inserts were carried out in a 1:5 ratio at room temperature with 1µl ligase (Takara) for 30min. The concentration of the DNA was measured using the NanoDrop.

Bacterial transformation using ligation products of XL1-blue supercompetent cells (Agilent) was followed by the inoculation of agar plates containing the appropriate antibiotic. The next day, individual colonies were picked for overnight growth at 37°C/220 rpm before plasmid DNA was extracted with GeneJET Midiprep (Thermo Scientific) and the colonies were screened for the corresponding insert size by

restriction enzyme digestion with suitable enzymes (NheI, HindIII, BamHI from NEB). The correct insert was confirmed by sequencing from Eurofins Genomics.

Likewise, bacterial transformation of competent *E. coli* with DpnI digested PCR mutagenesis product was followed by inoculation of agar plates containing the appropriate antibiotic. The next day, individual colonies were picked for overnight growth at 37°C/220 rpm before plasmid DNA was extracted using GeneJET Midiprep kit (Thermo Scientific). Colonies were screened and mutants were confirmed through sequencing (Eurofins Genomics).

2.3. Cell culture

All the handling of the cells was carried out in sterile laminar flow hoods and cells were maintained in 5% CO_2/37°C incubators.

2.3.1. Primary neuronal culture

Experimental procedures were performed in accordance with the guidelines outlined in the “Animals (Scientific Procedures) Act 1986” and the University of Bristol policy on working with animals.

Neurons were obtained weekly from E17 Han Wistar rat embryos following brain dissection and separation into cortical and hippocampal neurons. The pregnant female adult rat was sacrificed according to Schedule 1 regulations by cervical dislocation after being anaesthetised with isoflurane (Piramal). All dissection procedure were carried out in Hank’s balanced salt solution, (HBSS, Gibco) Embryos were removed from the embryonic sack and immediately decapitated. The separation of hippocampal and cortical neurons was carried out under the Leica microscope. The brains were removed from the skull using sharp, sterile forceps and the meninges were removed. The hippocampus was separated from the rest of cortex.

The following steps were carried out in the sterile hoods. The hippocampus was transferred to a sterile 15ml falcon tube before three 10ml HBSS washes were carried out. In order to trypsinise the tissue, the hippocampus was incubated with 10ml HBSS containing 0.005% trypsin-EDTA for 10min at 37°C in the water bath. After another

three 10ml HBSS washes, a final 1ml wash with plating medium was done. The hippocampal neurons were dissociated by gently pipetting up and down with a 1ml pipette tip. The cell suspension was diluted to 5ml and the number of cells was counted using a haemocytometer.

The hippocampal neurons were plated at a density of 300,000 per 3.5 cm glass bottom dish that had been previously incubated with poly-D-lysine (1 mg/ml) for 4h. The plating medium used during dissociation contained 2% B27 supplement (Thermo Fisher), 0.1mg/ml penicillin/streptomycin, 2mM glutamax and 5% horse serum in neurobasal medium (Thermo Fisher). The following day, the 2ml of plating medium was replaced with 3ml of feeding medium of the same composition but without horse serum. The neurons were cultured for 13-17 days at 37°C, 5% CO_2 in the incubator before being subsequently used for experiments.

2.3.2. Cell line culture of HEK293 and COS-7 cells

HEK293 and COS-7 cells were purchased from ATCC. The growth medium used was Dulbecco's Modified Eagle Medium (DMEM, Lonza) supplemented with 10% fetal bovine serum (Sigma), 2mM glutamine (Sigma) and 0.1mg/ml penicillin/streptomycin (Sigma). The cells were plated at densities of 200,000 per glass bottom dish for imaging, or at 400,000 per dish for biochemistry experiments. The cells were maintained at 37°C, 5% CO_2 until confluence levels of approximately 80% were reached.

2.3.3. Cell passage

A T75 flask of HEK293 and COS-7 cells was kept in the same conditions and passaged every 4-5 days once cells had reached 80% confluence. The culture was washed once in 1X PBS in cell culture grade water (Gibco). For the removal of the adhered cells, 1ml of 1% trypsin/EDTA (Gibco) was added to the flask before the cells were returned to the incubator for 5min. The COS-7 are harder to dislocate and were shaken every minute or so in order to improve cell count after passaging. The cell suspension was diluted to 10ml using growth media before centrifugation at 2000rpm for 2min. The cells were resuspended by trituration in 10ml growth media. After the

cells were counted using a haemocytometer, plating took place and 1ml of cell suspension was used to seed a new T75 flask in 15ml growth media.

2.3.4. Cryopreservation

For cryopreservation, passaged HEK293 and COS-7 cells were aliquoted into 3 million per ml DMEM with 20% glycerol and frozen overnight in the -80°C freeze before being transferred to liquid nitrogen. These stocks were thawed out when necessary and allowed to recover for a week before subsequent use in experiments.

2.3.5. Neuronal and cell line transfection

DIV14 to DIV18 neurons were transfected with various fluorophore- and PICK1-expressing pcDNA3.1 plasmids. The transfection cocktails were prepared using 5µl Lipofectamine 2000 (Thermo Fisher) and 2µg plasmid per dish. The Lipofectamine was initially diluted in 100µl plain neurobasal medium/dish and allowed to sit for 5min before being added to another 100µl neurobasal medium containing the plasmid dilutions. The lipofectamine and DNA were mixed together on the vortex before being allowed to sit for 30min at room temperature. The culture medium of the neurons was removed and replaced with 2ml plain neurobasal medium before the 200µl transfection cocktail was added. The neuronal cultures were returned to the incubator for 1h, after which the transfection medium was washed off with plain neurobasal medium and replaced with the previously saved culture medium. HEK293 and COS-7 cells were transfected based on a similar protocol, with the same DNA:Lipofectamine ratio but in plain DMEM and without being washed off.

2.4. Protein purification

Protein purification was carried out using pET vectors expressing his_6-tagged proteins. BL21(DE3) (Agilent) bacteria were transformed and allowed to grow onto kanamycin plates overnight at 37°C. The following day, colonies were picked to inoculate 20ml LB cultures (kanamycin 30µg/ml) which were incubated again overnight at 37°C, 220rpm. The next morning, the 20ml culture was used to inoculate 1l LB broth with kanamycin and returned to the incubator until an optical density between 0.7 and 1 was measured at 600nm using the spectrophotometer. At this point, the temperature was reduced to 30°C and 1mM IPTG was added to the cultures the for the next 3-4h of protein expression. The samples were then centrifuged at 14,000rcf at 4°C before being resuspended in his_6 buffer (150mM KCl, 50mM HEPES, 10% glycerol, 1mM DTT, pH 7.4). For cellular lysis, his_6 buffer containing 25mM imidazole, 1% Triton and EDTA-free protease inhibitors (Roche) was added to the bacterial suspension and set on ice for 20 minutes. The samples were then sonicated for three rounds of three 30s pulses in the cold room before being centrifuged for 30min at 20,000rpm at 4°C. This was done in order to extract the purified protein from the bacterial cells. The cellular extracts were then incubated with 200µl Ni-NTA coated beads (QIAGEN) with rotation for 2-3h at 4°C. Five rounds of washes were then performed using his_6 buffer with 55mM imidazole in order to remove unbound protein contaminants before the purified protein was eluted using his6 buffer with 300mM imidazole, pH 6.8.

2.5. Bradford assay

Protein concentration was determined using Bio-Rad reagent to generate a standard curve. Serial dilutions were made from 0.1mg/ml to 2mg/ml using BSA. Prior to incubation with 5µl protein, the BioRad reagent was diluted 1:5 with dH_2O and a total volume of 1ml was used in appropriate 1ml cuvettes. The corresponding buffer for the solubilised protein was used to normalise the spectrophotometer and the optical density was measured at 595nm. These values were used to generate the standard curve in Microsoft Excel before the protein concentration was extrapolated accordingly.

2.6. DSS crosslinking assay

2.6.1. DSS crosslinking using HEK293 cell cultures

In the case of HEK293 experiments, the crosslinking buffer used was 2ml PBS (GE Lifesciences) with 0.3mM DSS. After the reaction was quenched with 50mM Tris for 15min, the cells were lysed in 150mM NaCl/20mM HEPES containing EDTA-free protease inhibitors (Roche) and 0.5% Triton X. Laemmli buffer (65mM Tris, 25% glycerol, 2% SDS, 0.01% bromophenol blue, 5% mercaptoethanol) was added in a 1:1 ratio to cellular lysates before being loaded onto polyacrylamide gels.

2.6.2. DSS crosslinking using purified protein

For purified protein crosslinking, the crosslinking buffer was 150mM NaCl, 20mM HEPES, pH=7.4 and buffered to the appropriate calcium concentration (section 2.6.). 100nM purified PICK1 was treated with 10µM DSS for 20min at room temperature before the reaction was quenched with 50mM Tris for 15min. Laemmli buffer (65mM Tris, 25% glycerol, 2% SDS, 0.01% bromophenol blue, 5% mercaptoethanol) was added in a 1:1 ratio to cellular lysates before being loaded onto polyacrylamide gels.

2.7. Calcium buffered solutions and ionomycin treatment

The ionomycin treatment was carried out by incubating HEK293 cells with different calcium buffers (see below) for 5min at 37°C with 3µM ionomycin (Cayman Chemicals). The extracellular calcium solutions used were prepared using the following recipe in HBS buffer (140mM NaCl, 5mM KCl, 25mM HEPES, 10mM glucose, pH=7.4):

0mM: 50ml HBS

1mM: 49.5ml HBS + 0.5ml 100mM $CaCl_2$

3mM: 48.5ml HBS + 1.5ml 100mM $CaCl_2$

5mM: 47.5ml HBS + 2.5ml 100mM $CaCl_2$

The buffers used for purified protein crosslinking were obtained as follows in 150mM NaCl/20mM HEPES, pH=7.4:

0µM: 5mM HEDTA

2µM: 5mM HEDTA + 0.75mM $CaCl_2$

5µM: 5mM HEDTA + 1.5mM $CaCl_2$

12µM: 5mM HEDTA + 2.5mM $CaCl_2$

26µM: 5mM HEDTA + 3.4mM $CaCl_2$

The concentrations were calculated using the MaxChelator online tool for calculating free metal in solution (MaxChelator). The pH and ionic strength of the buffer was taken into account when making the calculations.

2.8. SDS-PAGE and Western blot

2.8.1. SDS-PAGE

Sodium dodecyl sulphate-polyacrylamide gel electrophoresis (SDS-PAGE) was used to separate proteins based on molecular weight. 6%, 7% or 12% polyacrylamide gels (55-70 kDa for monomer PICK1 used 12%, 130-170 kDa for dimer PICK1 used 6-7%) were prepared by allowing resolving gel solutions to polymerise at room temperature between 1.5mm glass plates (Bio-Rad). The gel solution contained H_2O, Acrylamide/bis (30% 37.5:1; Bio-Rad), Tris–HCl (1.5M, pH 8.8), SDS, N,N,N′,N′-tetramethylethylene-diamine (TEMED) (Bio-Rad) and ammonium persulfate and was covered with isopropanol to ensure level polymerisation. Once the resolving gel was set, the isopropanol was removed, and a 5% stacking gel was loaded on top before 10 or 15-well combs were inserted to produce wells. Once the gels were fully set, they were assembled into the Bio-Rad electrophoresis system before 5µl pre-stained ladder and 20µl sample was loaded. The gels were run for 1.5h at a constant voltage of 150V in running buffer (25mM Tris, 250mM glycine, 0.1% SDS).

2.8.2. Wet transfer

When the dye front had reached the bottom of the gel, the transfer apparatus was prepared. For the transfer, a PVDF membrane (Merck) that had been activated in methanol was placed onto the gels and a transfer cassette containing 4 sheets of blotting paper and one sponge on each side was assembled. During assembly, the gel and membrane were submerged in transfer buffer and a roller was used to eliminate any potential disruption caused by bubbles. The assembled cassettes were then placed inside the Bio-Rad electrophoresis system and the powerpack was run at 400mA for 1h in transfer buffer (50mM Tris, 40mM glycine, 20% methanol). An ice pack also placed inside the transfer box, in addition to being constantly stirred by a magnetic stirrer in order to maintain a consistent, low temperature to avoid inappropriate transfer.

2.8.3. Immunoblotting

The membranes were blocked by incubation with 5% milk (Own brand powdered milk, Co-op) in PBS-T (PBS + 0.1% Tween) for one hour at room temperature on the shaker. Primary antibody incubation was done using mouse antibodies against PICK1 (1/1000, Neuromab), and GFP (1/1000, Neuromab) diluted in 5% milk, either overnight at 4˚C or for at least 2h at room temperature on the shaker. After three 10min PBS-T washes, the anti-mouse HRP-linked secondary antibody (1/10000, GE Healthcare) was added for 45 minutes at room temperature. Another round of three 10min PBS-T washes followed, after which the membranes were incubated for 1min with either the Classico, Crescendo (Millipore) or the Femto (Thermo Scientific) ECL substrates depending on the intensity of the signal. The signal was detected by exposing and developing X-ray films which were then scanned in grayscale before using ImageJ for quantification. The data were normalised by assigning the value of 1 to the highest dimer signal and expressing the rest of the dimer values in relation to this. A second normalisation step was carried out to control for gel loading differences by assigning a value of 1 to the highest monomer signal before expressing the rest of the values in relation to this. The normalised dimer values were then divided by the normalised monomer values. The normalised data were statistically analysed using GraphPad Prism.

2.9. NMDA treatment

Transfected neuronal cultures were allowed to express for 24h before chemical LTD induction with 0.5μM TTX (Tocris), 20μM glycine (Sigma) and 50μM NMDA (Tocris) in HBS buffer (140mM NaCl, 5mM KCl, 25mM HEPES, 1.8mM $CaCl_2$, 0.8mM $MgCl_2$, 10mM glucose, pH=7.4). The feeding medium was removed and replaced with the NMDA treatment for 3 minutes, followed by a HBS wash and the re-addition of the feeding medium for the duration of the time course. The cells were then washed twice in HBS before 4% formaldehyde (Thermo Scientific) was added for 15min in order to fix the neurons. After fixation, the neurons were washed twice with PBS before being covered with 2ml PBS and used for imaging in the Wolfson Bioimaging Facility at room temperature.

2.10. FLIM-FRET data acquisition and analysis

Live and 4% formaldehyde fixed cells were imaged using the Leica SP8 CLSM system within the Wolfson Bioimaging Facility at the University of Bristol. The system is equipped with a pulsed laser, single molecule detectors and SymPhoTime software to facilitate TCSPC (time correlated single photon counting) FLIM. Data acquisition for the mGFP-sREACh pair was carried out within the 490-510nm window, extended for the mGFP-mCherry pair to 490-550nm and cells were inspected for RFP expression at 600-650nm. The scanning frequency was set to 80MHz and the image resolution was 512x512 pixels. IRF (instrument response function) measurements were taken at regular intervals in order to measure the instrument response which is taken into account during data fitting. Data analysis was carried out using the FLIMfit 5.1.1. fitting software tool developed at Imperial College London with the pixel-wise fitting algorithm (Warren *et al.*, 2013). The data were spatially binned to 2x2 and temporally binned to 32ps/bin to compress data for processing ease, cropped between 500-12000ps to exclude scattered marginal data and the threshold was set at an integrated minimum of 100 counts/pixel. The pixel-wise data were used to generate heatmaps showing the degree of the decline in measured lifetime in an intensity-adjusted manner and the data was exported as an average lifetime per image. Data was analysed for statistical significance using GraphPad Prism.

2.11. COS-7 cell tubulation assay

COS-7 cells which had been expressing GFP-tagged PICK1 or GFP-tagged 4A mutant for 24-32h were incubated in HBS containing the 0-5mM calcium range with 3µM ionomycin for 15min at 37˚C to allow for tubulation to occur. The cells were washed in PBS before being fixed with 4% formaldehyde for 15min. After a further two washes, 2ml of PBS was added to the imaging grade dishes containing the cultures. Prior to imaging, the samples were blinded with the help of a colleague to ensure that there is no bias in determining the extent of tubulation present in cells. Confocal imaging was carried out using the 63x and the 100x, N.A 1.4 oil immersion lenses in the green channel (490-550nm) with gating on between 0.3 and 8, an optimised pixel size of 70nm and a line average of 6 scans. A total of 20 cells per condition were counted and assigned as tubulated or non-tubulated. The tubulated cells were further analysed in order to detect the average number and the length of tubules per cell. A semi-automated script was developed with the help of Dr Dominic Alibhai from the Wolfson Bioimaging Facility based on Dr Steven Cross' Modular Image Analysis plugin for FIJI (ImageJ) (Cross, 2021). The manual component of the analysis involved selecting areas of suitable saturation within the cytoplasm and the exclusion of the plasma membrane. The automated component applied two filters to the images, a median filter with a radius of 1 and a difference of gaussian filter with a radius of 2 before using the Ridge Detection plugin for the detection and quantification of tubule data. The settings for ridge detection included a threshold of 25 pixels (roughly 1.8µm for my dataset) for minimum tubule length, intensity thresholds between 6-10 and sigma 1.8. An example of the data analysis workflow using a representative image can be viewed in Figure 2.1.

2.12. Statistical analysis

All graphs were prepared with GraphPad Prism version 7.0 after statistical analysis using the same software. The number of individual repeats is indicated in the figure legends, but also on the graph itself with a single dot represented a repeat of the experiment. Data is presented as mean values +/- standard error of the mean (SEM). Western blot data was first normalised by calculating dimer:monomer ratios. Data was first tested for normality. Multiple t-tests were carried out to analyse the differences

between PICK1 and other BAR domain proteins, with Bonferroni's correction for repeated tests. One-way ANOVAs were carried out to analyse the significance of the different conditions in FLIM-FRET experiments. Two-way ANOVAs were performed for the comparison between WT PICK1 and the mutants tested under various calcium conditions. ANOVAs are considered significant if $p<0.05$ and followed by Tukey's post-hoc analysis to determine any significance between the different groups. *$p<0.05$, **$p<0.01$, ***$p<0.001$.

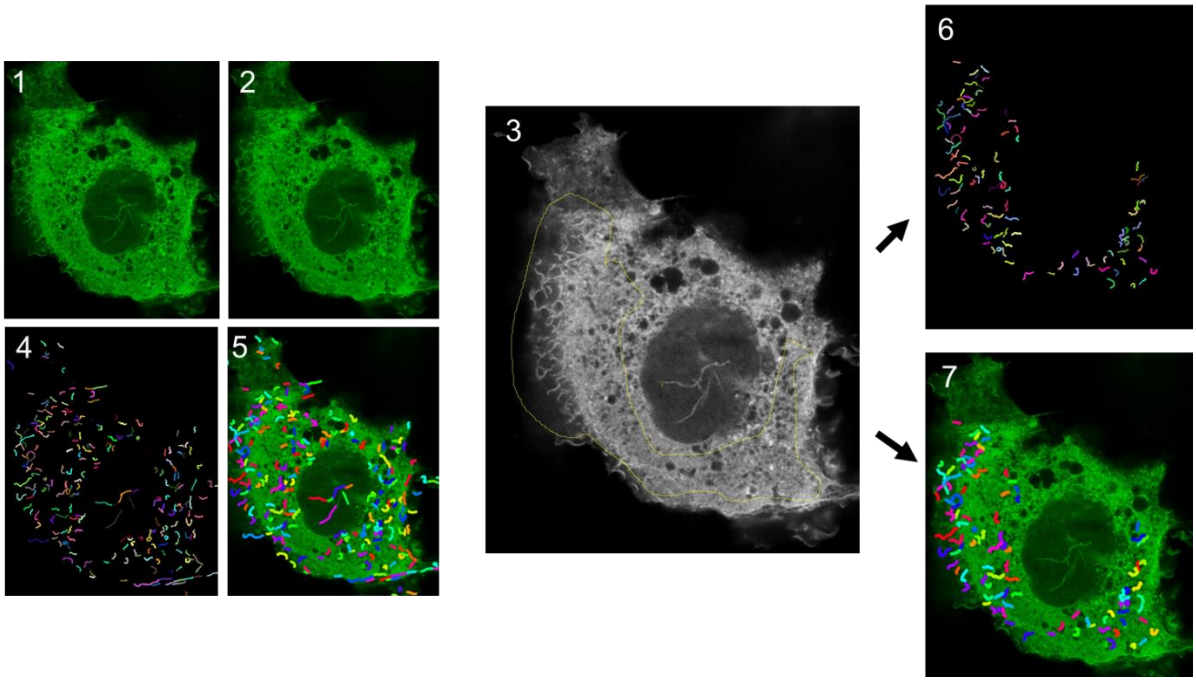

Figure 2.1.: Data analysis workflow used for the detection and measurement of tubules from COS-7 cellular assays. The images were acquired by confocal imaging of COS-7 cultures which had been transfected to express GFP-PICK1 24h prior to being subjected to 3µM ionomycin treatment in the presence of various calcium concentration buffers. (1) The raw images were pre-processed by selecting a single, suitable plane from a Z-stack, or if appropriate a maximum intensity projection from two planes. (2) The images were processed further by applying a median filter followed by a difference of gaussian filter in order to reduce background and improve contrast. (3) The next step involved the manual selection of cytoplasmic areas suitable for analysis while excluding the areas immediately adjacent to the plasma membrane and the nucleus. (4 and 5) The analysis script automatically analyses the entire image for tubular structures using the parameters defined within the Ridge detection plugin settings. The number of tubules is counted and their lengths are measured before an overlay image is generated to assist in assessing their subcellular localisation. (6 and 7) The manual exclusion area from panel 3 is applied, and tubules from outside the region of interest are eliminated in order to ensure that structures from within the nucleus, the nuclear envelope and the plasma membrane are not included in the analysis. An Excel spreadsheet with the individual lengths of all the detected tubules is exported and the data is pooled together to calculate the mean number and length of tubules in each condition.

Chapter 3

Characterisation of dynamic PICK1 dimerisation by using transfected cell lines and purified protein samples

3.1. Introduction

3.1.1. BAR domains are essential structural and functional components for proteins involved in membrane trafficking

The BAR domain superfamily of proteins has been characterised as facilitators of cellular processes which involve membrane reshaping and trafficking events ranging from clathrin-dependent and -independent endocytosis (Bertot *et al.*, 2018) to secretory vesicle biogenesis (Holst *et al.*, 2013) and endosomal retrograde transport (Kvainickas *et al.*, 2017; Simonetti *et al.*, 2017). Indeed, many authors explain in detail how the molecular composition of lipid membranes dictates properties such as intrinsic curvature and propensity for membrane reshaping (McMahon & Gallop, 2005; Stefan *et al.*, 2017), while others focus on how the interactions between BAR domain proteins and membranes drives remodelling (Simunovic *et al.*, 2015; Salzer *et al.*, 2017). In short, the lipid bilayer is made up of various types of lipids, while accommodating many transmembrane and membrane associated proteins. BAR domain-containing proteins have evolved to recognise and bind to negatively charged phospholipid group heads and it is believed that lipid recognition together with the curvature of their secondary structure determines their preferential membrane binding (Peter *et al.*, 2004). As well as a plasma membrane delimitating the exterior, cells contain a variety of intracellular membranous compartments and trafficking to and from these is essential for maintaining appropriate cell signalling (Vieira *et al.*, 1996). In fact, membrane remodelling events are inseparably tied to the expression of surface receptors, the activation and termination of signalling pathways and to protein turnover. This is particularly important in the context of neuronal communication, where neurotransmitter surface receptors are continuously endocytosed and recycled back to the surface in an activity dependent manner (Moretto & Passafaro, 2018). The essential role in neurotransmission of the BAR domain protein PICK1 is highlighted by the fact that mutations which abolish its ability to bind lipid membranes also result in impaired receptor trafficking and synaptic plasticity (Jin *et al.*, 2006; Pan *et al.*, 2007).

3.1.2. BAR domain-containing proteins are expressed as functional dimers

As outlined previously in chapter 1, a well characterised property of the BAR domain family members is their ability to form dimers. From early investigations into the interactions of amphiphysin and endophilin it became obvious that both proteins shared a richly charged N-terminal region with a high probability of coiled-coil structural domain formation (Ramjaun *et al.*, 1999; Ringstad *et al.*, 2001). Studies revealed this N-terminal sequence, now referred to as a BAR domain, mediated not only membrane targeting but also dimerisation in amphiphysin (Ramjaun *et al.*, 1999), while endophilin rat brain expression studies confirmed the stability of expressed homodimers (Ringstad *et al.*, 2001). The availability of a crystal structure for amphiphysin soon offered concrete proof for the existence of three α-helices forming an anti-parallel coiled-coil secondary structure motif in each monomer, coming together to form a six-helix bundle around the hydrophobic dimer interface (Peter *et al.*, 2004).

3.1.3. PICK1 is a BAR-domain family member involved in neuronal plasticity

The protein of interest in this study, PICK1 contains a PDZ domain in addition to the BAR domain and small-angle X-ray scattering revealed that the PICK1 dimer associates into a crescent-shaped molecule through its BAR domains, while the PDZ domains remain flexible in relation to the BAR domain scaffold via the linker region (Karlsen *et al.*, 2015). Interestingly, others have suggested that the PICK1 PDZ domain folds into the concave surface of the PICK1 dimer due to the stabilising effect of hydrophobic interactions (He *et al.*, 2011), and this is consistent with the proposed auto-inhibition of PICK1 where deletion of the PDZ domain results in increased clustering (Lu & Ziff, 2005; Madsen *et al.*, 2008).

The cellular function of PICK1 was outlined by studies which showed how the protein interacts with activated PKCα leading to redistribution to the neuronal cell surface, where following the phosphorylation of S880 on GluA2 subunits, it promotes the removal of GluA2-containing AMPARs from the surface (Staudinger *et al.*, 1997; Perez

et al., 2001). Of course, further investigations revealed a more complex role for PICK1 in AMPAR trafficking because it appears that the protein is involved in multiple stages including AMPAR internalisation, surface recycling and synaptic targeting (Jin *et al.*, 2006; Madsen *et al.*, 2012; Anggono *et al.*, 2013). In fact, PICK1 has been shown to function not only under basal conditions (Nakamura *et al.*, 2011; Fiuza *et al.*, 2017), but also during the expression of synaptic plasticity where it plays an essential role. Several studies show how PICK1 is an integral part in the induction of LTD due to its role in AMPAR trafficking by participating in clathrin-mediated endocytosis (Fiuza *et al.*, 2017), spine morphology through interactions with the Arp2/3 complex (Rocca *et al.*, 2008) and miRNA repression of gene expression through interactions with Ago2 (Antoniou *et al.*, 2014). Furthermore, PICK1 has been previously characterised as a calcium-sensor capable of directly binding calcium ions through its N-terminal acidic stretch in a manner which regulates its interaction with GluA2 subunits and their intracellular retention following NMDA-induced LTD (Hanley & Henley, 2005; Citri *et al.*, 2010).

Because LTD requires transient increases in local calcium concentration in the spine (Miyata *et al.*, 2000) and because the BAR domain minimal functional requirement is dimerisation (Peter *et al.*, 2004), I set out to explore whether there is a link between the activation of PICK1 in neurons following activity-induced calcium influx and its dimerisation status. PICK1 has been implicated in the bidirectional regulation of both LTP and LTD (Sossa *et al.*, 2006; Terashima *et al.*, 2008) which makes the calcium-sensitive relationship between dimerisation and PICK1 activation a very attractive regulatory mechanism which could act as a potential switch between the two types of neuronal plasticity.

3.2. Chapter aims

The main aim of this chapter is to investigate whether PICK1 dimerisation can be influenced by calcium concentration. In order to achieve this, several goals have been set:

- To determine whether PICK1 differs in terms of basal dimerisation levels observed in comparison to other BAR domain-containing proteins;
- To assess whether different calcium concentrations promote a change in the levels of dimer that are detected;
- To determine if calcium-sensitive upregulation in PICK1 dimerisation is direct or mediated through a calcium sensing protein;
- To investigate whether the deletion of calcium-binding regions in PICK1 abolishes dynamic PICK1 dimerisation.
- To determine whether single point mutations are sufficient to disrupt the BAR domain interface.

3.3. Results

3.3.1. Basal levels of dimerisation for BAR domain-containing proteins

In order to assess how the formation of PICK1 dimers compares to other BAR domain-containing proteins, a ratio between the dimer:monomer fractions was measured and analysed. HEK293 cells were transfected with plasmid constructs encoding GFP-tagged versions of PICK1, endophilin1, endophilin2 and the short splicing variant of amphiphysin2. The membrane-permeable crosslinker DSS was used to covalently stabilise dimers which could then be separated based on their size through SDS-PAGE and visualised by immunoblotting with antibodies against GFP (Figure 3.1.).

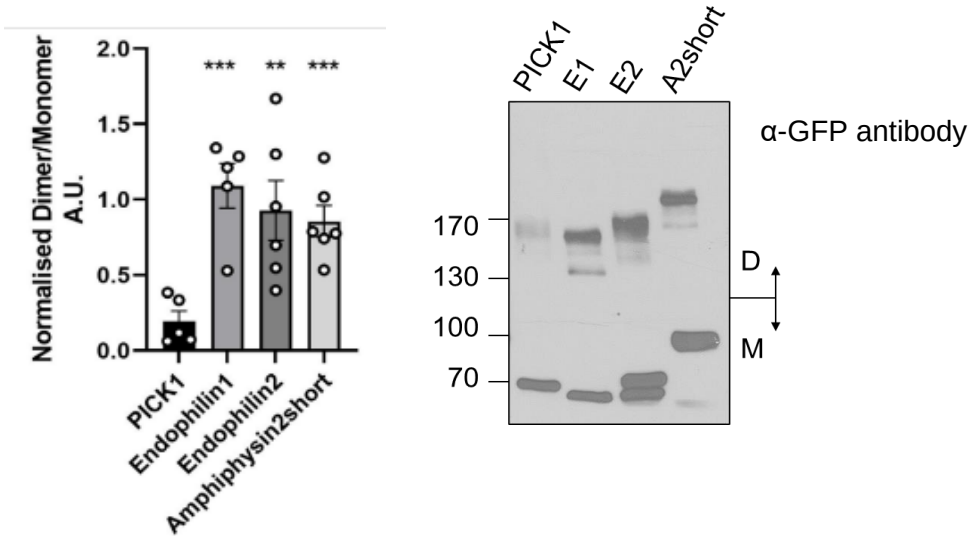

Figure 3.1.: Comparison between basal levels of dimerisation of BAR domain proteins in transfected HEK293 samples. GFP-tagged versions of the endophilin1, endophilin2 and amphiphysin2short were expressed in heterologous HEK293 cells for 24h before 20min incubation with 0.3mM DSS. The reactions were quenched with 50mM Tris for 15mins before lysis with 150mM NaCl/20mM HEPES with 0.5% Triton. Following lysis, proteins were separated by SDS-PAGE and detected by Western blotting with anti-GFP antibody. The representative image shows both monomeric and dimeric protein fractions, with PICK1 showing lower dimerisation compared to the other proteins. Quantification of the ratio between detected dimer:monomer levels shows that endophilin and amphiphysin self-associate approximately five-fold more than PICK1 under basal conditions (N=5-6, multiple t-test, P1 vs E1 $p<0.001$, P1 vs E2 $p<0.01$, P1 vs A2s $p<0.001$. Bonferroni's post-hoc correction applied). Error bars represent +/-SEM. D, dimer; M, monomer.

By analysing the representative blot, it becomes apparent that all four proteins tested were capable of self-association into dimeric forms, with limited or no amounts of higher order oligomers detected. The levels of monomers as well as dimers were measured using ImageJ and the data were normalised by calculating the ratios between the dimeric:monomeric species recorded. The results show that under basal conditions, PICK1 had the lowest amount of dimer being expressed compared to the other members of the BAR domain family which all had comparable levels of dimerisation to each other. The approximately five-fold difference between PICK1 and the other proteins was statistically significant. The other BAR domains chosen for this experiment have well defined roles in membrane curvature generation and it has been shown that dimeric forms of endophilin and amphiphysin are involved in synaptic recycling endocytosis that occurs under basal conditions (Wigge *et al.*, 1997; Pant *et al.*, 2009; Ross *et al.*, 2011; Sundborger *et al.*, 2011). This suggests that PICK1 has the potential for increasing its level of dimerisation which could be inhibited by mechanisms that are alleviated in response to stimulation.

3.3.2. PICK1 dimerisation is upregulated in the presence of calcium

The next logical step was to investigate whether PICK1 dimerisation could be influenced by external factors such as calcium concentration. As discussed in previous chapters, calcium is one the most important small signalling factors within neurons and particularly relevant for the appropriate expression of synaptic plasticity. PICK1 has also been defined as a calcium-sensing protein whereby it is capable of directly binding calcium ions through its acidic regions in a way which affects AMPAR trafficking (Hanley & Henley, 2005; Citri *et al.*, 2010). For these reasons, we hypothesise that calcium could influence the amounts of PICK1 dimer present in cells. In order to investigate this, the expression of PICK1 in HEK293 cell cultures was achieved via transfection and different samples were treated with 3µM ionomycin in the presence of increasing calcium concentrations in order to allow extracellular calcium to enter the cells. After crosslinking with 0.3mM DSS, proteins were again separated based on size through SDS-PAGE and Western blotting with an anti-PICK1 antibody allowed the visualisation of monomer/dimer fractions (Figure 3.2.).

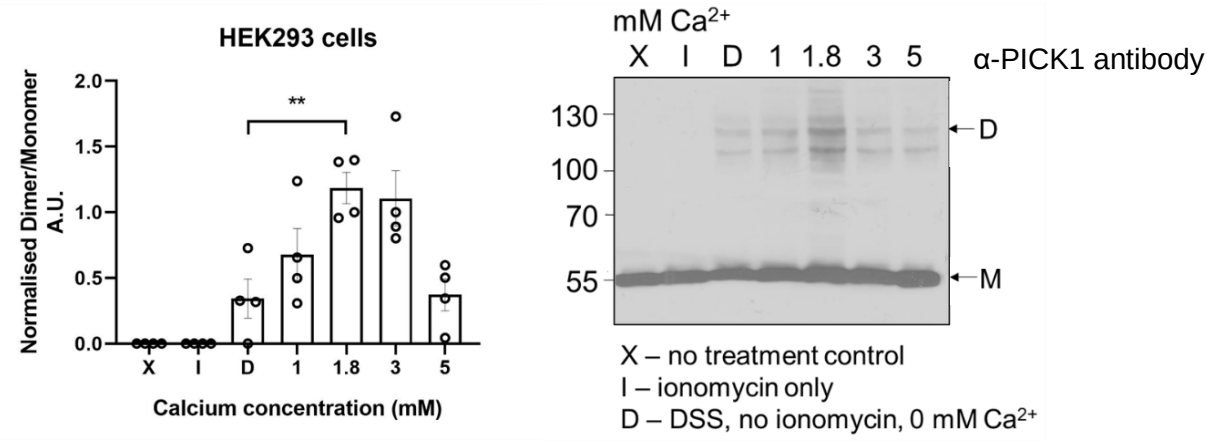

Figure 3.2.: PICK1 dimerisation is upregulated in the presence of calcium in heterologous cells. HEK293 cells were transfected with wild-type PICK1-expressing constructs and were treated with 3µM ionomycin for 5mins followed by 0.3mM DSS for 20mins in the presence of various extracellular calcium concentrations before lysis and SDS-PAGE/Western blotting with an anti-PICK1 antibody. Representative blot shows monomer and dimer fractions are detectable after DSS crosslinking in a concentration-dependent manner. Quantification of the ratio between detected dimer:monomer levels indicates that PICK1 dimerisation shows a biphasic response to calcium concentration. Peak dimerisation occurred between 1.8 and 3mM extracellular calcium, with dimer levels returning to basal levels at 5mM calcium (One-way ANOVA, N=4, F (6, 21) =12.01, $p<0.0001$; Tukey's post-hoc test $p<0.005$). Error bars represent +/-SEM. D, dimer; M, monomer.

The results clearly showed that PICK1 dimerisation was increased in samples that had been treated with ionomycin/DSS in the presence of calcium and that this effect was concentration dependent. The data were analysed by normalising the amount of dimer to how much monomer was expressed, and the results indicate that there is an approximately four-fold difference between basal conditions and 3mM calcium. Interestingly, this increase in dimerisation returns towards basal levels at 5mM extracellular calcium, suggesting that there is a biphasic effect of calcium concentration on PICK1 self-association. Of note, two distinct bands seem to appear in the range where the PICK1 dimer is expected. The dimer fraction normally runs as a smeared band supposedly because of slightly different DSS crosslinking conformations. In this case, one of the bands could represent PICK1 crosslinked with a smaller molecule in the same calcium-sensitive manner as dimerisation, but because the calcium effect is identical for both bands, it is also possible that the smaller band represents PICK1 crosslinked with partially degraded PICK1. Peak dimer levels occur

between 1.8 and 3mM calcium, however it is important to clarify that this refers to the extracellular calcium concentration and does not necessarily imply that equilibration of intracellular calcium concentration is reached within cells. However, it can be reasonably concluded that calcium influx into the cell determines the extent of PICK1 self-association, either as a direct consequence of altering local, subcellular calcium concentrations or indirectly through calcium signalling mediated by calcium-sensing enzymes. Overall, these results suggest that PICK1 is capable of reaching relative dimerisation levels similar to those described above with the other BAR domain proteins (3.3.1.) and that this increase in dimer levels is dependent on intracellular calcium influx.

3.3.3. Other BAR domain-containing proteins are not sensitive to calcium induced dimerisation

Another important question which arose was whether any other BAR domain-containing proteins showed the same effect of upregulated dimerisation in response to calcium stimulation. As such, various BAR domain proteins were tested in the same ionomycin/DSS crosslinking protocol in the absence or presence of calcium as previously used for PICK1 (Figure 3.3.).

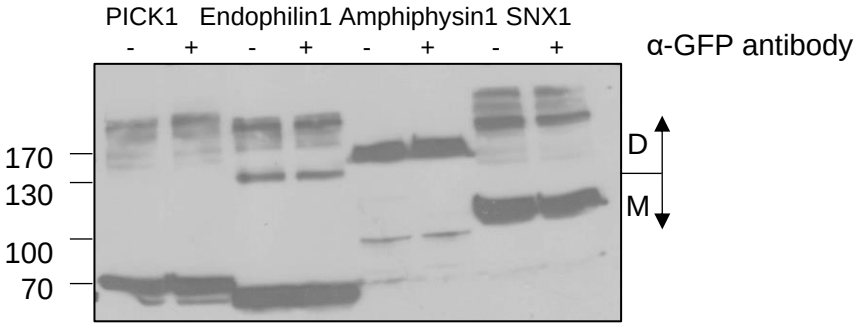

Figure 3.3.: Other BAR domain-containing proteins are not sensitive to calcium-induced dimerisation. Representative blots obtained from HEK293 cellular lysates after 24h expression of GFP-tagged PICK1, endophilin1, amphiphysin1 and SNX1. The samples were incubated either under no calcium conditions (-) or with 1.8mM calcium (+) in the presence of 3µM ionomycin for 5min before being crosslinked for 20 minutes with 0.3mM DSS. PICK1 shows a slight increase in its dimer:monomer ratio as compared to the other BAR domain-containing proteins. D, dimer; M, monomer.

Plasmids containing several different GFP-tagged versions of representative BAR domain containing-proteins were obtained as gifts in order to investigate whether calcium stimulation would also promote increased dimerisation in them. From the image above, it can be noted that only PICK1 shows a slight increase in the dimer levels present when the samples were incubated with the 1.8mM calcium buffer as compared to the negative controls. The various proteins have different molecular weights and for ease of visualisation the dimer is delimitated from the monomer by arrows pointing to their corresponding fraction (D or M). Endophilin has the closest molecular weight to PICK1, with GFP-endophilin1 monomers running at around 70kDa, while the dimer is separated close to the 170kDa band, just below PICK1. The GFP-amphiphysin1 monomer runs just below the 100kDa marker, however the only other fraction which appears is at around 170kDa which would be slightly lower than expected for a dimer. GFP-SNX1 monomer running just above the 100kDa marker is crosslinked into the dimer seen just above the 170kDa band. These results suggest that the ability of PICK1 to upregulate dimerisation in response to calcium stimulation is specific to this protein and is not a general property of the BAR domain.

3.3.4. The isolated PICK1 BAR domain does not show increased dimerisation after extracellular calcium stimulation

The next question that I wanted to address was whether the effect of calcium on PICK1 self-association was mediated through the BAR domain itself or involved any of the other structural components discussed in Chapter 1. To this extent, GFP-tagged versions of WT-PICK1 or the isolated PICK1 BAR domain were expressed in HEK293 cells and the same crosslinking/western blot protocol from before was followed (Figure 3.4.). Interestingly, the self-association of the BAR domain did not show the same calcium-dependent effect as observed for the full-length protein. Instead, when the isolated BAR domain is expressed it appears to have a higher dimer:monomer ratio than WT-PICK1. This is clearly noticeable when comparing the amount of dimer present in the absence of calcium for the two protein constructs. Moreover, the dimerisation levels of the isolated BAR domain show how truncation of full-length

PICK1 results in the loss of its ability to be upregulated in response to increased calcium concentration.

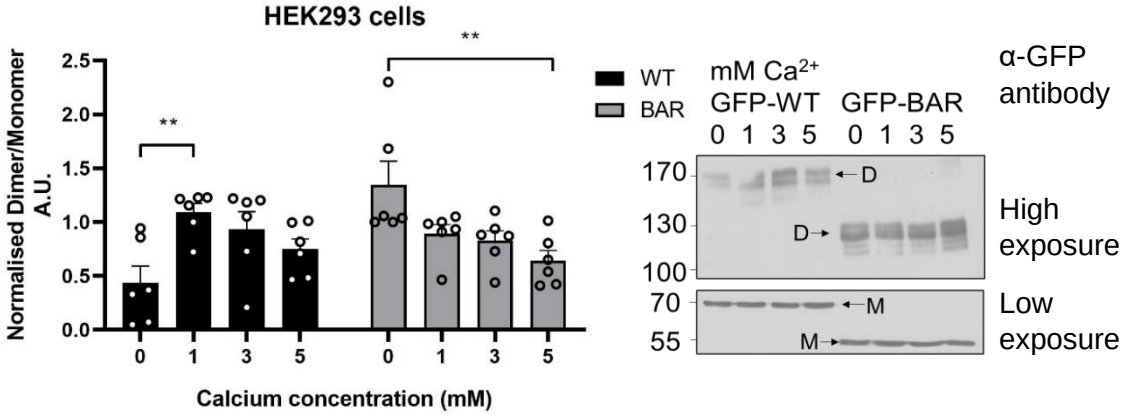

Figure 3.4.: The isolated PICK1 BAR domain does not show increased dimerisation after extracellular calcium stimulation. HEK293 cells were transfected to induce expression of either WT-PICK1 or the isolated PICK1 BAR domain as GFP-tagged constructs. Following 24h expression, the samples were subjected to 3µM ionomycin for 5mins followed by 0.3mM DSS incubation for 20mins in the presence of a range of extracellular calcium concentrations before SDS-PAGE and anti-GFP immunoblotting. Representative blot shows that WT-PICK1 dimerisation follows a concentration-dependent response, whereas the BAR domain dimer levels are elevated even in the absence of calcium. Quantification of the ratio between dimer:monomer fractions reveals that there is a statistically significant calcium-dependent increase in WT-PICK1, whereas the opposite effect is observed for the isolated BAR domain (Two-way ANOVA, N=6, $F(3, 40) = 7.848$, $p<0.001$; Tukey post-hoc tests, $p<0.01$). Error bars represent +/-SEM. M, monomer; D, dimer.

Surprisingly, there is a significant decrease in the dimer levels of the BAR domain as a consequence of calcium addition. One possible explanation for this could be that higher calcium concentrations have an inhibitory effect on the PICK1 BAR domain similar to that observed for the full-length protein, but because peak dimerisation occurs even in the absence of calcium the reduction in dimers can be observed earlier. Overall, these results suggest that the PICK1 BAR domain readily dimerises when expressed in HEK293 cells regardless of the calcium concentration present within the cell. This further shows that the other PICK1 regions are involved in accommodating the protein response to calcium and the two most plausible candidates are the N- and C-terminal acidic regions which previous work carried out in our laboratory has shown to directly bind calcium and regulate other aspects of PICK1 function (Hanley & Henley, 2005; Rajgor *et al.*, 2017).

3.3.5. The dimerisation of purified PICK1 in response to calcium is increased for WT but not for NT-lacking PICK1

In order to further decipher the mechanisms that regulate PICK1 self-association in response to calcium, I decided to adapt the DSS crosslinking protocol for use with purified protein samples. By performing this assay with purified WT-PICK1 and a mutant which lacks the acidic stretch of amino acids present at the N-terminus of the protein (ΔNT-PICK1), two distinct questions can be answered: whether PICK1 calcium-dependent dimerisation occurs through direct PICK1-calcium interactions as opposed to being mediated by cellular regulatory mechanisms such as phosphorylation, and whether this is facilitated by the N-terminal sequence of the protein (Figure 3.5.).

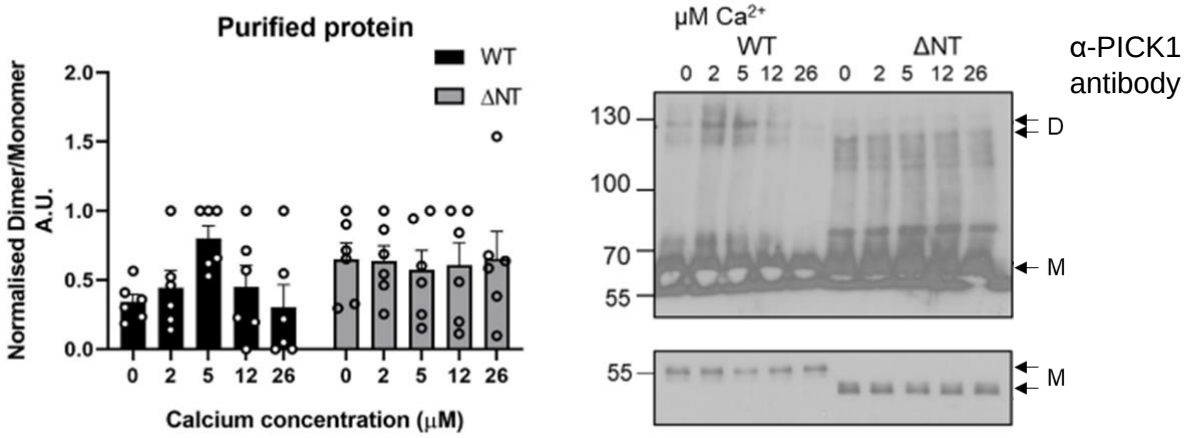

Figure 3.5.: WT-PICK1 dimerisation is upregulated in response to calcium stimulation, while the ΔNT-PICK1 mutant is not. 100nM purified his_6WT-PICK1 or his_6ΔNT-PICK1 protein samples were incubated with 10μM DSS in the presence of various calcium concentrations for 20mins and the reaction was quenched with 50mM Tris for 15mins before being separated based on size through SDS-PAGE and detected with anti-PICK1 antibodies. The representative blot shows dimeric and monomeric fractions which were quantified in order to obtain dimer:monomer ratios for comparison. While WT-PICK1 shows an effect of calcium concentration on the levels of dimerisation, the ΔNT mutant remains unaffected by the addition of calcium. The monomer blot represents a lower exposure of the top blot. N=6 repeated experiments. Error bars represent +/-SEM.

The results showed that WT-PICK1 maintained its calcium-induced dimerisation properties in the new assay and levels of detectable dimer increased in a concentration-dependent manner, as previously observed with cellular samples.

When the mutant was tested, however, there was no significant change between the different calcium conditions and the amount of dimer present. Additionally, the amount of dimer observed throughout the calcium range was comparable to the levels of dimerisation achieved in the presence of calcium for WT-PICK1 self-association. Two-way ANOVA statistical analysis was carried out and the results were statistically significant in terms of differences between the WT and mutant in response to calcium stimulation ($F(4, 50) = 2.899$, $p<0.05$), however Bonferroni's post-hoc analysis of the differences between the WT zero calcium and 5μM condition revealed a p-value of 0.10. I believe that one more repeat of this experiment would be sufficient to achieve statistical significance between these two groups as well, but unfortunately due to time constraints I was unable to achieve this. Nevertheless, this demonstrates that calcium can regulate PICK1 dimerisation directly, without necessarily activating an intermediate calcium-sensitive signalling protein as a signal transducer. In addition, this experiment also provides evidence for the role of the N-terminal acidic region of PICK1 in the response to calcium, such that deletion of this region mimics and occludes the presence of calcium, therefore suggesting an inhibitory regulatory mechanism.

3.3.6. The PICK1 dimer interface associates strongly and is not affected by mutations that disrupt hydrophobic interactions

One of the aims of this chapter was to determine whether the PICK1 BAR domain interface could be disrupted through single point mutations. In order to fully investigate the importance of calcium-sensitive BAR domain-mediated dimerisation, a mutant is required which maintains its monomeric folding but is unable to dimerise for loss of function experiments. The best way to identify prospective residues is to analyse the BAR domain region of PICK1 for hydrophobic amino acid residues such as phenylalanine. In order to gain insight into the potential consequences of disrupting the hydrophobic interactions surrounding these residues, I collaborated with Dr Deborah Shoemark who specialises in computational modelling of protein-protein interactions. The molecular dynamics simulation came up with three prospective phenylalanine residues present within the BAR domain which would contribute substantially to the hydrophobic interface due to their bulky, non-polar side chains.

Because of the antiparallel assembly of the PICK1 dimer, residues 187 and 210 are located in the proximity of residue 337 from the partner molecule. In order to achieve maximal disruption, it was suggested that the phenylalanine residues should be replaced with positively charged lysines to introduce charge in an otherwise hydrophobic region (Figure 3.6.).

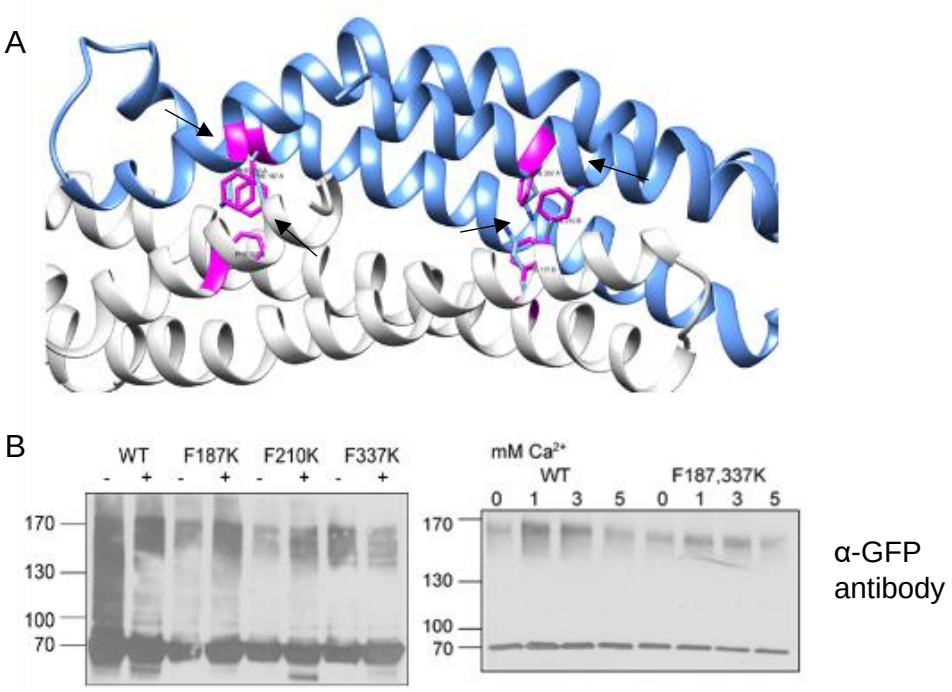

Figure 3.6.: Mutations targeting the hydrophobic PICK1 dimer interface do not impair dimer formation. (A) Molecular modelling showing the dimerised BAR domains of two PICK1 molecules (blue and white). Phenylalanine residues that are packed tightly within the hydrophobic interface are represented in pink. Of note is the location of residue F337 in proximity to the F187 and F210 residues belonging to the partnering PICK1 molecule. Dynamic simulations suggest that mutating these residues to positively charged lysine will disrupt the assembly of the PICK1 dimer. (B) HEK293 cells expressing GFP-tagged versions of WT PICK1 and the three phenylalanine mutants F187K, F210K, F337K as well as the F187,210K double mutant were treated with 3µM ionomycin and 0.3mM DSS before SDS-PAGE and Western blotting with anti-GFP antibody. Representative images showing the testing of the different phenylalanine mutants for their dimerisation capacity using the previous ionomycin/DSS protocol either in the presence of 3mM (+) or lack of calcium (-). The three individual mutations (F187K, F210K and F337K) as well as the F187,337K double mutant show a similar pattern of dimerisation as observed with the WT-PICK1 protein, regardless of calcium concentration.

The mutants that were generated are the single mutants F187K, F210K and F337K, as well as the double mutant F187,337K. These were cloned and expressed as GFP-tagged versions in HEK293 cells before being treated with the same DSS crosslinking and Western blot detection protocol as before. Surprisingly, the results showed that neither of the individual mutations were sufficient to disrupt dimer formation for the full-length protein. Additionally, the double mutant was also unsuccessful and resulted in comparable levels of dimerisation to the WT, while the effect of calcium was also maintained in a similar manner. These results suggest that the PICK1 dimer interface is a strong interaction that is not easily disrupted by single point mutations which affect its hydrophobicity.

3.4. Discussion

Over the course of this chapter, I have described the biochemical investigation into the dimerisation of PICK1, showing how it compares to other BAR domain-containing proteins and how calcium is an important factor which upregulates PICK1 dimerisation in the case of purified protein as well as in a cellular environment. Taken together, the results comprise strong evidence that supports the hypothesis that the cellular function of PICK1 is regulated through intracellular calcium influx in a direct manner.

3.4.1. PICK1 basal dimerisation levels are low compared to other BAR domain proteins

Firstly, by comparing basal levels of dimerisation between PICK1 and other members of the BAR domain family it becomes apparent that PICK1 differs significantly from the rest. Endophilin and amphiphysin are important for the coordination of clathrin-mediated endocytosis which supports the internalisation of surface expressed proteins in response to stimulation or as part of constitutive recycling pathways (Haucke & Kozlov, 2018; Nishimura *et al.*, 2018). For example, dimeric endophilin1 has been shown to activate the GTPase activity of dynamin (Ross *et al.*, 2011), while the interaction between amphiphysin and dynamin underlies the constitutive endocytosis of $GABA_A$ receptors (Kittler *et al.*, 2000). This would suggest that they are expressed at their maximum level of dimerisation and it is worth noting that dimer:monomer levels

for endophilin1, endophilin2 and the short variant of amphiphysin2 are comparable to one another. Indeed, there has been no evidence to support a mechanism for upregulated dimerisation for these proteins and there is evidence from our research that calcium concentration has no effect on the dimerisation levels of endophilin1, amphiphysin1 and SNX1. On the other hand, the majority of PICK1 is present in its monomeric form when expressed in HEK293 cells, with a five-fold reduction between the amount of dimer detected in cellular lysates as compared to the other BAR domain proteins. This result suggests either that PICK1 is a less efficiently dimerising protein and functions mainly as a monomer, or that PICK1 is maintained in a monomeric state in order to allow for upregulation of dimerisation in response to certain signals. The first option would be in contradiction with the established literature on how BAR domains function, which suggests that the curvature sensing and generating properties of the BAR domain are intrinsically connected to the radius of the BAR domain concave surface that is formed as a consequence of dimerisation (Peter *et al.*, 2004). Indeed, there are a several papers that demonstrate that BAR domain dimerisation is a prerequisite for membrane remodelling and appropriate protein-protein interactions (Wigge *et al.*, 1997; Gallop *et al.*, 2006; Ross *et al.*, 2011; van Weering *et al.*, 2012). The second option offers an intriguing possibility that PICK1 BAR domain dimerisation could be dynamic and could serve as a regulatory mechanism allowing for the integration of external signalling into a cellular outcome. This hypothesis has not been explored in the literature because most studies assume steady-state PICK1 dimer levels occur similar to other members of the BAR domain family. For these reasons, the results presented in the rest of this chapter represent an exciting discovery describing a newly identified mechanism for the regulation of BAR domain function in response to external factors or cellular activation.

3.4.2. PICK1 dimerisation is upregulated in response to intracellular calcium influx

The finding that PICK1 dimerisation increases with calcium concentration when expressed in HEK293 cells has implications for the neuronal function of the protein. As discussed in detail in chapter 1, calcium is an essential molecule for neuronal communication, not only in terms of contributing to the depolarisation of the cell due

to its large positive charge, but also because it serves as a co-factor for a number of calcium sensing enzymes such as kinases and phosphatases which in turn activate further downstream effects. PICK1 has already been established as a calcium binding protein through its N- and C-terminal acidic regions and more importantly it has been shown that the presence of calcium is able to regulate its cellular function. Calcium binding to the N-terminal region underlies NMDA-induced AMPAR trafficking (Hanley & Henley, 2005; Citri *et al.*, 2010), whereas calcium binding to the C-terminal region results in reduced interaction with Ago2 (Rajgor *et al.*, 2017). In this study, I have shown that PICK1 dimerisation is facilitated after the addition of calcium in a biphasic manner, such that optimal PICK1 dimerisation is achieved between 1.8 and 3mM calcium and returns towards basal levels at 5mM calcium. This concentration refers to the extracellular concentration present within the buffer and it would be difficult to correlate this to a potential intracellular calcium concentration that is achieved after membrane permeabilisation with ionomycin. However, it indicates a clear relationship between the intracellular influx of calcium and the enhanced formation of PICK1 dimers. Also interesting to note is the low presence of oligomeric species or lack thereof which could suggest that dimeric PICK1 is the main species being formed at least initially and that further self-association into higher order oligomers required either a more prolonged exposure to the calcium signal than the five minute incubation period used in this experiment or another signal. Because this experiment occurs in cells, the effect of calcium on dimerisation could be either mediated through direct binding to PICK1 or by other calcium sensitive molecules. For example, calcium sensing proteins such as calmodulin and PKCα are classical sensors of calcium concentrations within neuronal microenvironments, as well as integrating spatial and temporal factors into downstream signalling (Zhang *et al.*, 2012; Jin *et al.*, 2019). Plausible regulatory mechanisms which emerged at this stage were either changes in conformation directly caused by the binding of calcium to PICK1 or through post-translational modifications such as phosphorylation of specific residues which in turn affect PICK1 dimerisation. Nevertheless, the fact that calcium dimer levels are only favoured within a particular calcium concentration range is very interesting and it could provide a potential mechanism in which PICK1 could be one of the proteins that orchestrate the switch from LTP to LTD. This is in line with previous studies which showed that PICK1 is involved in both types of synaptic plasticity (Sossa *et al.*, 2006; Terashima *et al.*, 2008).

3.4.3. The isolated PICK1 BAR domain does not increase dimerisation after calcium stimulation

The next steps in our investigation focused on determining which regions of PICK1 are important for calcium dependent dimerisation. It is well known that one of properties of the BAR domain is self-association and this has been described in detail in chapter 1. In the case of PICK1, it is also known that other domains can influence the activity of the protein, such as the example of the N-terminal acidic region regulating AMPAR trafficking (Hanley & Henley, 2005) or the C-terminal acidic region having an inhibitory effect on PICK1 lipid binding (Jin *et al.*, 2006). During the investigation into the calcium sensitive dimerisation of the PICK1 BAR domain it was revealed that unlike WT-PICK1, the dimers formed by the isolated BAR domain were not upregulated with the addition of calcium although they still dimerised strongly. These findings suggest that indeed the BAR domain of PICK1 has the capacity to dimerise more efficiently, yet a larger proportion of the full-length protein is a monomeric in the absence of calcium. Therefore, one or more of the other regions in PICK1 are involved in the inhibition of PICK1 dimerisation and this inhibition is alleviated by their deletion which mimics and occludes the addition of calcium. Indeed, previous studies have been able to show that both the N- and C-terminal acidic regions of PICK1 can bind calcium and the deletion of both acidic regions still results in low levels of calcium binding (Hanley & Henley, 2005), which suggests that a potential third calcium binding site exists within the structure of PICK1.

3.4.4. The PICK1 N-terminal acidic region regulates of calcium-sensitive dimerisation

For further investigating the potential inhibitory structures for PICK1 dimerisation, I decided to use a PICK1 truncation which eliminated the N-terminal acidic region of the protein called ΔNT-PICK1 (Hanley & Henley, 2005). As previously mentioned, this region has been characterised for directly binding calcium and modulating the binding of PICK1 to GluA2 in a calcium sensitive manner. In order to also address whether the effect of calcium on dimerisation is direct or mediated through other proteins, I used purified WT- and ΔNT-PICK1 samples in a similar DSS crosslinking protocol but using a calcium concentration range that is physiologically relevant for the intracellular

environment. Whereas WT-PICK1 maintained a biphasic response to increasing calcium with regards to its dimer:monomer ratio, the ΔNT mutant on the other hand did not show any calcium sensitivity. The deletion of the acidic N-terminal region mimics and occludes the addition of calcium, eliminating the capacity for calcium sensitive upregulation of dimerisation similar to what is observed for the isolated BAR domain. This suggests that the N-terminus of the PICK1 protein acts as an inhibitory structure for the dimerisation of the full-length protein, and this inhibition is alleviated in the presence of calcium. It is interesting to note however, that in the absence of calcium the levels of ΔNT-PICK1 dimers relative to the WT are not as high as compared to the WT-relative isolated BAR domain levels. This implies that there are other regions within PICK1 which contribute to the regulation of dimerisation. Indeed, there is some evidence from our laboratory that deletion of the C-terminal acidic region also has a similar effect on dimerisation as the ΔNT deletion. Taken together, these results point towards a direct role for both terminal acidic regions for the translation of calcium signalling into PICK1 dimerisation levels.

3.4.5. Point mutations that disrupt the hydrophobicity of the BAR domain interface do not block dimerisation

At this point in the investigation, it became apparent that in order to understand the functional role of PICK1 dimerisation, a mutant must be generated that was impaired in calcium-dependent dimerisation yet maintained structural integrity and other protein-protein interactions in its monomeric form. To date, no such mutant has been described for PICK1 or any other BAR domain proteins so in collaboration with Dr Deborah Shoemark, who was able to run molecular dynamics simulations in order to narrow down potential residues that are essential for dimerisation, I was able to identify three potential residues located within the BAR domain. The F187, F210 and F337 amino acids were highlighted because they contain large, hydrophobic side chains which are traditionally located within hydrophobic pockets of proteins. The suggested mutation for maximal disruption to the dimeric interface was F->K because the introduction of a positively charged side chain massively disrupted the assembly of the dimer. Additionally, it was suggested that the three mutations would have an additive effect such that the triple mutant would only exist in a monomeric form, whereas the

F187,337K double mutation would have the largest impact on dimerisation due to these residues coming together on opposite sides of the dimer interface. However, the outcome suggested through molecular modelling was not replicated experimentally. Instead, the three single mutants were found to dimerise just as efficiently as the WT protein, as well as the F187,337K double mutant which also maintained the upregulation effect of calcium concentration on its dimerisation. This suggested that PICK1 dimer formation is mediated through strong hydrophobic interactions which are not easily disrupted. Because the double mutant that was most susceptible to disruption was unaffected, it appears that F->K mutations are not appropriate for preventing PICK1 dimerisation. One possible explanation could be that other hydrophobic interactions in proximity are strong enough to compensate for the mutations, however it is also necessary to mention that lysine groups participate in the crosslinking reaction and perhaps had the unintended effect of improving dimerisation.

Chapter 4

Investigating the dimerisation of PICK1 in neurons using FLIM-FRET microscopy

4.1. Introduction

4.1.1. The role of PICK1 in neurons during synaptic plasticity

Soon after it was first identified in the late 90s due to its PDZ-domain mediated interaction with PKCα (Staudinger *et al.*, 1995; Staudinger *et al.*, 1997), it became apparent that PICK1 is a protein that is relevant for neuronal function (Perez *et al.*, 2001; Hanley & Henley, 2005; Nakamura *et al.*, 2011). Importantly, it was established that the PICK1 PDZ domain can also recognise and bind the short C-terminal tails of AMPAR subunits GluA1, GluA2 and GluA4c which share the -SVKI/-SIKI PDZ binding motif (Xia *et al.*, 1999). Furthermore, PICK1 expression is enriched in synaptosomes and it colocalises with GluA2/3 at excitatory synapses in neurons, while co-expression of PICK1 and GluA2 in heterologous cells leads to the clustering of the AMPAR subunit indicating a role for PICK1 in the subcellular targeting of its interaction partners (Xia *et al.*, 1999). Because PICK1 only contains one PDZ domain, it was suggested that its ability to co-localise multiple PDZ motif-containing proteins (Perez *et al.*, 2001; Anggono *et al.*, 2013) was supported through the BAR domain which functions as a dimerisation module in addition to recognising and binding lipid membranes (Jin *et al.*, 2006; Karlsen *et al.*, 2015). Therefore, it is hypothesised that PICK1 self-association into dimers and into further order oligomers allows the protein to orchestrate cellular processes that require the precise subcellular targeting of kinases such as PKCα in the proximity of GluA2 AMPAR subtypes expressed at the surface of dendritic spines (Perez *et al.*, 2001).

Indeed, there is substantial evidence to support a dynamic role for PICK1 in response to neuronal activation. Firstly, disrupting the interaction between PICK1 and GluA2 with small interfering peptides resulted in the inhibition of LTD in hippocampal neurons in a manner which is dependent upon the activation of NMDARs (Terashima *et al.*, 2004). Secondly, PICK1 was shown to participate in the internalisation of GluA2-containing AMPARs from the synapse following the targeting of activated PKCα and phosphorylation of S880 on GluA2 (Perez *et al.*, 2001). Moreover, the disassociation of PICK1 from GluA2-containing endosomes can also promote the surface recycling of internalised AMPARs under basal conditions as well as in response to neuronal activity via extrasynaptic regions adjacent to the PSD (Gardner *et al.*, 2005; Sossa *et*

al., 2006; Jaafari *et al.*, 2012). Taken together, these studies suggest that PICK1 plays a complex role in the trafficking of AMPARs particularly during to NMDAR-mediated synaptic plasticity but also under basal conditions through constitutive recycling. As such, it is anticipated that PICK1 performs most of its cellular function in the presence of membranes which either form the neuronal cell surface or have been internalised into an endosomal pool of vesicles. In addition, there is evidence that suggests that the lipid binding capacity of PICK1 is essential for its ability to form clusters with GluA2 and that this is facilitated through the PICK1 BAR domain (Jin *et al.*, 2006; Lin & Huganir, 2007). Traditionally, BAR domain-containing proteins are believed to readily dimerise in solution as the minimal requirement for a fully functional BAR domain is dimerisation (Peter *et al.*, 2004). This has also been confirmed for PICK1 through SAXS studies which were used to determine the conformation of the full length PICK1 dimer which assembles into an antiparallel crescent with the two PDZ domains on each side of the concave membrane binding surface (Karlsen *et al.*, 2015; Madasu *et al.*, 2015). However, there have not been any investigations characterising PICK1 dimerisation within a cellular environment. For this reason, I decided to use FLIM-FRET, an imaging technique which can be applied to live cells in order to study the extent of PICK1 dimerisation in neurons.

4.1.2. Principles of FRET imaging

Förster resonance energy transfer (FRET) is a physical process first described in 1946 which refers to the non-radiative energy transfer which occurs between two or more light-sensitive molecules (Förster, 2012). The principle behind FRET requires the excitation of a donor molecule before this energy can be transferred to a second acceptor molecule provided there is sufficient spectral overlap between the emission and absorption spectra of the two chromophores and that their spatial orientation can allow dipole-dipole coupling of the two molecules. Because the efficiency of FRET is dependent upon the inverse of the sixth power of the distance between the donor and acceptor, it is highly sensitive to small intermolecular distances such that a typical distance of 10nm is accepted as the upper limit for FRET to be detectable (Bajar *et al.*, 2016). Indeed, FRET microscopy and its variations are considered the most accurate methodology for detecting protein-protein interactions due to their capacity

to resolve smaller intermolecular distances than colocalization studies, and the suitability of the method to be used with live cellular cultures recommends FRET as the gold standard for detecting direct protein-protein interactions in a relevant cellular environment (Sun *et al.*, 2013).

FLIM-FRET (Fluorescence lifetime imaging) is a variation of FRET microscopy which focuses on the characteristics of the donor molecule. A fluorophore enters an excited state by absorbing a photon; in order to return to the ground state, the molecule can emit the photon in a different wavelength, it can internally transform the energy into heat or it can pass the energy to its molecular environment (Becker, 2012). The amount of time it takes for an excited fluorophore to reach the ground state represents the lifetime decay. For example, the normal GFP lifetime decay amounts to approximately 2400ps. For a homogenous sample of fluorophores, the lifetime decay will be defined by a single exponential function, however when appropriate FRET pairs are co-expressed, several lifetime decays can be subsequently measured depending on the efficiency of FRET. In the case of FLIM, only the fluorescent lifetime decay of the donor is measured and as such the method is less sensitive to inter-channel bleed-through and the relative intensities of the donor/acceptor signals. A reduction in lifetime observed with appropriate fluorescently-tagged proteins as compared to the control is indicative of direct protein-protein interaction.

In order to investigate the dimerisation of PICK1 in a neuronal context, I decided to use FLIM-FRET microscopy on live hippocampal neurons. Previous research suggested that data acquisition by Time-Correlated Single Photon Counting (TCSPC) was sensitive enough to allow detection of FLIM-FRET in live neurons when using small fluorescent dyes as reporters (Duncan *et al.*, 2004; Zheng *et al.*, 2015). Others focused on fluorescently-labelled donor/acceptor protein pairs and found that two-photon-FLIM was appropriate for the detection of FRET signal in live neuronal cultures (Yasuda *et al.*, 2006; Laviv *et al.*, 2020). In particular, a paper describing the quantitative use of an mGFP-sREACh FRET pair for the investigation of actin polymerisation in dendritic spines provided the basis for designing suitable PICK1 FRET constructs (Murakoshi *et al.*, 2008). sREACh is a ‘dark’ variant of YFP which contains mutations that abolish its ability to emit fluorescence when excited, making it an ideal acceptor for mGFP, a monomeric version of eGFP. The spectral map of the

excitation and emission profiles of the mGFP/sREACh fluorophore pair show an almost perfect overlap between mGFP emission and sREACh absorption (Figure 4.1.).

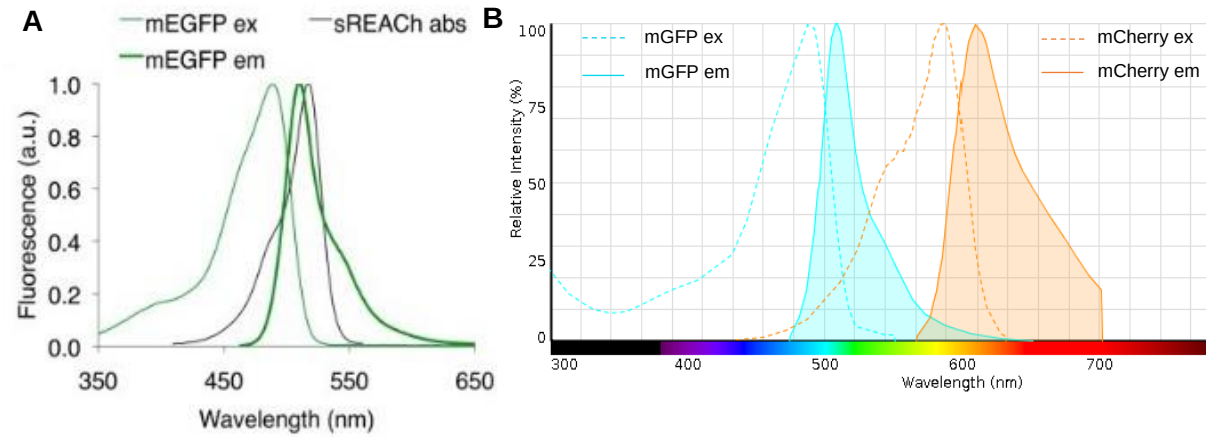

Figure 4.1.: Excitation and emission spectra of FRET donor/acceptor fluorescent protein pairs. (A) The spectral profile of mGFP and sREACh fluorophores shows that sREACh is a 'dark' fluorescent protein meaning it does not emit light, therefore sREACh absorbance is plotted instead. The considerable overlap between mGFP emission and sREACh absorbance is noticeable. Figure taken from (Bajar *et al.*, 2016). (B) The spectral profile of mGFP and mCherry, another classic FRET fluorophore pair, is included for comparison. The emission of mCherry is well separated from mGFP, while still maintaining significant overlap between mGFP emission and mCherry absorption. Figure made with ThermoFisher SpectraViewer.

4.2. Chapter aims

This chapter focuses on the investigation of PICK1 dimerisation in a live neuronal context. As mentioned, FLIM-FRET is the ideal methodology for the detection of protein-protein interactions directly within a cellular environment. Therefore, the main aim of this chapter is to determine whether PICK1 exists in a homodimeric state under basal conditions in neurons and whether the relative state of dimerisation for PICK1 changes during to synaptic plasticity. In order to achieve this, several goals must be fulfilled:

- An appropriate fluorophore pair to be used in the expression of differentially tagged-PICK1 constructs must be validated for the acquisition of FLIM-FRET data from hippocampal neurons;

- The FLIM-FRET method must reliably detect differences between the co-transfection of tagged-PICK1 and the free fluorophore control in HEK293 cells and in neurons;
- Neuronal cultures must be subjected to NMDA stimulation to induce LTD prior to FLIM-FRET data acquisition for assessing changes in relative dimerisation.

4.3. Results

4.3.1. Validation of FLIM imaging in neurons

To ensure that accurate measurements are recorded through FLIM-FRET, I began my investigation with the validation of the methodology in neurons by using a mGFP-sREACh fluorophore pair which has been previously used for FLIM data acquisition within a neuronal environment (Murakoshi *et al.*, 2008; Lee *et al.*, 2009; Ueda & Hayashi, 2013). The plasmids containing both fluorophores in the form of a fusion protein was obtained from Addgene (Plasmid #21947). The mGFP fluorescent protein is a variant of the classical GFP, containing the A206K mutation which abolishes its ability to dimerise (Zacharias *et al.*, 2002), and the sREACh fluorophore is a variant of YFP which has been modified such that it has no emission spectrum and is also monomeric (Murakoshi *et al.*, 2008). These modifications are proposed to have a beneficial effect on the quality of FLIM data collected (Martin *et al.*, 2018), firstly because it eliminates the non-specific interactions between potentially dimerising GFP molecules and secondly because it eliminates any inter-channel bleed-through which would occur from the stimulation of the acceptor molecule.

In order to validate the efficiency of the mGFP-sREACh FLIM-FRET donor-acceptor pair, neurons were transfected 24h prior to imaging with mGFP alone, the mGFP-sREACh fusion protein and co-transfected with mGFP and sREACh (Figure 4.2.). The lifetime decay that was measured with mGFP alone showed the intrinsic post-excitation decay properties of mGFP, while the mGFP-sREACh fusion protein lifetime decay represents the optimal FLIM-FRET signal which can possibly be achieved. The mGFP plus sREACh condition represents an important control which shows that the signal detected is not a consequence of non-specific interactions between the donor and acceptor fluorophores. Indeed, the results showed a strong reduction in lifetime

decay from approximately 2300ps in the case of mGFP to about 1700ps for the mGFP-sREACh fusion protein. Therefore, the maximal transfer of energy which can be recorded in neurons between this pair of fluorophores with an intermolecular distance of 0nm is approximately 600ps. The mGFP plus sREACh control showed little difference to the mGFP only condition indicating a lack of non-specific binding between the pair. This confirms previous reports that mGFP and sREACh are efficient FRET energy transfer partners and suggests that the mGFP-sREACh pair can be used further for FRET signal detection within a neuronal environment.

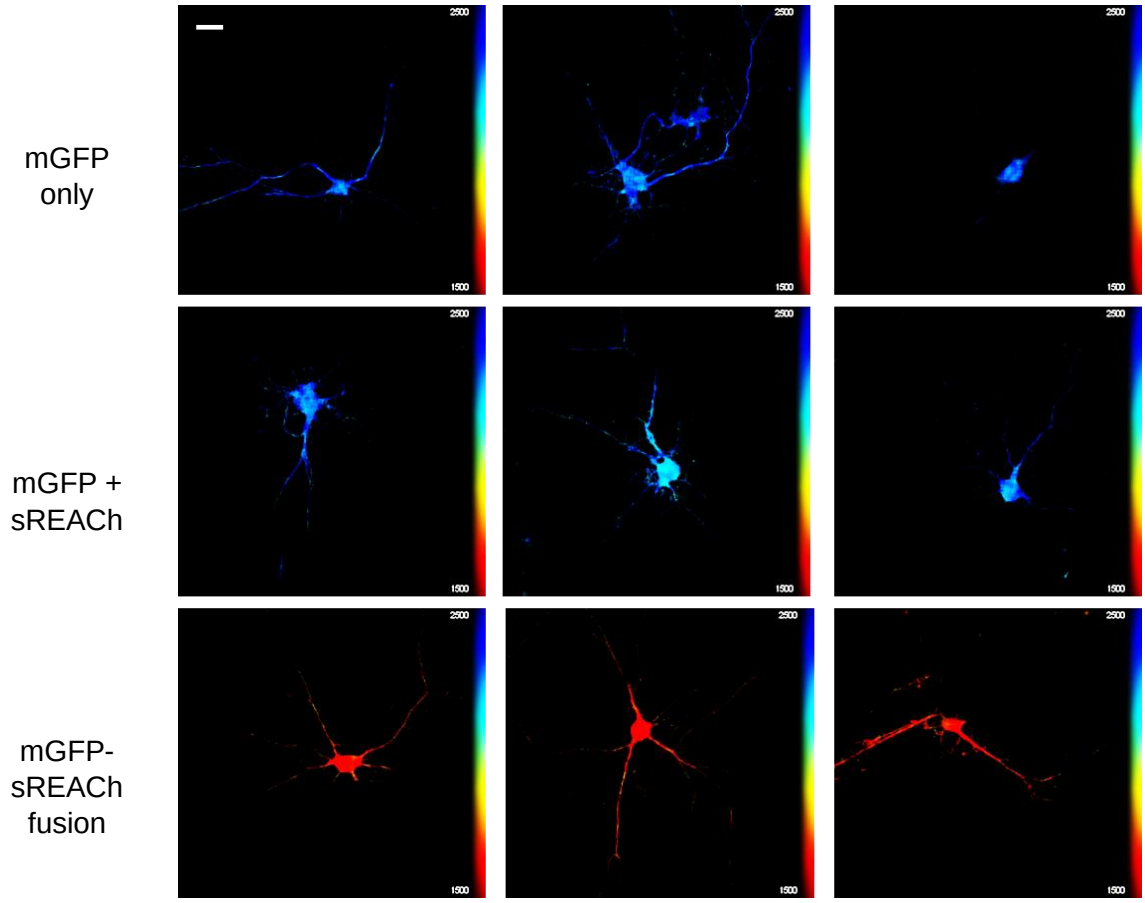

Figure 4.2.: Validation of the mGFP – sREACh fluorophore pair for the acquisition of FLIM-FRET signal in a neuronal intracellular environment. DIV14 neuronal cultures were transfected with vectors expressing mGFP only, mGFP and sREACh separately and the mGFP-sREACh fusion protein. The large reduction in lifetime observed with the fusion protein is indicative that mGFP and sREACh are a suitable donor-acceptor pair for FLIM data acquisition from neurons. Images were acquired in the green detection channel (490-510nm) using the 20x magnification lens. Collected data were fitted using the FLIMfit 5.1.1. software and heatmaps showing lifetime decay were generated. The coloured gradient bar on the right-hand side represents the lifetime of mGFP ranging from 1500ps (red) to 2500ps (blue). Lifetime signal is intensity-adjusted. Scale bar is consistent throughout panels and represents 20µm. Image courtesy of Dr Dominic Alibhai.

4.3.2. FLIM imaging of PICK1-PICK1 interactions using the mGFP-sREACh fluorophore pair in live HEK293 cells and neurons

The next step was the generation of mGFP- and sREACh-tagged versions of PICK1 in pcDNA3.1 through molecular cloning. Further optimisation steps were required for determining the appropriate expression levels of the PICK1-tagged constructs, as well as testing different acquisition settings for establishing a FLIM imaging protocol. Our initial aim was to use the FLIM methodology within a live cellular environment such that the formation of dimers could be observed and quantified in real time. For simplicity, I decided to test the success of tagged-PICK1 FLIM by using live HEK293 cell cultures expressing mGFP alone, mGFP-PICK1 together with sREACh-PICK1, as well as using the co-expression of mGFP-PICK1 with sREACh for the control (Figure 4.3.).

Results showed that when mGFP-PICK1 and sREACh-PICK1 are co-expressed, there is a reduction of approximately 80ps in the lifetime decay of the fluorophore-tagged PICK1 that is significant when compared to the mGFP-PICK1 only control. From the representative images it becomes apparent that the reduction in lifetime decay occurs at particular subcellular locations in the form of red puncta. The images are presented in an intensity-adjusted manner such that differences in local concentration are taken into account when generating the lifetime decay map. The second control condition which contained mGFP-PICK1 and free acceptor showed a small, but not significant decrease in lifetime decay.

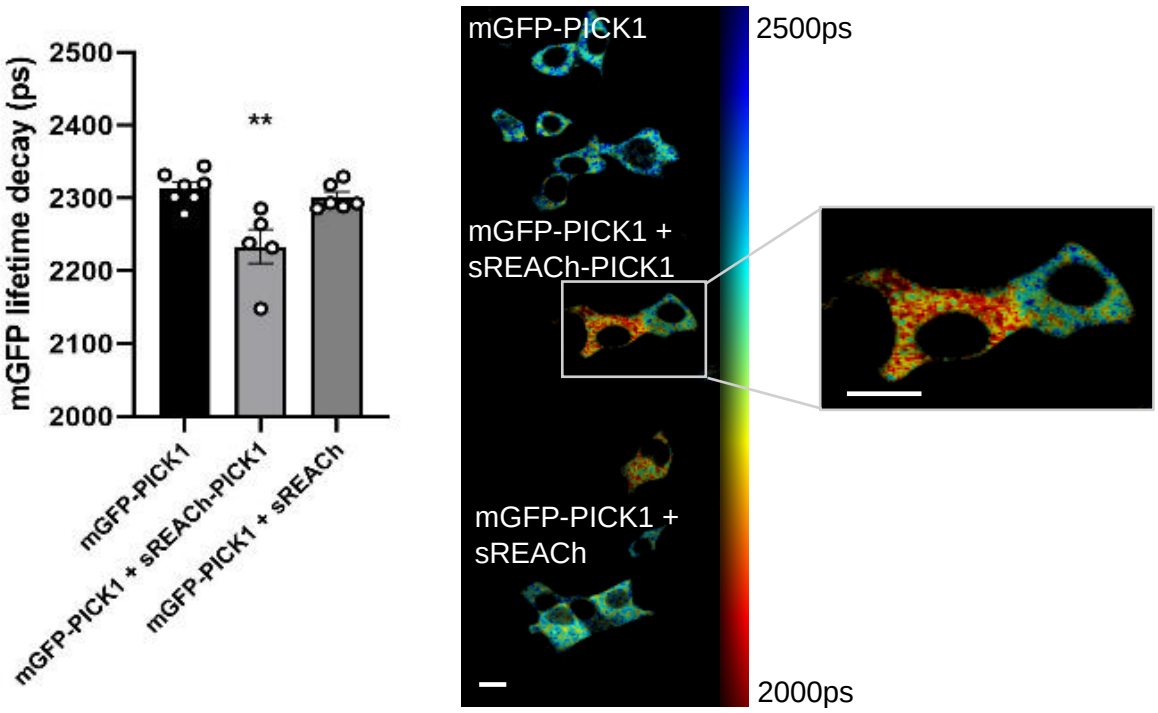

Figure 4.3.: PICK1-PICK1 interaction in live HEK293 cells as observed by FLIM-FRET with the mGFP-sREACh fluorophore pair. Cultures were transfected and allowed to express mGFP-PICK1, mGFP-PICK1 and sREACh-PICK1 or mGFP-PICK1 and free sREACh for 24h before FLIM data were acquired in the green channel (490-510nm) using the 20x magnification lens. mGFP-PICK1 showed a significant reduction in lifetime decay when co-expressed with sREACh-PICK1, consistent with dimerisation (N= 4-6 fields of view, one-way ANOVA, $F(2, 15)= 9.871$, $p<0.01$). Error bars represent +/- SEM. The collected data were fitted using the FLIMfit 5.1.1. software and heatmaps were generated ranging from 2000ps (red) to 2500ps (blue). The magnification in the inset allows for clearer observation of the punctate pattern of lifetime reduction in the dimerisation condition. Lifetime signal is intensity-adjusted and scale bar is consistent between panels at 20µm. **p<0.01

Surprisingly, when the same experimental procedure was undertaken with live neurons, the results were different (Figure 4.4.). There were no differences observed between the mGFP-PICK1 only control and the co-expression of both fluorescently-tagged versions of PICK1, regardless of whether the analysis included the whole neuron or only focused on the neuronal projections. In fact, there was a decline observed in the lifetime decay of the second control, mGFP-PICK1 + sREACh. Together with observations that there is potential bleed-through from the sREACh fluorophore, it was decided that a different FLIM pair be tried.

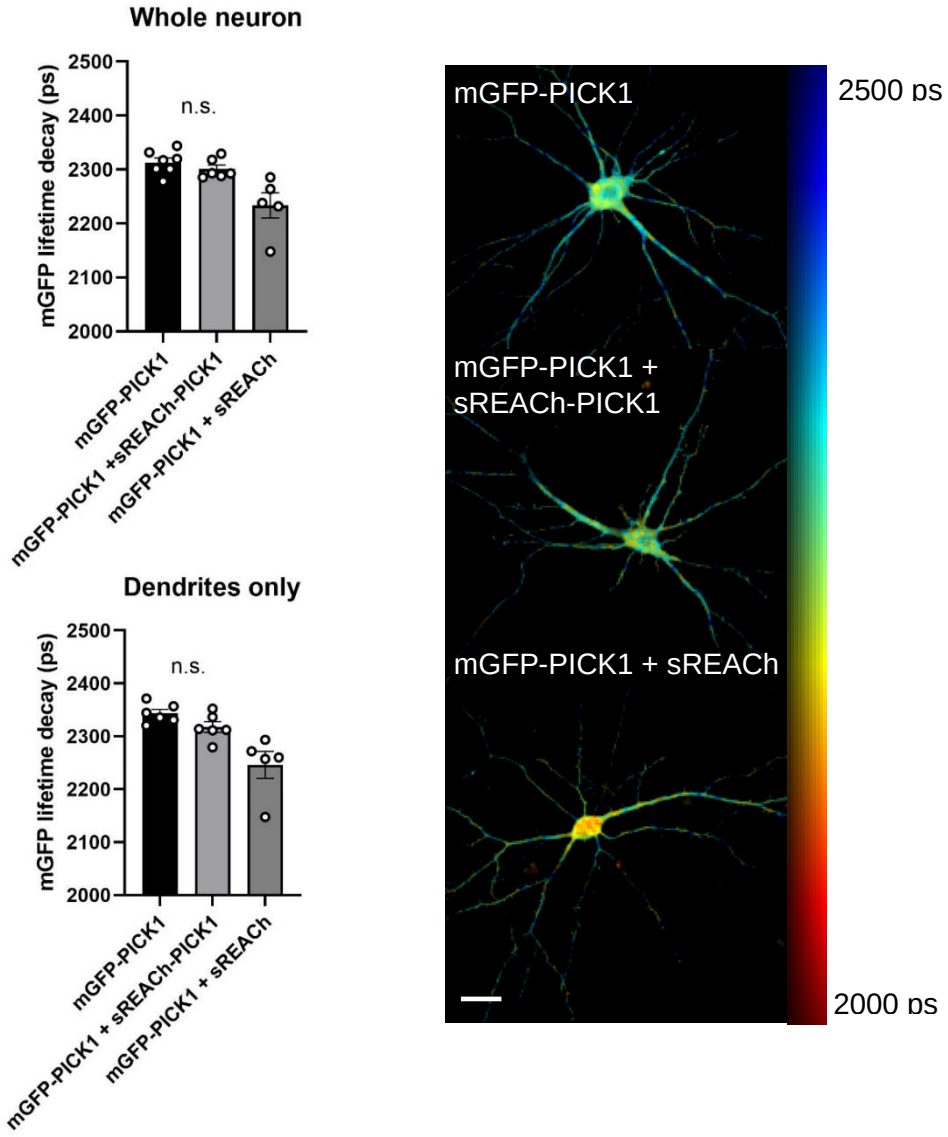

Figure 4.4.: Detection of PICK1-PICK1 interactions in live neurons using the mGFP-sREACh fluorophore pair is not possible. DIV14 neuronal cultures were transfected to induce the expression of mGFP-PICK1, mGFP-PICK1 together with sREACh-PICK1 as well as mGFP-PICK1 with free sREACh. Data were collected 24h later in the green channel (490-510nm) using the 20x magnification lens and were fitted using FLIMfit 5.1.1. software to generate heatmaps corresponding to mGFP lifetime decay on a scale from 2500ps (blue) to 2000ps (red). No significant difference could be observed between the PICK1 double transfection and the mGFP-PICK1 control. Instead, the mGFP-PICK1 and free sREACh control showed a reduction in lifetime decay. Error bars represent +/-SEM. Lifetime signal is intensity-adjusted and scale bar is consistent between panels at 20µm. N= 5-7 fields of view.

4.3.3. FLIM imaging of PICK1-PICK1 interaction using the mGFP-mCherry fluorophore pair in live HEK293 cells and neurons

As discussed in the introduction for this chapter, there are a number of different fluorophore pairs which have been previously used for FLIM-FRET imaging, as long as there is sufficient spectral overlap between the donor emission and acceptor absorption spectra (Bajar *et al.*, 2016; Martin *et al.*, 2018). Due to inefficient live neuronal detection of PICK1 interactions with the previous donor-acceptor pair, as well as signs of spectral bleed-through, I decided to test the mGFP-PICK1 donor against an already existing mCherry-PICK1 construct from our laboratory. The experimental procedure and control conditions were kept the same as before. Interestingly, the lifetime decay measured in live HEK293 cells was improved from 80ps in the previous mGFP-sREACh pair to approximately 100ps in the mGFP-PICK1 + mCherry-PICK1 condition compared to the controls. The second control which expressed mGFP-PICK1 together with free mCherry also showed improvements from before, such that no reduction in lifetime decay could be observed between this condition and mGFP alone (Figure 4.5.). This is an important data quality control step because it suggests that there is no non-specific interaction between mGFP and mCherry. Moreover, the distribution of the regions with the highest decline in FRET signal remained punctate, suggesting again that the PICK1-PICK1 interaction occurs within particular subcellular localisations.

Due to the successful acquisition of better-quality data with the mGFP-mCherry fluorophore pair in live HEK293 cells, I decided to test whether the improvement was reflected in the acquisition of FRET data from live neurons. Surprisingly, there was no difference between the three conditions yet again (Figure 4.6.). There are various possible explanations for the failure to detect PICK1-PICK1 interactions in live neurons, including the fact that PICK1 endogenous expression is higher in neurons than compared to HEK293 cells and therefore might interfere with the formation of the mGFP-PICK1/mCherry-PICK1 FLIM-FRET pairs. Alternatively, PICK1 dimerisation could potentially be differentially regulated depending on cell type with the possibility of a less detectable transient interaction occurring in neurons. Nevertheless, because FLIM-FRET data acquired with the mGFP-mCherry fluorophores showed a more pronounced lifetime reduction in HEK293 cells in comparison to the mGFP-sREACh pair and it was decided to continue using mCherry as an acceptor moving forward.

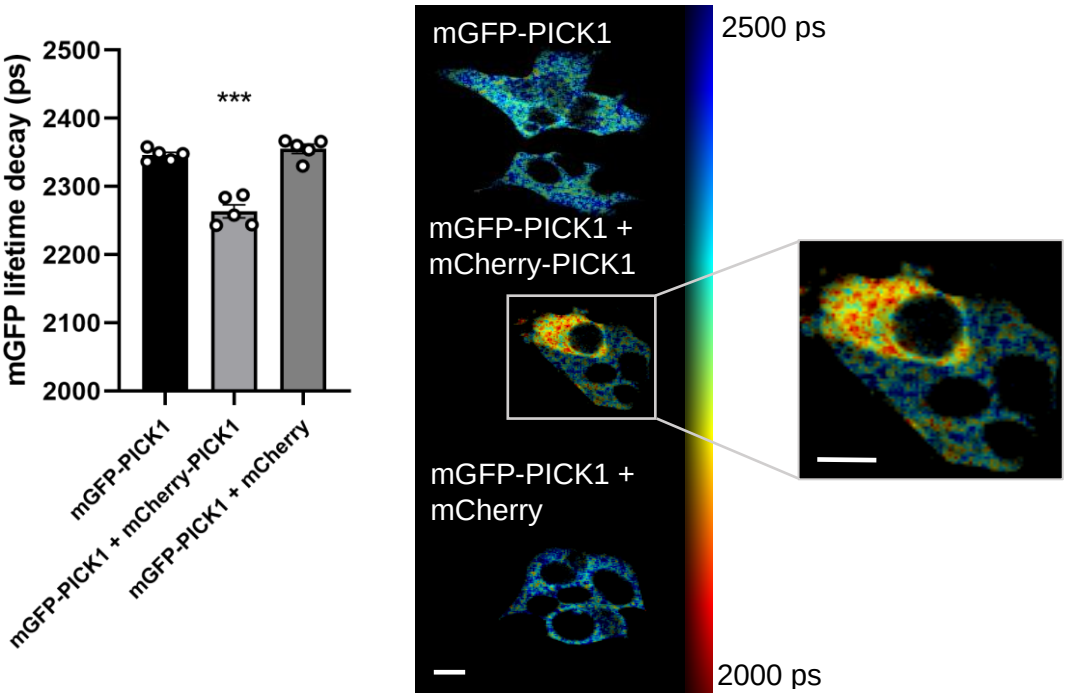

Figure 4.5.: PICK1-PICK1 interaction in live HEK293 cells as observed by FLIM-FRET with the mGFP-mCherry fluorophore pair. Culturess were transfected 24h prior to imaging induce the expression of mGFP-PICK1, mGFP-PICK1 together with mCherry-PICK1 and free mCherry. Data were acquired in the green channel (490-550nm) using the 20x magnification lens before being analysed using the FLIMfit 5.1.1. software. Heatmaps on the scale of 2500ps (blue) to 2000ps (red) were generated to illustrate the lifetime decay of mGFP-PICK1 which was reduced in the presence of mCherry-PICK1 (N=5 fields of view, one-way ANOVA, $F(2, 12)= 50.53$, $p<0.001$). Error bars represent +/-SEM. The magnification in the inset allows for clearer observation of the punctate pattern of lifetime reduction in the dimerisation condition. Lifetime signal is intensity-adjusted and scale bar is consistent between panels at 20µm. ***$p<0.001$.

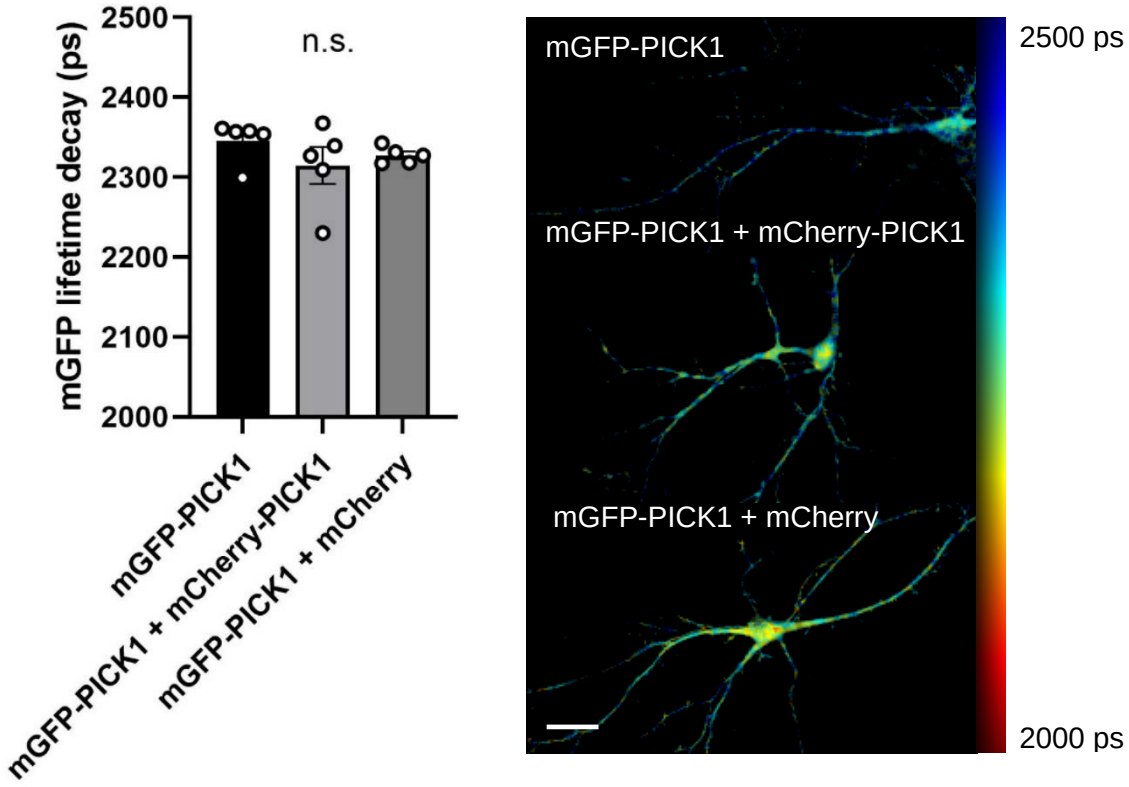

Figure 4.6.: FLIM-FRET measurement of PICK1 dimerisation acquired from live neurons using the mGFP-mCherry fluorophore pair. DIV14 neuronal cultures were transfected to induce the expression of mGFP-PICK1, mGFP-PICK1 together with mCherry-PICK1 as well as mGFP-PICK1 with free mCherry. Data were collected in the green channel (490-550nm) using the 20x magnification lens and fitted using FLIMfit 5.1.1. software to generate heatmaps corresponding to mGFP lifetime decay on a scale from 2500ps (blue) to 2000ps (red). No significant difference could be observed between the mGFP-PICK1 + mCherry-PICK1 condition and the controls. Error bars represent +/-SEM. Lifetime signal is intensity-adjusted and scale bar is consistent between panels at 20µm. N= 5 fields of view.

4.3.4. Calcium-dependent changes in PICK1 dimerisation could potentially be detected by FLIM-FRET imaging

I wanted to investigate whether the effect of calcium on the levels of PICK1 dimerisation which was seen during biochemical experiments in Chapter 3 can be replicated with FLIM-FRET data acquisition. HEK293 cultures were transfected to express mGFP-PICK1 together with mCherry-PICK1 or with free mCherry as a control for 24 hours before being incubated with a range of calcium concentrations in the presence of ionomycin to promote intracellular calcium influx. After the samples were fixed in order to preserve transient interactions, FLIM-FRET imaging was carried out and data was analysed with FLIMfit 5.1.1. software using the same parameters as in previous experiments (Figure 4.7.).

The results suggest that a similar pattern for calcium stimulation can be detected through the measurement of the lifetime decay of mGFP-PICK1, with the highest reductions in lifetime being observed at 3mM extracellular calcium and the signal returning towards basal levels at 5mM calcium. However, the reduction in lifetime decay is statistically non-significant even for the 3mM calcium condition, showing only a 15ps decline as compared to other calcium concentrations, or a non-significant 25ps decline compared to the free mCherry controls. Although the quantification of the data does not produce any statistically significant results, some interesting observations can be made from the representative images. There appears to be a high degree of lifetime variability between the cells that are expressing mGFP-PICK1 and mCherry-PICK1 compared to those in the control conditions. Although similar differences between cells were observed in previous experiments used for the optimisation of the FLIM-FRET methodology, the effect seems more consequential in this dataset. In particular, the zero calcium control for the mGFP-PICK1+mCherry-PICK1 condition contained several cells which were showing very pronounced reductions in lifetime which shifted the average value for the entire image. The correlation between these data and the biochemical assays is important because it indicates that FLIM-FRET imaging is appropriate for the quantification of PICK1 dimerisation and not reporting the association of PICK1 into higher order oligomers. Further experiments must be performed in order to resolve this question.

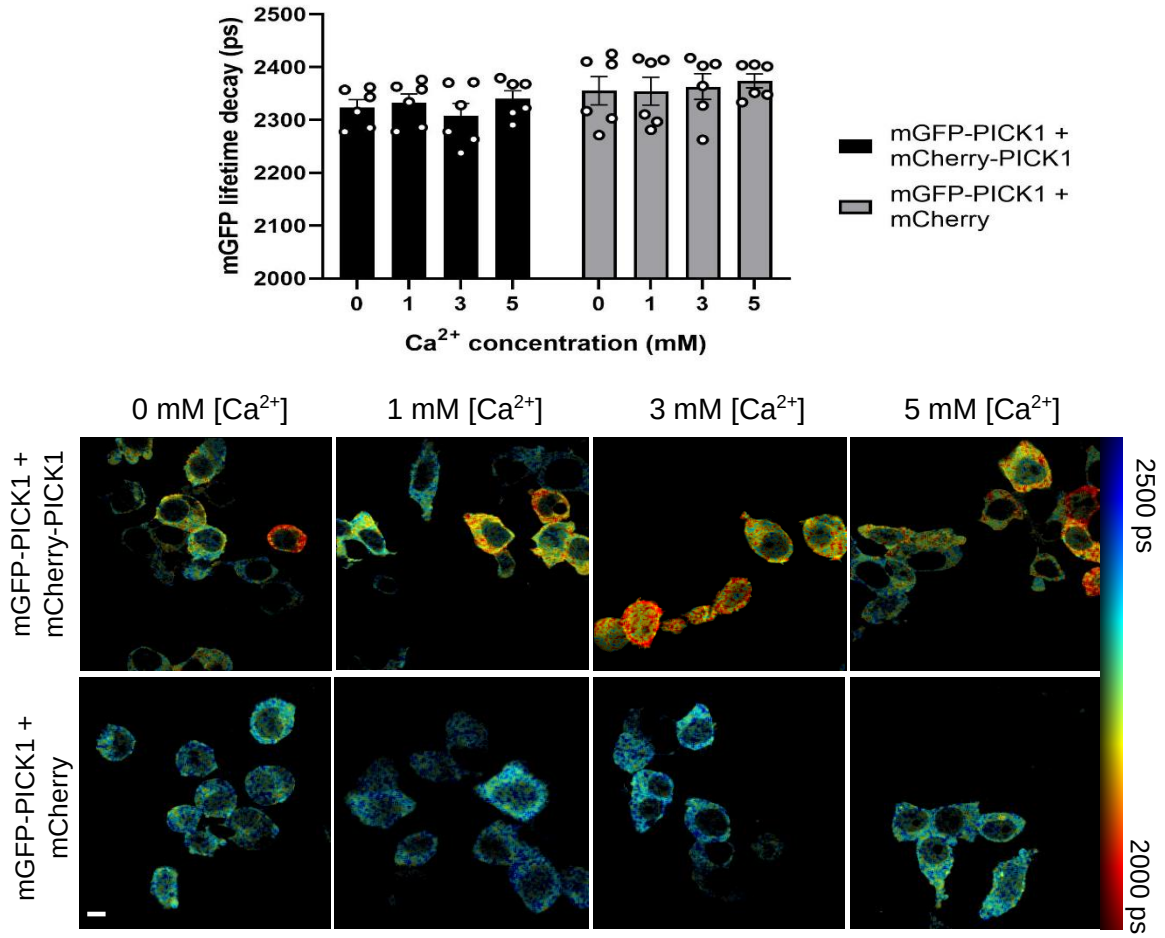

Figure 4.7.: PICK1 dimerisation in fixed HEK293 cells in the presence of increasing calcium concentrations detected through FLIM-FRET microscopy. HEK293 cultures were transfected to induce the expression of mGFP-PICK1 together with mCherry-PICK1 or with free mCherry for the control. 24h later, cultures were incubated with 0.3µM ionomycin for 5min in the presence of NaCl/HEPES buffers containing calcium over the range of 0mM to 5mM before being fixed with 4% PFA. Images were acquired in the green channel (490-550nm) using the 20x magnification lens before the data were fitted using FLIMfit 5.1.1. in order to generate heatmaps that show the mGFP lifetime decay on a scale ranging from 2500ps (blue) to 2000ps (red). No significant difference could be observed between the conditions. Error bars represent +/-SEM. Lifetime signal is intensity-adjusted and scale bar is consistent between panels at 20µm. N= 6 fields of view over 2 repeats.

4.3.5. PICK1 dimerisation is increased in neurons following chemically induced LTD

Because the main role of PICK1 during the expression of LTD is to promote the removal of GluA2-containing AMPARs from the synapse (Perez *et al.*, 2001; Hanley & Henley, 2005; Anggono *et al.*, 2013), it is likely that the protein is targeted to the surface of dendritic spines in response to neuronal activation. Activity-dependent AMPAR trafficking occurs in a regulated manner through clathrin-mediated endocytosis (Man *et al.*, 2000) and PICK1 could be involved in the internalisation of GluA2 subunits via BAR domain-mediated membrane remodelling. It is well established that one of the signalling factors which is altered during the induction of synaptic plasticity is calcium, whose local concentration increases at excited synapses either through NMDAR-mediated calcium influx or release from intracellular stores (Miyata *et al.*, 2000). Results from the previous chapter suggest that PICK1 dimerisation is upregulated within certain calcium ranges. In order to investigate whether the detection of PICK1 dimerisation through FLIM-FRET is possible in neurons during synaptic plasticity, I decided to stimulate DIV18 hippocampal neurons with an already established protocol for the induction of chemical LTD. The same imaging control conditions as before were included and FLIM-FRET was measured in neurons which had been fixed prior to the expression of LTD, immediately after LTD induction and following a 5min recovery period (Figure 4.8.).

As seen previously during the initial testing of the mGFP-mCherry FRET pair in live neurons, there are no significant differences between the mGFP-PICK1 lifetime recorded when co-expressed with mCherry-PICK1 and the mGFP-PICK1 only/with free mCherry controls (Figure 4.8.A). This seems to suggest that under basal conditions, there are minimal levels of PICK1 dimerisation detectable through FLIM-FRET. Interestingly, there was a significant reduction in the lifetime decay of mGFP-PICK1 of approximately 60ps when co-expressed with mCherry-PICK1 in measurements recorded immediately after NMDAR-mediated LTD. This reduction returns to baseline at the 5min timepoint after NMDA treatment which indicates that PICK1 dimerisation is a transient interaction elicited during synaptic plasticity.

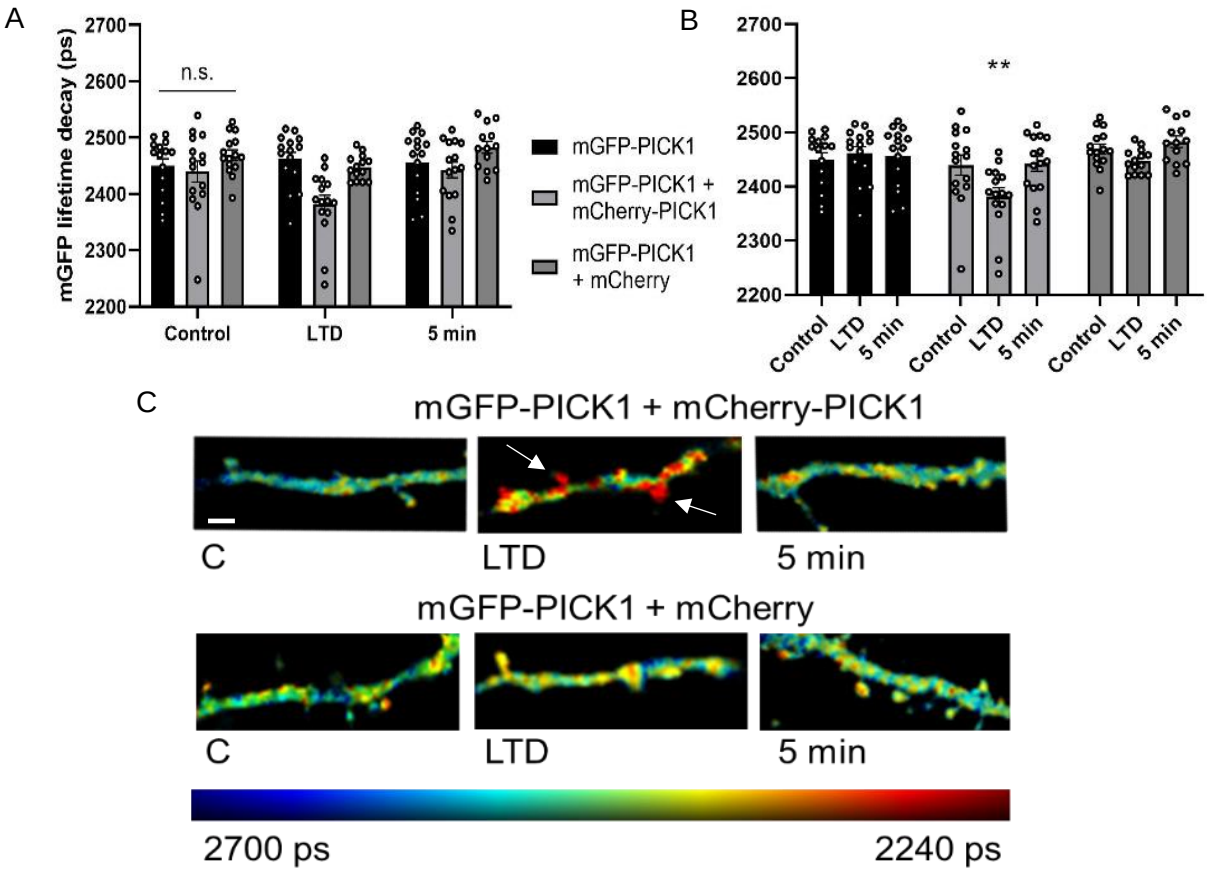

Figure 4.8.: PICK1 dimerisation in fixed neurons as observed by FLIM-FRET with the mGFP-mCherry fluorophore pair. DIV16-17 neurons were transfected to express mGFP-PICK1 alone, together with mCherry-PICK1 or with free mCherry for 24-48h before being treated with 50µM NMDA for 3 minutes to induce LTD. Samples were fixed with 4% PFA either prior to the NMDA treatment, immediately after LTD induction (LTD) or after a 5min recovery period. Data collected over the course of five experiments were quantified and showed a significant reduction in lifetime for mGFP-PICK1 when expressed together with mCherry-PICK1 immediately after LTD (N= 15 fields of view over 5 repeats, two-way ANOVA, $F(4, 123)= 2.296$, $p<0.05$). Images were acquired in the green channel (490-510nm) using the 63x magnification lens before the data were analysed using FLIMfit 5.1.1. software in order to generate heatmaps representative of mGFP-PICK1 lifetime decay on a scale from 2700ps (blue) to 2240ps (red). Error bars represent +/-SEM and the legend applies to both (A) and (B). Lifetime signal is intensity-adjusted and scale bar is consistent between panels at 5µm. Arrows point towards dendritic spines in order to highlight areas of lowest lifetime decay.

From the representative images it appears that the highest reduction in lifetime occurred within circular puncta located at the level of the dendritic spine, whereas the lifetime generated from mGFP-PICK1 that was present within the dendritic branch remained high. These results suggest that the induction of LTD promotes the self-association of PICK1 molecules into dimers and this takes place within the post-synaptic component of the synapse.

4.4. Discussion

4.4.1. Classic fluorescent proteins have been modified to improve their suitability for FRET

In this chapter, I set out to establish a FLIM-FRET imaging protocol for use in live neurons to determine the dimerisation status of PICK1 before and after the chemical induction of synaptic plasticity in the form of LTD. An interesting paper showed how the Yasuda group were able to detect FLIM-FRET in a live neuronal environment using the mGFP-sREACh fluorophore pair to differentially tag actin monomers (Murakoshi *et al.*, 2008). Fluorescent proteins are inherently prone to self-association (Constantini *et al.*, 2012) and in order to overcome this artefact, which poses potential ramifications for FLIM detection, mGFP represents an EGFP mutant (A206K) with limited dimerising capacity (Zacharias *et al.*, 2002) and sREACh also contains several mutations (F46L, Q69M, F223R) which function to abolish its dimerisation, as well as enhancing the appropriate folding of the protein (Murakoshi *et al.*, 2008). In addition, sREACh also functions as a ‘dark’ acceptor, meaning that it is a YFP variant which absorbs light in the 450-550nm range without emission. For these reasons, it is believed to form an ideal donor-acceptor pair for FLIM-FRET detection together with mGFP due to the high level of spectral overlap between mGFP emission and sREACh absorption with a limited chance of inter-channel bleed-through (Figure 4.1). Indeed, some groups were able to use GFP-sREACh pairings to investigate dimerisation and spine formation in live cells (Ueda & Hayashi, 2013; Presman *et al.*, 2014), but others found that additional sREACh mutations were necessary to fine-tune FLIM-FRET detection (Ma *et al.*, 2018; Hirata & Kiyokawa, 2019).

4.4.2. mGFP-sREACh fusion protein shows significant FLIM-FRET in neurons

I began my investigation by purchasing a commercially available plasmid (Plasmid #21947) from Addgene containing a mGFP-sREACh fusion protein, subcloning each fluorophore individually and then testing for the expression of the construct in neurons. The single transfection of mGFP shows a population that is homogenous in lifetime decay at 2300ps and so does the co-transfection of mGFP and sREACh. The expression of the fusion protein results in a substantial decay in lifetime of approximately 600ps representing the maximal extent of energy transfer between mGFP and sREACh. This suggested that the fluorophore pair is appropriate for FLIM-FRET detection in live neurons and I was able to subclone N-terminally tagged versions of PICK1 with either mGFP or sREACh into the mammalian expression vector pcDNA3.1.

4.4.3. PICK1-PICK1 interactions are detected through FLIM-FRET with mGFP-sREACh in live HEK293 cells

For simplicity reasons, I decided to initially test the suitability of the mGFP-PICK1 and sREACh-PICK1 pair for the detection of dimerisation in HEK293 cells by transfecting them 24 hours prior to data acquisition in order to reach stable expression of both proteins. Currently, there are no studies using imaging techniques such as co-localisation or FLIM-FRET to investigate the dimerisation of PICK1. Based on heterologous expression, the expectation was that PICK1 will readily self-assemble into dimers diffusely within the cytoplasm, in a similar manner to other representative BAR-domain proteins (Peter *et al.*, 2004; Ross *et al.*, 2011; Gortat *et al.*, 2012; van Weering *et al.*, 2012; Capraro *et al.*, 2013). Indeed, it was observed that there is a significant reduction in the lifetime of cells expressing both fluorescently-tagged proteins as compared to the mGFP-PICK1 control. A closer inspection of the representative images reveals that the pattern of dimerisation is a punctate one, possibly suggesting that PICK1 dimerisation co-localises with intracellular compartments which is in agreement with previous studies that showed PICK1 clustering on early endosomes following stimulation (Sossa *et al.*, 2006). Nevertheless, no link has been demonstrated between the ability of PICK1 to cluster

proteins and its dimerisation. The fact that mGFP-PICK1 lifetime is diffusely distributed within the cytoplasm, yet significant decline is only observed in certain punctate areas in the cell offers further support for the hypothesis that PICK1 dimerisation is spatially and temporally regulated. In addition, expressing mGFP-PICK1 with free sREACh did not result in a decrease in lifetime which confirms that the reduction observed with the co-expression of both fluorophore-tagged proteins is not a consequence of non-specific interactions between mGFP and sREACh.

4.4.4. PICK1-PICK1 interactions are not detected through FLIM-FRET with mGFP-sREACh in live neurons

When the same experimental procedure was repeated with DIV14 neurons, it was found that no differences could be measured in the lifetime of mGFP-PICK1 irrespective of co-expression with sREACh-PICK1. Because I noticed that the fluorescent signal present in the cell body was more intense than in the rest of the cell and because PICK1 is expected to perform its cellular function in proximity of the synapse (Xia *et al.*, 1999; Xu *et al.*, 2014), I decided to exclude the cell body from data analysis, but unfortunately this did not improve FLIM-FRET signal. Moreover, there was marked reduction in the lifetime observed with the second control which co-expresses free sREACh. Of note, observations made during data acquisition raised some questions for the efficiency of the energy transfer occurring between the donor and acceptor molecules. The sREACh molecule, which was supposed to function as a ‘dark’ fluorophore meaning it had optimal energy absorption and no emission, was surprisingly showing fluorescence in the green channel. Indeed, others have found that there is residual emission generated by sREACh which could affect FLIM data acquisition and further improvements have been made in order to generate the fluorophores called ShadowG and ShadowY to abolish emission (Demeautis *et al.*, 2017; Murakoshi & Shibata, 2017). This information taken together with the fact that the reduction in lifetime was considerably less robust than with the fusion protein tested in the previous subchapter, as well as the reduced lifetime for the mGFP-PICK1 + sREACh control seen with neuronal samples, was an indication that the mGFP-sREACh pair was not ideal for looking at PICK1 dimerisation.

4.4.5. PICK1-PICK1 interactions are detected through FLIM-FRET with mGFP-mCherry in live HEK293 cells but not in live neurons

One of the traditional FRET pairings which has been extensively characterised in various cellular systems and with various FRET methods of acquisition is between a green and red fluorophore such as GFP and mCherry (Bajar *et al.*, 2016). Interestingly, the extent of the lifetime decay of mGFP-PICK1 was enhanced in the presence of mCherry-PICK1, improving by 20% from a decline of 80ps observed with sREACh to approximately 100ps. However, when the experiment was performed in live neurons, there were no differences again between the controls and the cells co-expressing both fluorescently-tagged versions of PICK1. Because both fluorophore pairs tested so far have been shown in the past to be successful for the acquisition of FLIM-FRET data from live neurons (Ueda & Hayashi, 2013; Dore *et al.*, 2014), it is surprising that I was unable to detect dimerised PICK1 from our samples and several possible explanations have been raised. First, it is possible that endogenous PICK1 expression is interfering with the appropriate association of the fluorescently-tagged FLIM-FRET pairs. Indeed, when considering that there are six different combinations of two which result from the expression of three monomers, namely endogenous PICK1, mGFP-PICK1 and mCherry-PICK1, the likelihood of mGFP-PICK1 and mCherry-PICK1 coming together is low. Additionally, if a higher percentage of the population is represented by PICK1-mGFP-PICK1 or mGFP-PICK1 dimers than by the FRET pair dimers, it is possible that higher lifetime decay of uncoupled mGFP-PICK1 masks the effect of FLIM-FRET. The fact that endogenous expression of PICK1 in neurons is increased compared to the relatively low levels found in HEK293 kidney cells is relevant here because of the inability to detect FRET in live neurons as opposed to live HEK293 cells (Xia *et al.*, 1999).

4.4.6. Future work is required to correlate FLIM-FRET results with calcium-dependent dimerisation

In order to address whether the FLIM-FRET methodology can be used to detect distinct changes in PICK1 dimerisation, I decided to replicate my findings from the previous chapter which show that PICK1 dimerisation is improved in response to increasing calcium concentrations. As such, I found that although non-significant

differences exist between the conditions, there is a tendency for the 3mM calcium sample to show reduced lifetimes. A closer inspection of the representative images reveals that the population of cells showing a reduction in mGFP-PICK1 lifetime becomes more homogenous in the 3mM calcium condition in comparison to the other concentrations, similar to the control fields of view which contain cells that are comparable amongst themselves. Of note, several images collected for the no calcium condition expressing both mGFP-PICK1 and mCherry-PICK1 included one cell with a significantly lower lifetime decay. In these cells, the pattern of lifetime decay is diffuse within the cytoplasm as opposed to the punctate pattern observed during the optimisation of mGFP-mCherry fluorophore pair and the fluorescent signal is of higher intensity than the rest of the cells in the image. Because BAR domain dimerisation and oligomerisation are dependent on the concentration of the protein (Karlsen *et al.*, 2015; Madasu *et al.*, 2015), this suggests that the data could be skewed towards a lower lifetime average in the overall image because of the higher levels of PICK1 overexpression. More work is required in order to address these shortcomings, either by manually excluding the cells expressing PICK1 at a higher level than a defined threshold from the analysis or collecting over a smaller field of detection to limit variability. Nevertheless, there is an indication that there could be a correlation between the experiments performed with DSS crosslinking which show a calcium effect specifically on dimerisation with very little oligomerisation present and the decay in fluorescent lifetime observed with FLIM-FRET in the presence of various calcium concentrations.

4.4.7. PICK1 dimerisation in neurons is increased following LTD stimulation

Because PICK1 has been shown to perform its function during synaptic plasticity (Terashima *et al.*, 2004; Citri *et al.*, 2010; Nakamura *et al.*, 2011), I decided to investigate whether chemical LTD induction prior to FLIM-FRET data acquisition would result in any changes in PICK1 dimerisation levels in neurons that had been fixed in order to preserve transient interactions. Interestingly, PICK1 dimerisation was undetectable before stimulation, however there was a clear observation of lifetime reduction in the samples that were fixed immediately after 3 minutes of NMDA

treatment. Furthermore, the regions with the most reduction appeared to be within dendritic spines which is in agreement with previous studies which showed that PICK1 participates in AMPAR internalisation and recycling to and from the synapse in response to LTD (Lin & Huganir, 2007; Anggono *et al.*, 2013; Fiuza *et al.*, 2017). Nevertheless, the resolution used in this experiment is unable to clarify whether PICK1 dimerisation occurs at the plasma membrane or intracellularly within endocytic compartments. Because basal levels of PICK1 dimerisation returns to baseline after 5 minutes, this suggests that the self-association of PICK1 is indeed a transient interaction triggered by neuronal activation. The data also indicate that PICK1 dimerisation during synaptic plasticity is highly regulated both spatially and temporally and provide a possible explanation for the lack of dimeric PICK1 detection under basal condition. The quick induction of PICK1 dimerisation is also consistent with our hypothesis from the previous chapter in which PICK1 has been shown to upregulate its dimerisation as a consequence of direct calcium binding, without the time delay required for the activation of other calcium-sensitive signalling pathways.

In conclusion, this chapter represents the multiple steps that were undertaken in order to develop an appropriate imaging protocol for the FLIM-FRET acquisition of data reporting PICK1 dimerisation in neurons. Even though the initial fluorophore pair that was tested proved problematic, a suitable replacement acceptor molecule that showed improved energy transfer from mGFP was found in mCherry. And although imaging live neurons with the mGFP-PICK1 and mCherry-PICK1 pair was unable to detect PICK1 dimerisation, the combination of NMDA stimulation with PFA fixing at different timepoints was able to resolve that PICK1 dimerisation occurs immediately after the induction of LTD and quickly returns to basal levels. Importantly, this is the first demonstration of activity-dependent upregulation of BAR domain-mediated dimerisation. This is particularly relevant in a neuronal context where changes in PICK1 dimerisation could have potential consequences for AMPAR trafficking and the overall activation of the neuron.

Chapter 5

The role of PICK1 BAR domain dimerisation in membrane reorganisation and tubule formation

5.1. Introduction

5.1.1. BAR domain-containing proteins can induce membrane curvature

Several BAR domain-containing proteins have been shown to participate in the bending of membranes, in addition to sensing membrane curvature. Molecular dynamics simulations were able to calculate that the BAR domains of PACSIN, endophilin and amphiphysin can induce changes in membrane curvature (Blood & Voth, 2006; Mim et al., 2012; Mahmood et al., 2019), and this has been demonstrated experimentally by showing that liposomes in the presence of PACSIN, endophilin or amphiphysin adopt a tubular morphology (Peter et al., 2004; Wang et al., 2009; Mizuno et al., 2010).

Two cooperative models of BAR domain-mediated membrane curvature have been proposed. In one, it is proposed that helical scaffolding of BAR domain multimers around the membrane forces it to adopt their intrinsic curvature. Additionally, the amphipathic helix characteristic of BAR domain proteins may become embedded into the membrane, disrupting membrane tension.

In the case of PACSIN, which is an F-BAR protein that contains a wedge-loop similar to the short amphipathic helix seen in N-BARs, molecular dynamics simulations show the protein readily dimerises and quickly attaches to the membrane driven by electrostatic interactions between the positively charged concave dimer interface and the negatively charged lipid heads (Mahmood et al., 2019). Modelling studies suggest that, depending on the type of membrane modelled, PACSIN can induce curvature 40nm or 60nm in diameter – the latter corresponding to the length of the PACSIN dimer, suggesting PACSIN performs a scaffolding function that causes the membrane to adopt the intrinsic curvature of the dimer (Mahmood et al., 2019). Indeed, experimental evidence supports these findings such that incubating liposomes in the presence of PACSIN resulted in two different classes of striated tubules, with diameter averages of ~50nm or ~100nm being recorded through cryo-electron microscopy. Furthermore, they also found many smaller 35nm tubules, which suggests an ability for even further constriction and vesiculation by PACSIN, and this was attributed to the insertion of residues from the wedge-loop into the lipid bilayer (Wang et al., 2009).

When the structure of the amphiphysin BAR domain was first resolved, the authors also performed experiments examining the membrane binding properties of several other BAR domain-containing proteins (Peter et al., 2004). They showed that the BAR domains of centaurin and oligophrenin, which show poor tubulation activity, preferentially bound to curved membranes compatible with their intrinsic curvature. Conversely, the full N-BAR of amphiphysin, including the short amphipathic helix, was able to bind independent of membrane curvature (Peter et al., 2004), suggesting the tubulation activity of amphiphysin may be attributed to its ability to bind non-curved membranes. Subsequent simulations identified cooperation between the scaffolding of amphiphysin into helical oligomers around tubules, forcing them to adopt its own curvature, and insertion of the amphipathic helix into the lipid layer to disrupt membrane tension, as the likely mechanism underlying its tubulation ability (Blood & Voth, 2006).

Finally, endophilin has been suggested to also form scaffolds around lipid vesicles, although with a more variable degree of curvature, accommodating a range of diameters from 25nm to 32nm with such flexibility that multiple diameters could be observed through cryo-EM imaging on the same tubule (Gallop et al., 2006; Mizuno et al., 2010). Molecular dynamics simulations have highlighted the importance of a small internal amphipathic helix within its BAR domain structure, which becomes inserted into the membrane in a similar manner to the N-terminal amphipathic helix (Jao et al., 2010). Interestingly, deleting this region of endophilin results in reduced tubulation capacity, despite the mutant being able to bind the membrane similarly to the wild-type (Gallop et al., 2006). In further experiments, this mutant was demonstrated to be exclusively monomeric, underscoring the importance of dimerisation in endowing membrane-binding BAR domains with the ability to induce membrane curvature.

5.1.2. PICK1 could participate in AMPAR trafficking by regulating membrane remodelling

It is well established that one of the main functions of PICK1 in neurons is to mediate the removal of GluA2-containing AMPARs away from the synapse following the induction of LTD (Terashima *et al.*, 2004; Anggono *et al.*, 2013; Fiuza *et al.*, 2017). PICK1 has also been found to associate with endosomal compartments where it

colocalises with Rab11 which is a marker of recycling endosomes (Madsen *et al.*, 2008; Madsen *et al.*, 2012). Indeed, further evidence supporting the role of PICK1 in clathrin-mediated endocytosis shows that PICK1 can directly interact with AP2, an adaptor protein which is recruited at the site of endocytosis soon after LTD induction, as well as dynamin2, a GTPase which is responsible for the scission of the newly internalised vesicle (Fiuza *et al.*, 2017). Therefore, PICK1 is potentially involved throughout all stages of clathrin-mediated endocytosis, from the initial recognition of cargo such as GluA2-contaning AMPARs and other receptors, to the recruitment of adaptors such as AP2 to promote further assembly of the endocytic machinery and finally the recruitment of dynamin2 which causes intracellular release of the early endosome. In addition to orchestrating many different protein-protein interactions, PICK1 is also capable of binding lipid membranes of preferred phospholipid composition (Jin *et al.*, 2006) and contains an amphipathic helix which has been shown to participate in the recognition and preferential binding of 75nm liposomes (Herlo *et al.*, 2018). However, there is no evidence so far that shows a direct role for PICK1 in the generation of curvature.

An interesting question asks whether the calcium-dependent PICK1 dimerisation observed in this study has any consequences for the potential membrane remodelling capacity of the protein. So far, I have been able to demonstrate that wild-type PICK1 shows upregulated dimerisation in the presence of optimal concentrations of calcium both in heterologous cells and using purified protein in solution. Furthermore, levels of PICK1 dimer are immediately increased within the dendritic spines of neurons after prior treatment with NMDA in order to induce LTD. To address whether impairing PICK1 calcium-sensitive dimerisation affects its membrane dynamics, a short acidic stretch within the BAR domain sequence was substituted with 4 alanine residues (4A mutant). Molecular simulations of the PICK1 BAR-domain dimer suggested that the ^{271}DDEE^{274} region is located at the edge of the dimer interface where it forms a negatively charged binding pocket easily accessible to calcium ions from the surrounding environment, confirming this site's capacity to bind calcium (Figure 5.1.). In addition, the modelling also includes an orange overlay of the mutant on top of the blue wild-type which shows that the substitution of these residues with alanine does not significantly disrupt the PICK1 BAR domain from a structural point of view.

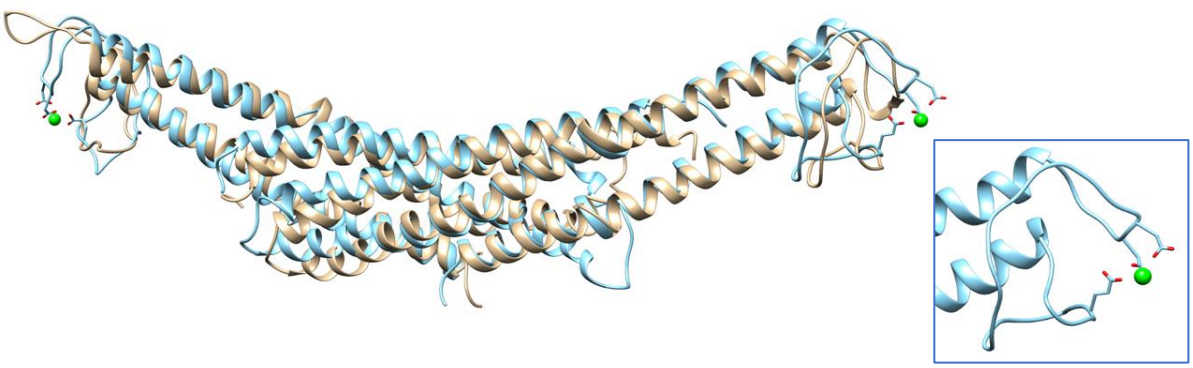

Figure 5.1.: Molecular modelling simulation showing the PICK1 BAR domain dimer and its association with calcium ions through residues ^{271}DDEE^{274}. Wild-type PICK1 is shown in blue and 4A mutant in orange. The inset represents the negatively-charged pocket that is formed by the acidic stretch and how these residues can coordinate the binding of a calcium ion. The orange overlay shows how the 4A mutant lacks the ability to bind calcium but the overall conformation of the BAR domain dimer remains unaffected. Image courtesy of Dr Deborah Shoemark.

5.2. Chapter aims

This chapter focuses on the characterisation of the PICK1 4A mutant in the context of its membrane remodelling properties in order to determine whether there is a mechanistic link between calcium-sensitive PICK1 dimerisation and potential changes in membrane curvature. In order to achieve this, several goals have been set:

- To determine whether PICK1 is able to tubulate liposomes in the presence of the optimal calcium concentration for dimerisation by means of cryo-EM imaging;
- To characterise the newly generated 4A mutant in terms of its dimerisation properties in solution and after heterologous expression;
- To establish whether PICK1 is capable of inducing tubulation in a COS-7 cellular assay and how this compares to the 4A mutant.

5.3. Results

5.3.1. PICK1 requires the presence of calcium to be able to tubulate membranes

In order to determine whether PICK1 is capable of inducing membrane curvature, I collaborated with Dr Hugh Tanner, a PhD student in Prof Paul Verkade's group who specialised in cryo-EM imaging of proteins in the presence of liposomes. Prior to incubation with liposomes, I purified wild-type PICK1 and allowed the protein to equilibrate overnight in dialysis cassettes incubated with calcium-free buffers or 5μM calcium which was shown to be the optimal calcium concentration for PICK1 dimerisation. Dr. Tanner subsequently incubated 100nM PICK1 with liposomes and cryo-EM imaging data was collected (data now shown).

From the data obtained, it appears that the morphology of lipid vesicles incubated with PICK1 is strongly influenced by additional calcium being present in the solution. In the absence of calcium, round liposomes which do not appear any different to typical liposome preparations can be observed. In contrast, the small, tubular structures present within the 5μM calcium concentration suggest that PICK1 requires calcium in order to initiate membrane remodelling.

5.3.2. The 4A mutant shows signs of impairment in its overall ability to dimerise irrespective of calcium concentration

In chapter 3 it was suggested that the acidic stretch of amino acids present within the N-terminal region of PICK1 can regulate calcium-dependent dimerisation such that its deletion occludes the upregulation seen with wild-type PICK1. Similarly, I identified a region within the BAR domain consisting of 4 negatively charged amino acids, ^{271}DDEE^{274}, and molecular modelling simulations indicated that they are involved in the formation of a negatively charged pocket capable of binding calcium ions (Figure 5.1.). Therefore, I decided to substitute this region with 4 alanine residues and tested the new mutant using the same protocols for DSS crosslinking of purified proteins or HEK293 overexpression as in the previous chapter (Chapter 3).

Initially the effect of increasing calcium concentration on the dimerisation of PICK1 in solution was explored. To this extent, purified his-tagged versions of wild-type PICK1 and the 4A mutant were incubated with 10µM DSS at room temperature before separation based on molecular weight through SDS-PAGE and subsequent Western blotting with an anti-PICK1 antibody. The results indicated that the 4A mutant is impaired in its overall ability to dimerise in addition to being insensitive to calcium-induced upregulation of dimerisation (Figure 5.2.).

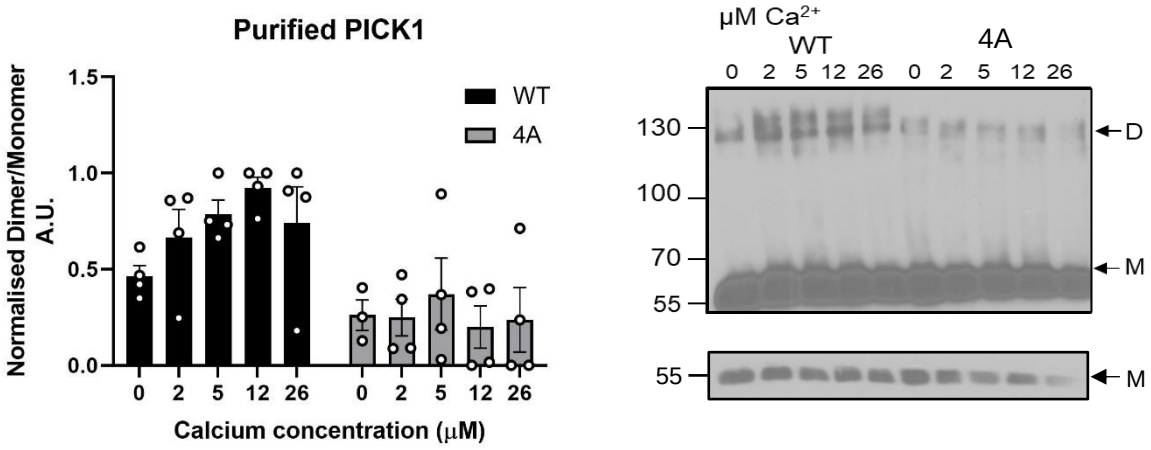

Figure 5.2.: Dimerisation of purified PICK1 4A mutant is impaired regardless of calcium concentration. 100nM his_6PICK1 was incubated with 10µM DSS for 20 minutes at room temperature before SDS-PAGE and immunoblotting with an anti-PICK1 antibody. The WT condition showed a near doubling of the amount of dimer detectable in the 5-12µM range as compared to the zero calcium control. The 4A mutant on the other hand did not present a calcium-dependent effect for its dimerisation and was impaired across all conditions. N=4 repeated experiments. Error bars represent +/-SEM. The representative blot on the right-hand side highlights the dimer fraction (arrow, D) and the monomer used for normalisation (arrow, M). The monomer blot for normalisation is a lower exposure of the top blot.

Interestingly, the amount of dimer detected in the 5 and 12µM calcium conditions for the WT was 1.7 and 2 times higher compared to the levels of WT dimerisation in the absence of calcium. This is in agreement with previous experiments which showed a doubling of the dimeric fraction from 0 to 5µM calcium and suggests that a range of 5-12µM calcium concentration maximally promotes PICK1 dimerisation. In contrast, the 4A mutant showed reduced levels of dimerisation across all conditions at approximately half the levels seen with WT PICK1 in the absence of calcium. Therefore, it appears that the ^{271}DDEE^{274} region within the PICK1 BAR domain is required not only for the appropriate maintenance of calcium-induced dimerisation but

also for overall dimer formation. Of note, the data presented were analysed using a two-way ANOVA which showed statistical significance only for the column factor ($F(1, 29)= 30.68$, $p<0.0001$) which indicated that WT PICK1 and the 4A mutant are different in their overall response to calcium. One or two more experiments should result in significant differences between the calcium ranges as well.

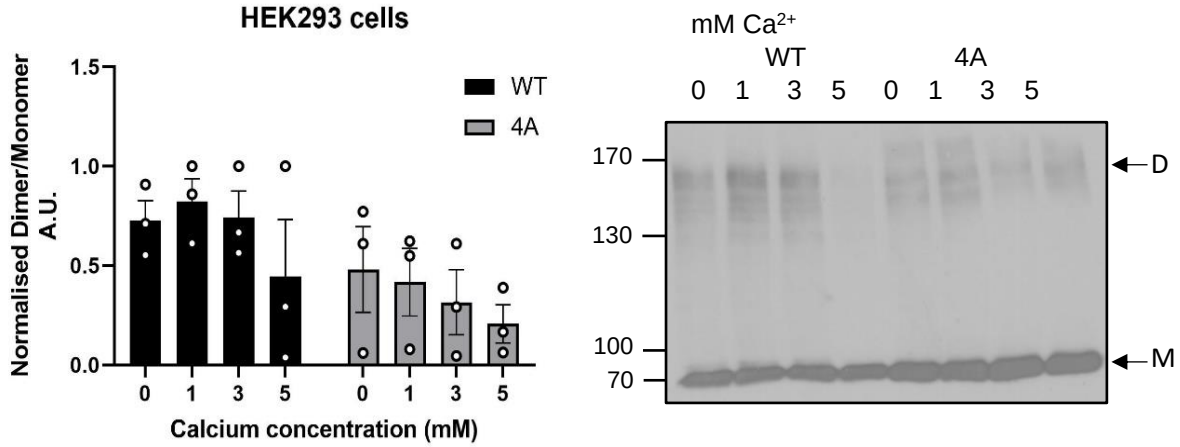

Figure 5.3.: Dimerisation of overexpressed PICK1 4A mutant in a cellular environment is impaired regardless of calcium concentration. HEK293 cultures were transfected to express either WT or mutant PICK1 24h prior to treatment with 0.3mM DSS/3µM ionomycin in the presence of increasing calcium concentrations. Although the effect of calcium on WT PICK1 is less pronounced in this data set, the difference observed with the mutant indicates an inability to dimerise efficiently regardless of calcium concentration. N=3 repeated experiments. The error bars represent +/-SEM. The representative blot on the right-hand side highlights the dimer fraction (arrow, D) and the monomer used for normalisation (arrow, M).

Next, I wanted to investigate whether the same effect is maintained within a cellular environment with the overexpression of PICK1 in HEK293 cells. As before, HEK293 cultures were transfected to express GFP-tagged versions of either WT PICK1 or the 4A PICK1 mutant for 24h before being subjected to 0.3mM DSS crosslinking in the presence of various calcium buffers. In agreement with the experiment using purified proteins, the results showed that even in the context of cellular expression, the 4A mutant shows a reduced capacity for dimer formation when compared to the WT (Figure 5.3.). Interestingly, the calcium effect on WT PICK1 dimerisation is less pronounced in this dataset than in previous experiments, but completely absent from the 4A mutant. In fact, there appears to be a downward trend for the dimer fraction detected with the 4A mutant similar to the effect seen with the truncated PICK1 BAR

domain (Figure 3.4.). Because this dataset is limited in N number, more repeats of this experiment are required in order to achieve statistical significance across the calcium range, however it is worth mentioning that a two-way ANOVA of the data confirms that the WT and 4A overall behave differently in response to calcium (column factor $p<0.05$, $F(1, 16)= 7.360$).

5.3.3. The 4A PICK1 mutant shows reduced capacity to induce the formation of tubules in COS-7 cells

Finally, I was interested in determining how PICK1 would behave in a COS-7 cellular assay in terms of its ability to generate membrane curvature in a cellular environment. In previous studies, COS-7 expression of BAR domain-containing proteins led to the detection of tubular structures emerging from the plasma membrane (Peter *et al.*, 2004; Itoh *et al.*, 2005; Gallop *et al.*, 2006). COS-7 cells are particularly suitable for this type of analysis because of their relatively flat morphology which allows for the detection of many tubular structures especially at the periphery of the cell. So far, there has been no evidence that PICK1 is capable of forming such tubules under any conditions. Therefore, I set out to investigate whether the addition of calcium to COS-7 cell cultures expressing GFP-tagged WT or 4A mutant PICK1 would result in the formation of tubular membrane structures.

From the representative images (Figure 5.4.), it becomes apparent that there are differences between the conditions. A cell is considered to be tubulated if two or more tubular structures can be detected across at least two Z planes in the cytoplasm. The tubules must also be at a reasonable distance (2-3µm) away from the plasma membrane in order to eliminate the possibility of mistaking membrane folds as internal tubules. The experiment was performed blinded to the sample identification in order to eliminate personal bias in the assessment of tubulation. The most striking observation concerns the increased levels of tubulation observed with WT PICK1 in the presence of calcium. Indeed, when the cells are incubated with ionomycin in calcium free buffer, there are few if any tubules initiated. However, the number of cells with tubules increases significantly with increasing calcium concentration. The extent of tubulation correlates with the previous finding that PICK1 dimerisation is optimal at 3mM extracellular calcium and is reduced at 5mM calcium. Interestingly, the 4A mutant

is incapable of forming tubules when expressed in COS-7 cells regardless of the extracellular calcium concentration. This seems to suggest that the ^{271}DDEE^{274} region required for the appropriate formation of the PICK1 dimer in response to calcium also promotes the membrane remodelling capacity of PICK1.

The images collected over the course of three experiments were used for data quantification in order to determine through statistical analysis whether the effect observed by visual inspection of the images is true. When acquiring the images, I assesed the tubulation status of 20 cells per condition and this count was used to calculate the percentage of cells showing tubules. The cells which contained at least one tubule were further analysed using a semi-automated script which measured the number and length of tubules in each cell (Figure 5.5.). For each condition, a representative image from the non-tubulated cells was run through the analysis to confirm the lack of tubule detection.

The quantification of the data confirmed that the differences noticed by visually inspecting the images are in fact statistically significant between conditions. The representative images from Figure 5.5.A offer an insight into how the Ridge Detection plugin from FIJI ImageJ detects and measures tubules. The settings were adjusted such that appropriate tubule detection is achieved across all three experiments while omitting aberrant detection of structures from the non-tubulated cells. Appropriate areas of the cytoplasm were manually selected to ensure the folds of the outer membrane were also not included in the analysis. Unfortunately, some tubules were still missed under these parameters and further processing could certainly improve the quality of the data. Nevertheless, the quantification shows that WT PICK1 in the presence of 3mM calcium differs significantly from the 4A mutant in terms of the percentage of cells presenting with tubules ($p<0.01$) as well as the average length of tubules per cell ($p<0.001$). As such, there is an approximately 10-fold upregulation in both of these parameters when WT PICK1 is expressed in the presence of 3mM calcium.

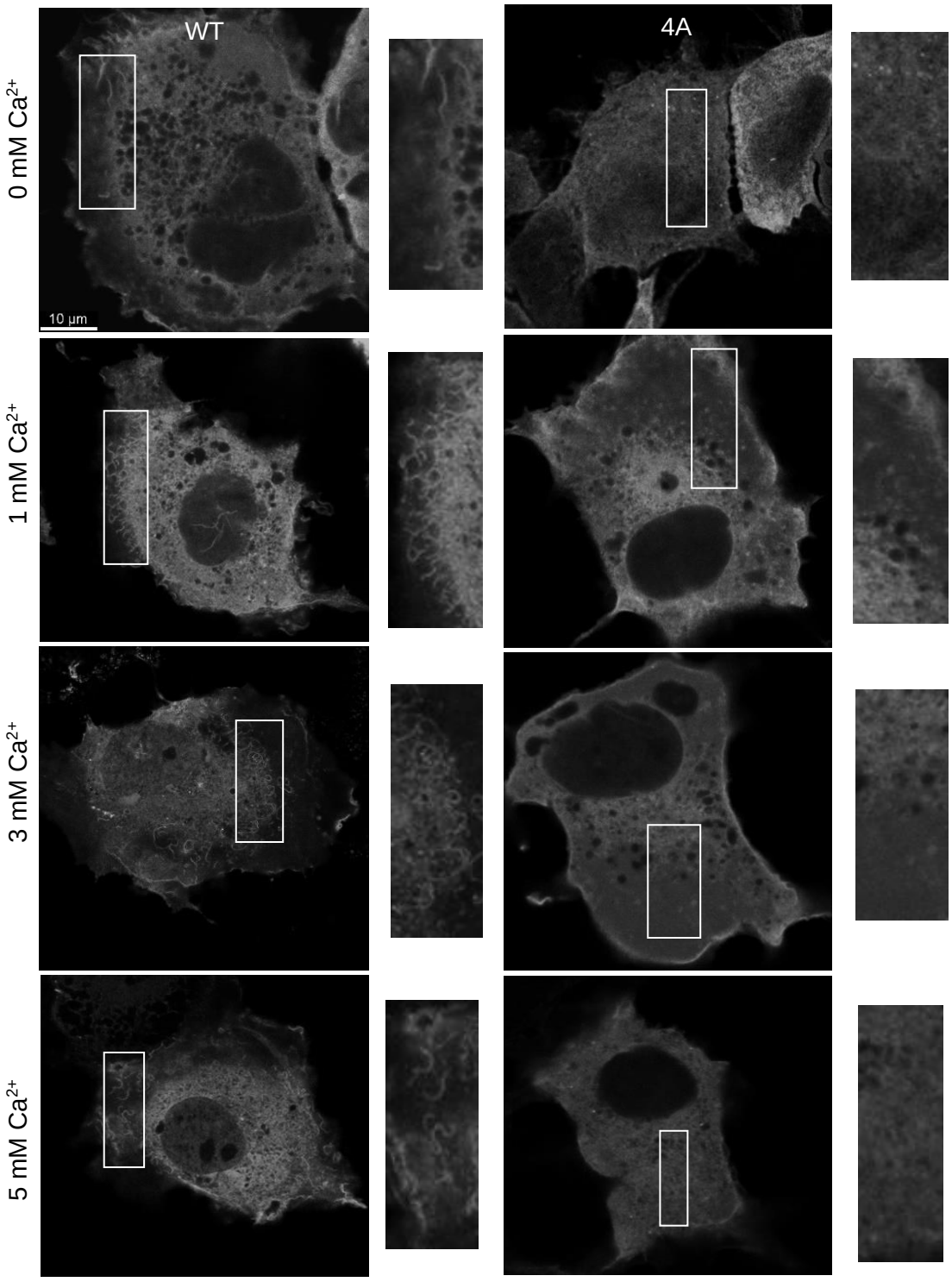

Figure 5.4.: Representative images showing COS-7 cells expressing GFP-PICK1 or GFP-4A PICK1 in the presence of increasing calcium concentrations. COS-7 cells were transfected 24-32h prior to being incubated with 3µM ionomycin at 37°C for 15min in the presence of increasing calcium concentrations before being fixed. Images were acquired using confocal microscopy with the 100x lens acquiring in the green channel (490-550nm). Areas of interest showing the most tubulation or lack of tubulation are highlighted in rectangles and the magnification can be viewed in the insets and in Figure 5.6. Scale bar is consistent among panels at 10µm.

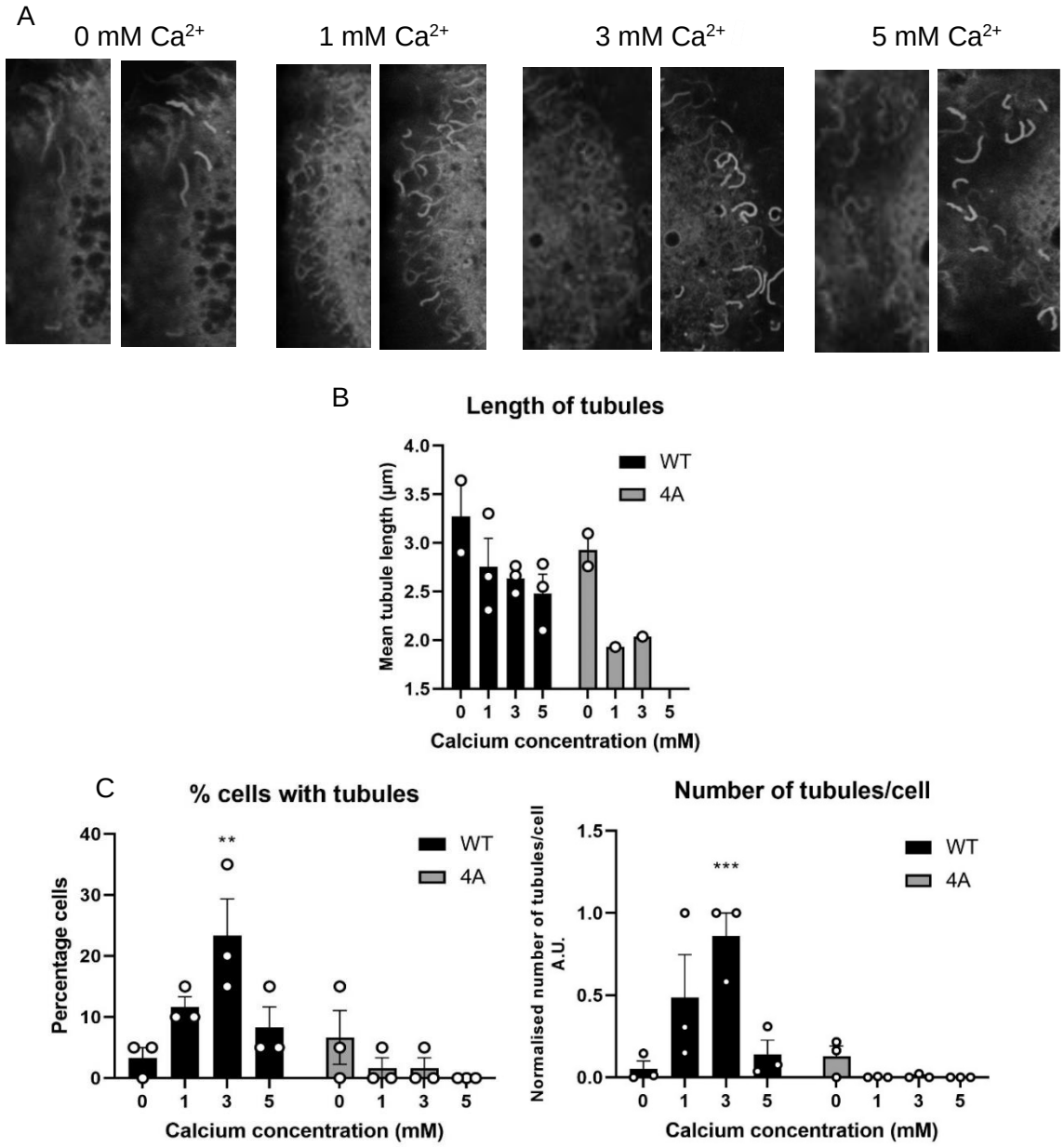

Figure 5.5.: Quantification of tubules observed by imaging COS-7 cells expressing GFP-PICK1 or GFP-4A PICK1 after being incubated with ionomycin in the presence of various calcium concentrations. A) Representative images corresponding to the panels for WT PICK1 in Figure 5.5. showing the tubules which were identified through Ridge Detection (FIJI software) from COS-7 cells expressing wild-type GFP-PICK1. In the images on the right, colourful overlays highlight the structures which are identified as tubules. B) Preliminary quantification of the mean length of tubules detected. N varies between 0-3 due to the lack of tubulation in some conditions in some experiments. More repeats are required for reliable conclusions to be drawn. C) Quantification of the percentage of cells showing tubules and of the number of tubules per cell comparing WT PICK1 to the 4A mutant. In the case of WT PICK1, the 3mM calcium condition shows a significant increase in both the percentage of cells presenting with tubules (two-way ANOVA, $F(3, 16) = 5.381$, $p<0.01$. Tukey's post-hoc analysis, $^{**}p<0.01$) and the average number of tubules per cell (two-way ANOVA, $F(3, 16) = 6.490$, $p<0.01$. Tukey's post-hoc analysis, $^{***}p<0.001$). N= 3 repeated experiments.

This result is significant because it represents the first evidence in support of a role for PICK1 in membrane bending in a cellular system. Furthermore, due to the striking lack of tubules in cells which express the 4A mutant PICK1, it is implied that the ^{271}DDEE^{274} region is necessary for the appropriate initiation of membrane remodelling which occurs in response to calcium addition. In fact, in the absence of calcium, the 4A mutant seems to induce tubulation at low levels comparable to the WT in the absence of calcium.

A preliminary analysis looking at the mean length of tubules was also conducted in order to determine whether the increased pattern of tubulation can be attributed to increases in length as well as in the number of tubules per cell. Of note, no statistical analysis could be performed due to the limited data set because of insufficient data for some conditions. However, there is an indication that there could be a calcium-dependent reduction in the mean length of the tubules formed by WT PICK1. This would suggest that the effect of increased tubulation is due to a larger number of smaller tubules being initiated rather than the continued elongation of already existing tubules.

5.4. Discussion

5.4.1. Purified PICK1 can induce tubulation in lipid vesicles only in the presence of calcium

The aim of this chapter was to investigate the induction of membrane curvature by PICK1 in a similar manner observed previously with other BAR domain-containing proteins (Peter *et al.*, 2004; Mizuno *et al.*, 2010). Indeed, with collaboration with Hugh Tanner who performed EM imaging using purified PICK1 which had been dialysed against zero calcium or 5µM buffer, we were able to detect that PICK1 causes liposome tubulation only when calcium is present. This finding is significant because direct tubulation with PICK1 has not been demonstrated before. Therefore, this constitutes the first evidence in support of the membrane-remodelling capacity of PICK1 as well as the first representation of stimulus-induced upregulation in the tubulation efficiency of a BAR domain-containing protein. However, this experiment was only performed once and further repeats are required to solidify this finding. The

experiment could also be extended to include mutants that are relevant for PICK1 calcium sensitivity such as the ΔNT and 4A mutant, and subtomogram averaging/ single particle analysis techniques could allow the visualisation of the PICK1 scaffold surrounding the tubulated membrane.

5.4.2. The PICK1 4A mutant is impaired in its ability to dimerise during heterologous expression and using purified protein regardless of calcium concentration

Another important aim pursued within this chapter was to generate a PICK1 mutant which is impaired calcium-dependent dimerisation. This is an important step required for investigating the contribution of PICK1 dimerisation to the appropriate remodelling of the membrane. Indeed, other studies have shown how single point mutations within the BAR domain can affect the dimerisation of BAR domain proteins. In the case of SNX9, it was shown single amino acid substitutions within the BAR domain can alter its dimerisation status from homodimeric SNX9 to heterodimeric SNX9/SNX33 complexes (Dislich *et al.*, 2010), suggesting that small mutations could alter the properties of BAR domain-mediated dimerisation without resulting in the complete misfolding of the domain. To this extent, I identified a stretch of negatively charged amino acid residues spanning across the ^{271}DDEE^{274} region within the BAR domain. Molecular modelling carried out by collaboration with Dr. Deborah Shoemark indicated that this region can indeed participate in the binding of calcium ions because it falls outside of the BAR domain dimer interface with easy access to the environment. After replacing the 4 acidic amino acids with alanine residues, the new mutant was impaired not only in its response to the addition of calcium, but also in the overall level of dimer detected. This effect was consistent when the DSS crosslinking assay was performed with purified proteins (Figure 5.2.) or in a cellular context through PICK1 overexpression (Figure 5.3.) and showed an approximate halving of the amount of dimer present compared to WT PICK1 in the absence of calcium. This suggests that the ^{271}DDEE^{274} region is required for the appropriate assembly of the BAR domain dimer interface, with noticeable impairement detected even in the absence of calcium and maintained across conditions. Although molecular modelling predicted that the substitution of ^{271}DDEE^{274} with 4 alanines would not significantly affect the folding of

the BAR domain dimer interface, it is possible that there is a coordination requirement between this region and the other functional and regulatory domains within the full length protein to promote the formation of the dimer.

5.4.3. WT PICK1 can induce membrane tubulation in COS-7 cells only in the presence of calcium and this is completely abolished with the 4A mutant

Finally, I decided to test the tubulation activity of PICK1 in a COS-7 imaging assay in order to visualise any emerging tubules in response to calcium stimulation. Previously, the expression of fluorescently-tagged BAR domain proteins in COS-7 cells had been used to assess the membrane remodelling properties of BAR domains (Peter *et al.*, 2004; Itoh *et al.*, 2005; Gallop *et al.*, 2006). Interestingly, the results showed that there is a significant increase in the percentage of cells presenting with tubules and also in the number of tubules detected per cell with WT PICK1 in the 3mM calcium condition (Figure 5.4.). The efficiency of tubulation appears to correlate with the pattern of increasing dimerisation in response to calcium analysed by DSS crosslinking (Figure 5.3.) which is reduced at 5mM calcium. Furthermore, the 4A mutant is significantly impaired in its ability to generate tubules, with the majority of cells analysed lacking any indication of tubulation. When correlated with the reduced dimerisation of the 4A mutant this supports the direct link between calcium-induced PICK1 dimerisation and the reshaping of the membrane. The analysis regarding average tubule length is still inconclusive with more experimental data required for the completion of the data set. Regardless, because tubule length does not increase across the calcium range but the number of tubules does, this could be an indication that PICK1 is more likely to participate in the initiation of new tubule formation rather than the elongation of already existing ones. An interesting observation is the fact that PICK1-mediated tubulation was not detected when expressing GFP-PICK1 in HEK293 during the FLIM-FRET experiments from chapter 4. However, the data generated during the optimisation of the FLIM-FRET pair were performed under basal conditions without calcium manipulation. Additionally, in the experiments testing the effect of calcium influx for dimerisation using FLIM-FRET, the resolution of the imaging using the 20x lens was not high enough to allow detection of any potential small intracellular tubular structure.

Future experiments should be performed with the 100x magnification lens in order to address this issue.

5.4.4. Improvements are required for more robust data analysis with the COS-7 protocol

The results from this experiment represent further new evidence in support of the stimulus-induced tubulation capacity of PICK1 which has not yet been reported elsewhere. However, there are some limitations in the design of the experiment which could be improved. Firstly, the semi-automated data analysis is very time-consuming and could be further optimised and adapted for full automation. The collection of high-quality images is paramount for the return of high-quality data from the analysis which is why the 100x lens or the highest quality of lens available should be used. Secondly, because the samples are blinded before data collection, this introduced complications in terms of collecting the same numbers of cells per each condition across the three experiments, depending on the efficiency of the tubulation. As such, in the future the same total number of tubulated and non-tubulated cells must be recorded for consistency. Finally, the experiment does not address the origin of the tubulated membranes so using an external fluorescent membrane dye such as FM4-64 would decipher what percentage of the tubules originate from the plasma membrane or from endosomes.

5.4.5. Future directions for the COS-7 tubulation assay to investigate the mechanisms involved in PICK1 membrane remodelling

The COS-7 tubulation assay has the potential to be extended with further investigations into the cellular mechanisms involved in the generation of membrane curvature by PICK1 in response to calcium. To assess whether the other calcium binding sites within the PICK1 structure have any influence on tubulation, COS-7 cells could be transfected with GFP-tagged versions of the ΔNT mutant or the ΔCT mutant using the same extracellular calcium influx protocol. Additionally, more information could be gained about the role of the PDZ domain and how its interactions are relevant for the dimerisation of PICK1 and subsequent membrane tubulation by inhibiting the

PDZ domain through the addition of PDZ ligands. Another possible avenue of exploration involves looking into the importance of other PICK1 protein-protein interactions that are relevant for membrane remodelling, such as the binding of the Arp2/3 complex and the downstream effect on actin tubulation, or the interaction with AP2 and dynamin, which are essential for clathrin-mediated endocytosis. Indeed, the potential for PICK1 to actively participate in CME is significant due to the discovery of its ability to generate membrane curvature and will be discussed in more detail in the next chapter.

Chapter 6

General Discussion

6.1. Reminder of aims and objectives

The main aim of this study was to characterise a novel mechanism for the regulation of BAR domain function in response to signalling factors that are relevant for neuronal communication. Specifically, the objectives previously outlined in chapter one fall into three main categories:

- Biochemical investigations using the cell-permeable irreversible crosslinker DSS in order to:
    - Assess how the dimerisation of PICK1 compares to other BAR domain proteins;
    - Determine whether PICK1 BAR domain-mediated dimerisation can be upregulated in response to calcium stimulation;
    - Discover which regions within the PICK1 structure are involved in the regulation of calcium-sensitive PICK1 dimerisation.
- Establishing a FLIM-FRET imaging protocol that can reliably detect PICK1-PICK1 interactions in neurons following chemical induction of LTD in order to assess whether PICK1 dimerisation is upregulated during synaptic plasticity.
- Investigations into the membrane remodelling capacity of PICK1 by:
    - Designing a mutant that is impaired in its overall dimerisation and also blocks the effect of calcium;
    - Testing the mutant in a COS-7 tubulation assay in order to determine whether calcium-sensitive PICK1 dimerisation is relevant for membrane tubulation.

Over the course of my thesis, I have been able to address each of these goals and as such I have been able to show that:

- Basal level PICK1 dimer:monomer ratios are low when compared to other BAR domain proteins such as endophilin and amphiphysin;
- PICK1 dimerisation is upregulated in response to intracellular calcium influx in HEK293 cells;
- Purified PICK1 dimerisation in an isolated system is also calcium-dependent and this effect is abolished after the deletion of the N-terminal acidic region;

- PICK1 dimerisation is increased in distinct puncta which localise at dendritic spines in neurons after NMDA-induced expression of LTD;

- The PICK1 4A mutant shows reduced dimer:monomer ratios regardless of calcium concentration;
- The PICK1 4A mutant shows reduced and calcium-insensitive tubulating activity in a COS-7 tubulation assay; in contrast, WT PICK1 showed a robust calcium-senstive increase in the number of tubulated cells and the number of tubules detected per cell.

6.2. Proposed mechanism for PICK1 calcium-sensitive AMPAR endocytosis during LTD

Taken together, the results presented in this thesis offer the first convincing evidence in support of a novel role for PICK1 in membrane remodelling. So far, no other studies have demonstrated a direct effect of PICK1 on membrane curvature generation even though many other BAR domain proteins have shown an ability to both preferentially bind and influence the diameters of liposomes (Peter *et al.*, 2004; Gallop *et al.*, 2006; Wang *et al.*, 2009). By taking into account how PICK1 performs its function in response to neuronal stimulation (Jin *et al.*, 2006; Terashima *et al.*, 2008) and how calcium is one of the signalling factors required for the synaptic plasticity (Hirsch & Crepel, 1992), as well as the fact that PICK1 has already been characterised as a calcium sensor involved the regulation of AMPAR trafficking (Hanley & Henley, 2005; Citri *et al.*, 2010), I have been able to integrate calcium signalling with PICK1 dimerisation and subsequent BAR domain-mediated membrane remodelling to define a novel mechanism for PICK1 function.

6.2.1. PICK1 dimerisation is upregulated in response to calcium

Dimerisation is considered the minimal requirement for a fully functional BAR domain because the appropriate recognition of specific membrane curvatures requires the formation of the angle between the two monomers (Peter *et al.*, 2004). Representative BAR domain proteins such as endophilin and amphiphysin have been shown to have

low micromolar dimerisation constants which suggests that they are readily assembled into their dimeric form when expressed in the cytoplasm (Gallop *et al.*, 2006; Capraro *et al.*, 2013; Gruber & Balbach, 2015). This idea is partially challenged in Figure 3.1. which shows that although endophilin1, endophilin2 and amphiphysin2 have much higher levels of basal dimerisation in comparison to PICK1, only a proportion of the protein fraction can be crosslinked into a dimeric form for any of the BAR domains tested. In the case of endophilin, some have proposed that the monomer is still capable of recognising lipid membrane (Gallop *et al.*, 2006) on its own and that the redistribution of the protein to the membrane promotes its dimerisation. This in turn leads to membrane curvature generation and the initiation of a cascade in which more protein is recruited to the membrane resulting in the assembly of the oligomeric protein scaffold and subsequent membrane remodelling (Simunovic *et al.*, 2016). This represents one possible scenario for the calcium-sensitive dimerisation of PICK1 observed following expression in HEK293 cells where the binding of calcium to PICK1 monomers could elicit conformational changes which either promote its dimerisation in the cytoplasm or promote the redistribution of monomers to the membrane where the membrane itself can assist dimerisation (Figure 3.2.). On the other hand, experiments performed with purified WT-PICK1 and the ΔNT mutant (Figure 3.5.) show that dimerisation is still possible in a reduced system in the absence of any membranes but occurs at much lower levels than in a cellular environment. This is indicated by the longer exposure required to be able to visualise the dimeric fraction of PICK1 on the blot in Figure 3.5. compared to the one in Figure 3.2.

The BAR domain of PICK1 has been proposed to exist in an autoinhibited manner such that the deletion of the PDZ domain and the C-terminal acidic region leads to enhanced clustering (Perez *et al.*, 2001). In addition, I found that the deletion of the N-terminal acidic region leads to improved dimerisation which suggests that this region is inhibitory for the assembly of the dimer in the absence of calcium and that this inhibition is alleviated after calcium binding (Figure 3.5.). Interestingly, the isolated BAR domain also showed high levels of dimerisation in the absence of calcium which suggests a lack of inhibition, but the levels of dimer went down with calcium addition (Figure 3.4.). This could indicate that in the case of the isolated BAR domain, the biphasic effect of calcium is shifted to the left such that the inhibitory effect on dimerisation is visible from 1mM. This is consistent with my observation that the BAR

domain contains at least one calcium-binding region within its structure which can influence its dimerisation. Indeed, this was later confirmed through molecular dynamics simulations which suggested that the negatively charged ^{271}DDEE^{274} region forms a binding pocket capable of accommodating a calcium ion on each side of the dimer interface (Figure 5.1.).

All in all, these findings offer an indication of how changes in local calcium concentration can influence the levels of PICK1 dimerisation through direct calcium binding of the PICK1 N-terminal acidic region as well as the ^{271}DDEE^{274} region within the BAR domain.

6.2.2. PICK1 dimers localise at dendritic spines during synaptic plasticity

Congruent with the hypothesis that PICK1 dimerisation occurs in the proximity of membranes, the results from FLIM-FRET experiments showed the highest levels of FRET signal occurring in distinct puncta located at the level of the dendritic spine (Figure 4.8.). This is where PICK1 is expected to perform its cellular function, as highlighted by studies which show enhanced expression in synaptosomes and colocalisation with GluA2 at synapses (Xia *et al.*, 1999). Because the increase in PICK1 dimerisation was only detected immediately after NMDA-induced chemical LTD, this indicates that PICK1 dimerisation is a transient response to rapid and tightly regulated increases in local calcium concentration elicited during synaptic plasticity (Neveu & Zucker, 1996; Miyata *et al.*, 2000). However, it is not clear whether PICK1 dimerisation occurs at the surface of the synapse or on membranes belonging to internalised endocytic vesicles or both. Interestingly, the fact that PICK1 expression is present throughout the cell yet dimerisation is restricted to specific subcellular localisations suggests that after LTD induction and the presumed binding of calcium to the monomer, the dimer is rapidly redistributed to membranes. Another possible explanation for the lack of PICK1 dimerisation measured by FLIM-FRET in the cytoplasm could be that PICK1 is forming heterodimers with another BAR domain protein. Indeed, heterodimerisation is not unusual for BAR domain proteins and previous studies have shown that two thirds of PICK1 is associated with ICA69 in a manner which inhibits the function of PICK1 (Cao *et al.*, 2007; Cao *et al.*, 2013; Xu *et al.*, 2014).

6.2.3. PICK1 can induce membrane tubulation potentially due to N-BAR amphipathic helix

BAR domain proteins can bind lipid vesicles of preferred curvature such as endophilin showing preference for 25-32nm vesicles (Mizuno *et al.*, 2010) or amphiphysin being mostly found on small liposomes with diameters less than 50nm (Peter *et al.*, 2004). When incubated with large liposomes of up to 400nm, BAR domain proteins are able to constrict the diameters of round vesicles into tubular structures with lower diameters (Gallop *et al.*, 2006). It is believed that this form of highly regulated membrane remodelling by BAR domains is essential for the appropriate generation of endocytic vesicles during clathrin-mediated endocytosis (Meinecke *et al.*, 2013). In the case of PICK1, it has been shown to participate in CME of AMPARs containing the GluA2 subtype via its interaction with AP2 and dynamin (Fiuza *et al.*, 2017). PICK1 also colocalises with endocytosed cargo on the surface of internalised early and recycling endosomes (Sossa *et al.*, 2006; Lin & Huganir, 2007). Furthermore, it has been shown in the case of other BAR domain proteins that the recognition of lipid curvature is an intrinsic property of their isolated BAR domain such that the amphiphysin BAR domain shows preferential binding to lipid vesicles smaller than 100nm (Peter *et al.*, 2004). Interestingly, when BAR domains are preceded by an amphipathic helix to form an N-BAR domain they also participate in the tubulation of the liposomes (Peter *et al.*, 2004; Gallop *et al.*, 2006). More recently, it has also been shown that PICK1 contains an N-BAR amphipathic helix located between residues 113-130 which dictates its preference for small liposomes of approximately 75nm in diameter (Herlo *et al.*, 2018). Mutating residues V121E, L125E in this region abolishes the density of PICK1 on small liposomes without affecting its membrane binding to larger 400nm liposomes. This would suggest that PICK1 also has the capacity to induce membrane curvature similar to the other N-BAR domain family members.

I was able to test the ability of PICK1 to induce changes in membrane shape in collaboration with Dr Hugh Tanner who performed cryo-EM imaging on liposomes after incubation with purified PICK1 (Figure 5.3.). In the absence of calcium, the lipid vesicles maintained their round morphology, however in the presence of 5µM calcium there were noticeable differences to the shape of the liposomes such that the vast majority became constricted to small, tubular structures. This correlates with the calcium concentration at which peak dimerisation occurs with purified PICK1. Another

method for determining the membrane bending activity of BAR domains proteins is through COS-7 cellular tubulation assay. Again, PICK1 showed a lack of tubulation in the absence of calcium, but maintained a calcium-dependent relationship in terms of the number of cells which presented with tubules and the number of tubules detected per cell (Figure 5.6.). These two results represent the first demonstration of the tubulating capacity of PICK1 both in a reduced system and within a cellular environment. The tubulation activity of PICK1 is different to other BAR domain containing proteins because it requires external stimulation in the form of calcium in order to promote membrane remodelling. Therefore, it is my understanding that this is a newly identified mechanism for BAR domain function which prompts further investigation.

6.2.4. PICK1 calcium-sensitive dimerisation could be a regulatory step for the initiation of membrane tubulation and the internalisation of GluA2-containing AMPARs

The generation of the PICK1 4A mutant which abolishes the ^{271}DDEE^{274} calcium binding site located within the BAR domain itself resulted in reduced overall dimerisation of the protein when expressed in cells or in purified form (Figures 5.3. and 5.4.). The mutant was insensitive to increasing calcium concentrations which suggests that the ability of PICK1 to form dimers depends on the cooperation between the calcium binding site located within the acidic N-terminal region to alleviate inhibition of dimerisation and the ^{271}DDEE^{274} region to promote dimerisation. Interestingly, the 4A mutant showed a calcium-dependent reduction in dimerisation starting from 1mM calcium similar to what is observed with the isolated BAR domain, which could suggest that the ^{271}DDEE^{274} site regulates concentration-dependent dimerisation, while the NT region regulates the overall extent of dimerisation in a calcium sensitive-manner. Furthermore, the binding of calcium to the NT region was shown to promote the interaction between PICK1 and GluA2 in a similar biphasic manner such that the peak was observed at 15μM calcium and was already reduced at 26 μM calcium (Hanley & Henley, 2005). This suggests that PICK1 dimerisation and the internalisation of GluA2 are connected and regulated in a similar manner in response to changes in local calcium concentrations induced during synaptic plasticity

resulting in the orchestration of the endocytic machinery. While WT-PICK1 showed a calcium relationship in terms of COS-7 tubulation, this was almost entirely abolished in the 4A mutant (Figure 5.5). Moreover, while the number of tubules per cells increased with calcium concentration, their lengths did not which suggests that calcium sensitive PICK1 dimerisation is important for the initiation of new tubules as opposed to the elongation of already existing ones. Based on molecular dynamics simulations assessing the conformation of the PICK1 dimer, Madasu and colleagues identified the region between residues 272-289 as critical for PICK1 function and proposed potential interactions with the PDZ domain or insertion within the membrane as possible mechanisms of action (Madasu *et al.*, 2015). Interestingly, the location of these residues is comparable to the N-terminal helix in endophilin, which has been shown to insert itself in the membrane during remodelling events (Gallop *et al.*, 2006; Ambroso *et al.*, 2014). This would suggest that PICK1 and endophilin share a similar mechanism employing two loop regions for membrane insertion and subsequent reshaping.

This offers interesting insight into what could be happening during PICK1-mediated AMPAR internalisation in response to LTD (Figure 6.1). The mechanism that I am proposing states that PICK1 is either maintained in a heterodimeric state of inhibition with ICA69 or another suitable BAR domain partner, or it is maintained at a relatively high level of monomers. In response to neuronal activity and the induction of LTD, calcium concentration is increased via NMDAR stimulation. When local calcium concentrations reach a certain threshold, calcium ions bind to the N-terminal acidic region of PICK1, the ^{271}DDEE^{274} region in the BAR domain and potentially other calcium-sensitive sites such as the C-terminal acidic region. This could either cause PICK1 to change its conformation or overall charge in a manner which promotes an upregulation in its homodimerisation within the cytoplasm or it could trigger membrane redistribution of the monomer where dimerisation could be favoured. Alternatively, PICK1 monomers could already be present in the proximity of membranes through their interaction with GluA2 and other transmembrane or membrane associated binding partners and the increase in calcium could promote dimerisation. Once the PICK1 dimer has been assembled, the activated PICK1 BAR domain can participate in membrane remodelling. This could be mediated by its amphipathic helix initiating curvature generation before other BAR domain proteins can be recruited to the emerging vesicle (Herlo *et al.*, 2018). Finally, PICK1 also recruits AP2 and dynamin2

to allow for the scission and internalisation of the newly formed endocytic vesicle (Fiuza *et al.*, 2017).

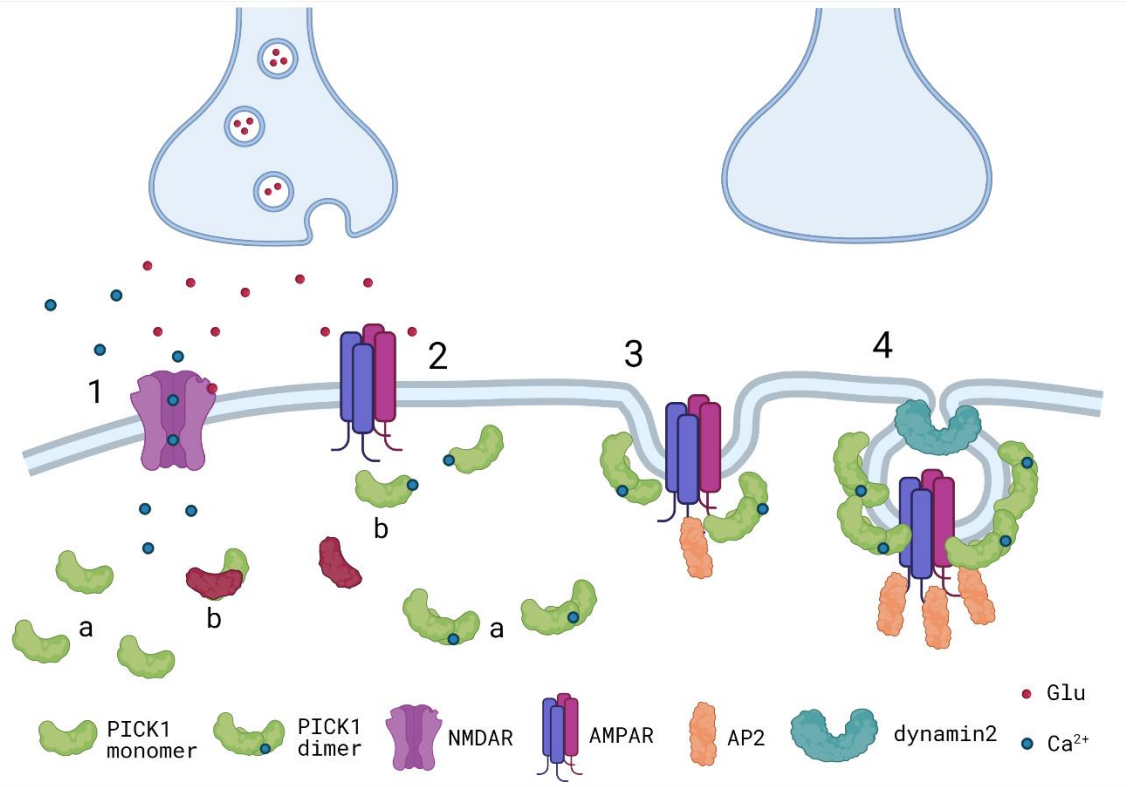

Figure 6.1.: Proposed mechanism for PICK1-mediated AMPAR endocytosis during synaptic plasticity. (1) PICK1 is maintained within the cytoplasm either in (a) a monomeric state or (b) in association with other suitable BAR domain-containing binding partners such as ICA69. (2) Neuronal signalling leads to the activation of AMPA and NMDARs in response to glutamate stimulation followed by intracellular calcium influx through opened NMDARs. Once calcium reaches a certain concentration, it is recognised and bound by PICK1 monomers which can then either (a) dimerise within the cytoplasm or (b) disassemble from heterodimers before redistributing to the plasma membrane where dimerisation could be favoured either by PICK1 interactions with the membrane or with PDZ-binding proteins. Alternatively, the dimers could be formed in the cytoplasm before localising to the membrane. (3) Once in the proximity of GluA2-containing AMPARs, PICK1 dimers could simultaneously promote the dissociation of AMPARs from synaptic anchoring proteins, the recruitment of AP2 and other proteins required for CME, as well as initiating membrane curvature generation. (4) The emerging vesicle is potentially surrounded by a scaffold consisting of PICK1 and other BAR domain-containing proteins which cooperate in order to achieve appropriate membrane constriction. PICK1 also then participates in the recruitment of dynamin2 to the neck of the vesicle to induce scission and intracellular release. Image generated with BioRender.com.

6.3. Future work

The results generated from this study outline a novel potential role for PICK1 in membrane remodelling, as well as a new regulatory mechanism for BAR domain function in response to external stimulation. However, many questions remain open and must be addressed in future work in order to gain full understanding of the implications that calcium-upregulated dimerisation has on PICK1 function during synaptic plasticity.

6.3.1. Where precisely does PICK1 dimerisation occur?

While I have been able to generate some evidence that PICK1 dimerisation is highest at the level of the dendritic spine in neurons and in distinct puncta within the cytoplasm of HEK293 cells, further resolution is required to distinguish between the plasma membrane and other various intracellular compartments. One possible strategy which could be adopted here is to perform FLIM-FRET imaging in conjunction with immunostaining for synaptic markers such as PSD-95, Homer1 or VGLUT, as well as immunostaining for various endocytic markers such as EEA1 for early endosomes and the Rab family of proteins for recycling or late endosomes. Furthermore, the importance of membrane binding for PICK1 dimerisation could be investigated by performing FLIM-FRET experiments with the lipid-binding deficient mutant 5KE which has been previously described in terms of its impaired membrane association (Citri *et al.*, 2010).

6.3.2. Does upregulated PICK1 homodimerisation represent a transition from a monomeric state or from a heterodimeric state?

It is yet unclear whether the changes in dimerisation levels recorded in response to NMDA stimulation through FLIM-FRET in neurons are a consequence of PICK1 monomers assembling into dimers, or whether it could represent a switch between PICK1 heterodimerisation with ICA69 and homodimerisation. One way to investigate this would be to co-transfect HEK293 cells with PICK1 and ICA69 in order to carry out the DSS/ionomycin crosslinking protocol in the presence of calcium before immunoblotting for ICA69 to assess whether there is a calcium-dependent decline in

the PICK1-ICA69 interaction. This could be confirmed later with FLIM-FRET investigations of the PICK1-ICA69 interaction after NMDA stimulation in neurons.

6.3.3. What is the calcium-binding kinetics for the ^{271}DDEE^{274} region within the PICK1 BAR domain?

Even though molecular dynamics simulations offered an indication that the ^{271}DDEE^{274} region is capable of forming a calcium binding pocket, it is important to verify this experimentally by isothermal titration calorimetry or liquid scintillation. By determining the calcium binding curve, more knowledge can be gained about the range of calcium concentrations which could affect this binding site.

6.3.4. Further characterisation of the different calcium-binding regions in PICK1 and their effect on dimerisation

In this study, I have looked at the N-terminal acidic region and the newly identified ^{271}DDEE^{274} region in terms of their effect on calcium-dependent dimerisation. However, it has also been shown that the C-terminal acidic region is able to bind calcium in a similar range to the N-terminal acidic region (Hanley & Henley, 2005). For a comprehensive understanding of the potentially different affinities and different roles that each of these regions might play, a separate investigation into the properties of each individual site is required by creating mutants which only contain one of the desired regions and testing them within the already established protocol for DSS crosslinking using purified protein and cell cultures. Furthermore, for an analysis of whether the different calcium sensing regions play differential roles during synaptic plasticity, the mutants could be used for FLIM-FRET imaging following LTD induction in neurons.

6.3.5. What is the effect of the 4A mutant on the tubulation of lipid vesicles in a reduced system? Does the tubulating activity of PICK1 in the presence of calcium depend on its amphipathic helix?

Further information about the newly described mechanism of calcium- and dimerisation-dependent tubulation of lipid vesicles by PICK1 can be obtained from EM imaging of purified 4A-PICK1 in the absence or presence of calcium after incubation with liposomes. Because the 4A mutant is unable to generate tubules in COS-7 cells, it would be interesting to see whether this is also impaired in a cell-free system. Further investigations could also address whether the amphipathic helix which has been recently shown to be essential for PICK1 curvature sensing (Herlo *et al.*, 2018) is also involved in calcium-dependent tubulation either through its complete deletion or through the V121E, L125E mutation which has been shown to impair curvature sensing.

6.3.6. What is the role of calcium-sensitive PICK1 dimerisation for the trafficking of GluA2-containing AMPARs during LTD?

Finally, more work is required in neurons in order to determine what the functional consequences of PICK1 calcium-sensitive dimerisation are for the removal of GluA2-containing AMPARs from the synapse during synaptic plasticity. The 4A mutant which is impaired in overall levels of dimerisation and insensitive to calcium upregulation of dimerisation will be useful in this approach. One possible technique to be used for studying AMPAR endocytosis is based on the antibody feeding assay where surface GluA2 is labelled with fluorescent antibodies prior to the induction of LTD, followed by fixing, permeabilization and differential labelling of the internalised GluA2. Another possibility is to use surface biotinylation were GluA2-containing AMPARs are labelled with biotin before LTD induction, after which the biotin label on the remaining surface receptors is cleaved and the extent of internalisation can be determined after neuronal lysis and Western blotting against biotin.

6.3.7. What is the role of calcium-dependent PICK1 dimerisation for the expression of synaptic plasticity in the form of LTP and LTD?

The investigation into the importance of calcium-induced PICK1 dimerisation for the expression of synaptic plasticity could be extended with electrophysiology experiments. Because PICK1 has been proposed to function during both forms of long-term synaptic plasticity (Sossa *et al.*, 2006; Terashima *et al.*, 2008), it would be interesting to assess the impact of dynamic PICK1 dimerisation on both LTP and LTD. To this extent, molecular replacement studies could be designed where wild-type PICK1 can be knocked out using viral vectors and replaced with the two mutants tested in my study before LTP and LTD induction via electrical stimulation. The effects observed with the ΔNT mutant could give an indication about what happens when PICK1 loses its ability to up-regulate dimerisation in response to calcium stimulation, whereas the 4A mutant would offer insight into whether impairing dimerisation overall has any significant detriments for either LTP or LTD. In addition, a deletion of the C-terminal acidic region in PICK1 could also be included in these experiments in order to achieve a full investigation into the three calcium-binding regions within the PICK1 structure. It would be interesting to assess whether dimerisation occurs as a consequence of the cooperation between these regions or whether certain regions have differential roles depending on the type of plasticity invoked.

6.4. Conclusion

In conclusion, the aim of this study was to characterise the dimerisation of PICK1 in response to stimulation that is relevant in the context of neuronal communication. Over the course of this report, I have shown that PICK1 dimerisation is dynamic in response to a certain calcium range and that this is mediated through acidic regions within the PICK1 structure which are capable of directly binding calcium ions. Furthermore, PICK1 dimerisation is significantly increased at the level of dendritic spine in neurons which had been chemically induced to express LTD. Importantly, PICK1 is capable of tubulating liposomes only in the presence of calcium, and the deletion of the ^{271}DDEE^{274} region within the BAR domain results in impaired dimerisation and abolished tubulation in a COS-7 assay. Together, these results provide the first evidence in support for a role for PICK1 in membrane remodelling, as well as the first

indication of upregulated BAR-domain dimerisation after stimulation. Moreover, these results offer preliminary insight into a potential mechanism for PICK1-mediated membrane curvature generation in response to intracellular calcium influx which could underlie AMPAR trafficking during synaptic plasticity. If extended with future work, the novel findings from this report could offer a significant contribution to the existing knowledge regarding PICK1 function during synaptic plasticity, as well as highlighting a new regulatory mechanism for BAR domain proteins.

References

Abraham, W.C., Jones, O.D. & Glanzman, D.L. (2019) Is plasticity of synapses the mechanism of long-term memory storage? *npj Science of Learning*, **4**, 9.

Ambroso, M.R., Hegde, B.G. & Langen, R. (2014) Endophilin A1 induces different membrane shapes using a conformational switch that is regulated by phosphorylation. *PNAS*, **111**, 6982-6987.

Ammendrup-Johnsen, I., Thorsen, T.S., Gether, U. & Madsen, K.L. (2012) Serine 77 in the PDZ domain of PICK1 is a protein kinase Cα phosphorylation site regulated by lipid membrane binding. *Biochemistry*, **51**, 586-596.

Anggono, V., Koc-Schmitz, Y., Widagdo, J., Kormann, J., Quan, A., Chen, C.-M., Robinson, P.J., Choi, S.-Y., Linden, D.J., Plomann, M. & Huganir, R.L. (2013) PICK1 interacts with PACSIN to regulate AMPA receptor internalization and cerebellar long-term depression. *PNAS*, **110**, 13976-13981.

Antoniou, A., Baptista, M., Carney, N. & Hanley, J.G. (2014) PICK1 links Argonaute 2 to endosomes in neuronal dendrites and regulates miRNA activity. *EMBO Reports*, **15**, 548-556.

Araki, Y. & Huganir, R.L. (2010) Plasma membrane insertion of the AMPA receptor GluA2 subunit is regulated by NSF binding and Q/R editing of the ion pore. *PNAS*, **107**, 11080-11085.

Babiec, W.E., Guglietta, R., Jami, S.A., Morishita, W., Malenka, R.C. & O'Dell, T.J. (2014) Ionotropic NMDA receptor signaling is required for the induction of long-term depression in the mouse hippocampal CA1 region. *Journal of Neuroscience*, **34**, 5285-5290.

Bajar, B.T., Wang, E.S., Zhang, S., Lin, M.Z. & Chu, J. (2016) A Guide to Fluorescent Protein FRET Pairs. *Sensors*, **16**, 1488.

Becker, W. (2012) Fluorescence lifetime imaging – techniques and applications. *Journal of Microscopy*, **247**, 119-136.

Bedecarrats, A., Chen, S., Pearce, K., Cai, D. & Glanzman, D.L. (2018) RNA from Trained Aplysia Can Induce an Epigenetic Engram for Long-Term Sensitization in Untrained Aplysia. *eNeuro*, 0038-0018.2018.

Bell, M., Bartol, T., Sejnowski, T. & Rangamani, P. (2019) Dendritic spine geometry and spine apparatus organization govern the spatiotemporal dynamics of calcium. *Journal of General Physiology*, **151**, 1017-1034.

Ben-Yaacov, A., Gillor, M., Haham, T., Parsai, A., Qneibi, M. & Stern-Bach, Y. (2017) Molecular Mechanism of AMPA Receptor Modulation by TARP/Stargazin. *Neuron*, **93**, 1126-1137.

Bertot, L., Grassart, A., Lagache, T., Nardi, G., Basquin, C., Olivo-Marin, J.-C. & Sauvonnet, N. (2018) Quantitative and Statistical Study of the Dynamics of Clathrin-Dependent and -Independent Endocytosis Reveal a Differential Role of EndophilinA2. *Cell Reports*, **22**, 1574-1588.

Bhatia, V.K., Madsen, K.L., Bolinger, P.-Y., Kunding, A., Hedegard, P., Gether, U. & Stamou, D. (2009) Amphipathic motifs in BAR domains are essential for membrane curvature sensing. *EMBO Journal*, **28**, 3303-3314.

Bissen, D., Foss, F. & Acker-Palmer, A. (2019) AMPA receptors and their minions: auxiliary proteins in AMPA receptor trafficking. *Cellular and Molecular Life Sciences*, **76**, 2133-2169.

Bliss, T.V.P. & Lomo, T. (1973) Long-lasting potentiation of synaptic transmission in the dentate area of the anaesthetized rabbit following stimulation of the perforant path. *Journal of Physiology*, **232**, 331-356.

Blood, P.D. & Voth, G.A. (2006) Direct observation of Bin/amphiphysin/Rvs (BAR) domain-induced membrane curvature by means of molecular dynamics simulations. *PNAS*, **103**, 15068-15072.

Bolia, A., Gerek, Z.N., Keskin, O., Ozkan, S.B. & Dev, K.K. (2012) The Binding Affinities of Proteins Interacting With the PDZ Domain of PICK1. *Proteins*, **80**, 1393-1408.

Brett, T.J., Traub, L.M. & Fremont, D.H. (2002) Accessory Protein Recruitment Motifs in Clathrin-Mediated Endocytosis. *Structure*, **10**, 797-809.

Breuer, A., Lauritsen, L., Bertseva, E., Vonkova, I. & Stamou, D. (2019) Quantitative investigation of negative membrane curvature sensing and generation by I-BARs in filopodia of living cells. *Soft Matter*, **15**, 9829-9829.

Burnashev, N., Monyer, H., Seeburg, P.H. & Sakmann, B. (1992) Divalent ion permeability of AMPA receptor channels is dominated by the edited form of a single subunit. *Neuron*, **8**, 189-198.

Callender, J.A. & Newton, A.C. (2017) Conventional protein kinase C in the brain: 40 years later. *Neuronal Signaling*, **1**, NS20160005.

Cao, M., Mao, Z., Kam, C., Xiao, N., Cao, X., Shen, C., Cheng, K.K.Y., Xu, A., Lee, K.-M., Jiang, L. & Xia, J. (2013) PICK1 and ICA69 control insulin granule trafficking and their deficiencies lead to impaired glucose tolerance. *PloS Biology*, **11**, e1001541.

Cao, M., Xu, J., Shen, C., Kam, C., Huganir, R.L. & Xia, J. (2007) PICK1–ICA69 Heteromeric BAR Domain Complex Regulates Synaptic Targeting and Surface Expression of AMPA Receptors. *Journal of Neuroscience*, **27**, 12945-12956.

Capraro, B.R., Shi, Z., Wu, T., Chen, Z., Dunn, J.M., Rhoades, E. & Baumgart, T. (2013) Kinetics of Endophilin N-BAR Domain Dimerization and Membrane Interactions. *Journal of Biological Chemistry*, **288**, 12533-12543.

Casares, D., Escriba, P.V. & Rossello, C.A. (2019) Membrane Lipid Composition: Effect on Membrane and Organelle Structure, Function and Compartmentalization and Therapeutic Avenues. *International Journal of Molecular Sciences*, **20**, 2167.

Chen, L., Chetkovich, D.M., Petralia, R.S., Sweeney, N.T., Kawasaki, Y., Wenthold, R.J., Bredt, D.S. & Nicoll, R.A. (2000) Stargazin regulates synaptic targeting of AMPA receptors by two distinct mechanisms. *Nature*, **408**, 936-943.

Chen, X., Levy, J.M., Hou, A., Winters, C., Azzam, R., Sousa, A.A., Leapman, R.D., Nicoll, R.A. & Reese, T.S. (2015) PSD-95 family MAGUKs are essential for anchoring AMPA and NMDA receptor complexes at the postsynaptic density. *PNAS*, **112**, E6983-E6992.

Chial, H.J., Wu, R., Ustach, C.V., McPhail, L.C., Mobley, W.C. & Chen, Y.Q. (2008) Membrane Targeting by APPL1 and APPL2: Dynamic Scaffolds that Oligomerize and Bind Phosphoinositides. *Traffic*, **9**, 215-229.

Chung, H.J., Xia, J., Scannevin, R.H., Zhang, X. & Huganir, R.L. (2000) Phosphorylation of the AMPA receptor subunit GluR2 differentially regulates its interaction with PDZ domain-containing proteins. *Journal of Neuroscience*, **20**, 7258-7267.

Cichon, J. & Gan, W.-B. (2015) Branch-specific dendritic Ca2+ spikes cause persistent synaptic plasticity. *Nature*, **520**, 180-185.

Citri, A., Bhattacharyya, S., Ma, C., Morishita, W., Fang, S., Rizo, J. & Malenka, R.C. (2010) Calcium Binding to PICK1 Is Essential for the Intracellular Retention of AMPA Receptors Underlying Long-Term Depression. *Journal of Neuroscience*, **30**, 16437-16452.

Citri, A. & Malenka, R.C. (2008) Synaptic Plasticity: Multiple Forms, Functions, and Mechanisms. *Neuropsychopharmacology Reviews*, **33**, 18-41.

Clarke, J.R., Cammarota, M., Gruart, A., Izquierdo, I. & Delgado-Garcia, J.M. (2010) Plastic modifications induced by object recognition memory processing. *PNAS*, **107**, 2652-2657.

Colgan, L.A., Hu, M., Misler, J.A., Parra-Bueno, P., Moran, C.M., Leitges, M. & Yasuda, R. (2018) PKCα integrates spatiotemporally distinct Ca2+ and autocrine BDNF signaling to facilitate synaptic plasticity. *Nature Neuroscience*, **21**, 1027-1037.

Constantini, L.M., Fossati, M., Francolini, M. & Snapp, E.L. (2012) Assessing the Tendency of Fluorescent Proteins to Oligomerize under Physiologic Conditions. *Traffic*, **13**, 643-649.

Cornelisse, L.N., van Elburg, R.A.J., Meredith, R.M., Yuste, R. & Mansvelder, H.D. (2007) High Speed Two-Photon Imaging of Calcium Dynamics in Dendritic Spines: Consequences for Spine Calcium Kinetics and Buffer Capacity. *pLoS One*, **2**, e1073.

Coultrap, S.J., Freund, R.K., O'Leary, H., Sanderson, J.L., Roche, K.W., Dell'Acqua, M.L. & Ulrich Bayer, K. (2014) Autonomous CaMKII mediates both LTP and LTD using a mechanism for differential substrate site selection. *Cell Reports*, **6**, 431-437.

Cross, S. (2021) SJCross/ModularImageAnalysis: Version v0.17.0. DOI 10.5281/zenodo.1201320. Last accessed 22.02.2021.

Demeautis, C., Sipieter, F., Roul, J., Chapuis, C., Padilla-Parra, S., Riquet, F.B. & Tramier, M. (2017) Multiplexing PKA and ERK1&2 kinases FRET biosensors in living cells using single excitation wavelength dual colour FLIM. *Scientific Reports*, **7**, 41026.

Dev, K.K., Nakanishi, S. & Henley, J.M. (2004) The PDZ Domain of PICK1 Differentially Accepts Protein Kinase C-α and GluR2 as Interacting Ligands. *Journal of Biological Chemistry*, **279**, 41393-41397.

Diering, G.H. & Huganir, R.L. (2018) The AMPA Receptor Code of Synaptic Plasticity. *Neuron*, **100**, 314-329.

Dislich, B., Than, M.E. & Lichtenthaler, S.F. (2010) Specific amino acids in the BAR domain allow homodimerization and prevent heterodimerization of sorting nexin 33. *Biochemical Journal*, **433**, 75-83.

Dore, K., Labrecque, S., Tardif, C. & De Koninck, P. (2014) FRET-FLIM Investigation of PSD95-NMDA Receptor Interaction in Dendritic Spines; Control by Calpain, CaMKII and Src Family Kinase. *PLoS One*, **9**, e112170.

Dudek, S.M. & Bear, M.F. (1992) Homosynaptic long-term depression in area CA1 of hippocampus and effects of N-methyl-D-aspartate receptor blockade. *PNAS*, **89**, 4263-4267.

Duke, C.G., Kennedy, A.J., Gavin, C.F., Day, J.J. & Sweatt, J.D. (2017) Experience-dependent epigenomic reorganization in the hippocampus. *Learning and Memory*, **24**, 278-288.

Duncan, R.R., Bergmann, A., Cousin, M.A., Apps, D.K. & Shipston, M.J. (2004) Multi-Dimensional Time-Correlated Single Photon Counting (TCSPC) Fluorescence Lifetime Imaging Microscopy (FLIM) to Detect FRET in Cells. *Journal of Microscopy*, **215**, 1-12.

Dunwiddie, T. & Lynch, G. (1978) Long-term potentiation and depression of synaptic responses in the rat hippocampus: localization and frequency dependency. *Journal of Physiology*, **276**, 353-367.

Ehlers, M.D. (2000) Reinsertion or Degradation of AMPA Receptors Determined by Activity-Dependent Endocytic Sorting. *Neuron*, **28**, 511-525.

Elias, G.M., Elias, L.A.B., Apostolides, P.F., Kriegstein, A.R. & Nicoll, R.A. (2008) Differential trafficking of AMPA and NMDA receptors by SAP102 and PSD-95 underlies synapse development. *PNAS*, **105**, 20953-20958.

Erlendsson, S. & Madsen, K.L. (2015) Membrane Binding and Modulation of the PDZ Domain of PICK1. *Membranes*, **5**, 597-615.

Erlendsson, S., Rathje, M., Heidarsson, P.O., Poulsen, F.M., Madsen, K.L., Teilum, K. & Gether, U. (2014) Protein Interacting with C-kinase 1 (PICK1) Binding Promiscuity Relies on Unconventional PSD-95/Discs-Large/ZO-1 Homology (PDZ) Binding Modes for Nonclass II PDZ Ligands. *Journal of Biological Chemistry*, **289**, 25327-25340.

Fiuza, M., Rostosky, C.M., Parkinson, G.T., Bygrave, A.M., Halemani, N., Baptista, M., Milosevic, I. & Hanley, J.G. (2017) PICK1 regulates AMPA receptor endocytosis via direct interactions with AP2 α-appendage and dynamin. *Journal of Cell Biology*, **216**, 3323-3338.

Förster, T. (2012) Energy migration and fluorescence. *Journal of Biomedical Optics*, **17**, 011002.

Foster, T.C. & Kumar, A. (2007) Susceptibility to induction of long-term depression is associated with impaired memory in aged Fischer 344 rats. *Neurobiology of Learning and Memory*, **87**, 522-535.

Frost, A., Perera, R., Roux, A., Spasov, K., Destaing, O., Egelman, E.H., De Camilli, P. & Unger, V.M. (2008) Structural Basis of Membrane Invagination by F-BAR Domains. *Cell*, **132**, 807-817.

Fujii, K., Maeda, K., Hikida, T., Mustafa, A.K., Balkissoon, R., Xia, J., Yamada, T., Ozeki, Y., Kawahara, R., Okawa, M., Huganir, R.L., Ujike, H., Snyder, S.H. & Sawa, A. (2006) Serine racemase binds to PICK1: potential relevance to schizophrenia. *Molecular Psyciatry*, **11**, 150-157.

Gallop, J.L., Jao, C.C., Kent, H.M., Butler, P.J.G., Evans, P.R., Langen, R. & McMahon, H.T. (2006) Mechanism of endophilin N-BAR domain-mediated membrane curvature. *EMBO Journal*, **25**, 2898-2910.

Gardner, S.M., Takamiya, K., Xia, J., Suh, J.-G., Johnson, R., Yu, S. & Huganir, R.L. (2005) Calcium-Permeable AMPA Receptor Plasticity Is Mediated by Subunit-Specific Interactions with PICK1 and NSF. *Neuron*, **45**, 903-915.

Gortat, A., San-Roman, M.J., Vannier, C. & Schmidt, A.A. (2012) Single Point Mutation in Bin/Amphiphysin/Rvs (BAR) Sequence of Endophilin Impairs Dimerization, Membrane Shaping, and Src Homology 3 Domain-mediated Partnership. *Journal of Biological Chemistry*, **287**, 4232-4247.

Greger, I.H., Khatri, L. & Ziff, E.B. (2002) RNA Editing at Arg607 Controls AMPA Receptor Exit from the Endoplasmic Reticulum. *Neuron*, **34**, 759-772.

Grienberger, C., Chen, X. & Konnerth, A. (2014) NMDA Receptor-Dependent Multidendrite Ca2+ Spikes Required for Hippocampal Burst Firing In Vivo. *Neuron*, **81**, 1274-1281.

Gruber, T. & Balbach, J. (2015) Protein Folding Mechanism of the Dimeric AmphiphysinII/Bin1 N-BAR Domain. *pLoS One*, **10**, e0136922.

Gu, X., Mao, X., Lussier, M.P., Hutchinson, M.A., Zhou, L., Hamra, F.K., Roche, K.W. & Lu, W. (2016) GSG1L suppresses AMPA receptor-mediated synaptic transmission and uniquely modulates AMPA receptor kinetics in hippocampal neurons. *Nature Communications*, **2**, 10873.

Guthrie, P.B., Segal, M. & Kater, S.B. (1991) Independent regulation of calcium revealed by imaging dendritic spines. *Nature*, **354**, 76-80.

Haglerod, C., Kapic, A., Boulland, J.-L., Hussain, S., Holen, T., Skare, O., Laake, P., Ottersen, O.P., Haug, F.-M.S. & Davanger, S. (2009) Protein interacting with C kinase 1 (PICK1) and GluR2 are associated with presynaptic plasma membrane and vesicles in hippocampal excitatory synapses. *Neuroscience*, **158**, 242-252.

Halder, R., Hennion, M., Vidal, R.O., Shomroni, O., Rahman, R.-U., Rajput, A., Centeno, T.P., van Bebber, F., Capece, V., Garcia Vizcaino, J.C., Schuetz, A.-L., Burkhardt, S., Benito, E., Sala, M.N., Javan, S.B., Haass, C., Schmid, B., Fischer, A. & Bonn, S. (2016) DNA methylation changes in plasticity genes accompany the formation and maintenance of memory. *Nature Neuroscience*, **19**, 102-110.

Han, D.S. & Weinstein, H. (2008) Auto-inhibition in the multi-domain protein PICK1 revealed by dynamic models of its quaternary structure. *Biophysical Journal*, **94**, 67-76.

Hanley, J.G. (2018) The Regulation of AMPA Receptor Endocytosis by Dynamic Protein-Protein Interactions. *Frontiers in Cellular Neuroscience*, **12**, 362.

Hanley, J.G. & Henley, J.M. (2005) PICK1 is a calcium-sensor for NMDA-induced AMPA receptor trafficking. *EMBO Journal*, **24**, 3266-3278.

Hanley, J.G., Khatri, L., Hanson, P.I. & Ziff, E.B. (2002) NSF ATPase and α-/β-SNAPs Disassemble the AMPA Receptor-PICK1 Complex. *Neuron*, **34**, 53-67.

Hansel, C., Artola, A. & Singer, W. (1997) Relation between dendritic Ca2+ levels and the polarity of synaptic long-term modifications in rat visual cortex neurons. *European Journal of Neuroscience*, **9**, 2309-2322.

Harmel, N., Cokic, B., Zolles, G., Berkenfeld, H., Mauric, V., Fakler, B., Stein, V. & Klocker, N. (2012) AMPA Receptors Commandeer an Ancient Cargo Exporter for Use as an Auxiliary Subunit for Signaling. *pLoS One*, **7**, e30681.

Harney, S.C., Rowan, M. & Anwyl, R. (2006) Long-Term Depression of NMDA Receptor-Mediated Synaptic Transmission Is Dependent on Activation of Metabotropic Glutamate Receptors and Is Altered to Long-Term Potentiation by Low Intracellular Calcium Buffering. *Journal of Neuroscience*, **26**, 1128-1132.

Haucke, V. & Kozlov, M.M. (2018) Membrane remodeling in clathrin-mediated endocytosis. *Journal of Cell Science*, **131**, jcs216812.

He, J., Xia, M., Yeung, P.K.K., Li, J., Li, Z., Chung, K.K., Chung, S.K. & Xia, J. (2018) PICK1 inhibits the E3 ubiquitin ligase activity of Parkin and reduces its neuronal protective effect. *PNAS*, **115**, E7193-E7201.

He, Y., Liwo, A., Weinstein, H. & Scheraga, H.A. (2011) PDZ binding to the BAR domain of PICK1 is elucidated by coarse-grained molecular dynamics. *Journal of Molecular Biology*, **405**, 298-314.

Hebb, D.O. (1949) The organization of behavior; a neuropsychological theory.

Henley, J.M. & Wilkinson, K.A. (2013) AMPA receptor trafficking and the mechanisms underlying synaptic plasticity and cognitive aging. *Dialogues in Clinical Neuroscience*, **15**, 11-27.

Henne, W.M., Kent, H.M., Ford, M.G.J., Hedge, B.G., Daumke, O., Butler, P.J.G., Mittal, R., Langen, R., Evans, P.R. & McMahon, H.T. (2007) Structure and Analysis of FCHo2 F-BAR Domain: A Dimerizing and Membrane Recruitment Module that Effects Membrane Curvature. *Structure*, **15**, 839-852.

Herlo, R., Lund, V.K., Lycas, M.D., Jansen, A.M., Khelashvili, G., Andersen, R.C., Bhatia, V., Pederson, T.S., Albornoz, P.B.C., Johner, N., Ammendrup-Johnsen, I., Christensen, N.R., Erlendsson, S., Stoklund, M., Larsen, J.B., Weinstein, H., Kjaerulff, O., Stamou, D., Gether, U. & Madsen, K.L. (2018) An Amphipathic Helix Directs Cellular Membrane Curvature Sensing and Function of the BAR Domain Protein PICK1. *Cell Reports*, **23**, 2056-2069.

Heynen, A.J., Abraham, W.C. & Bear, M.F. (1996) Bidirectional modification of CA1 synapses in the adult hippocampus in vivo. *Nature*, **381**, 163-166.

Hiester, B.G., Becker, M.I., Bowen, A.B., Schwartz, S.L. & Kennedy, M.J. (2018) Mechanisms and Role of Dendritic Membrane Trafficking for Long-Term Potentiation. *Frontiers in Cellular Neuroscience*, **12**, 391.

Higley, M.J. & Sabatini, B.L. (2012) Calcium Signaling in Dendritic Spines. *Cold Spring Harbor Perspectives in Biology*, **4**, a005686.

Hirata, E. & Kiyokawa, E. (2019) ERK Activity Imaging During Migration of Living Cells In Vitro and In Vivo. *International Journal of Molecular Sciences*, **20**, 679.

Hirsch, J.C. & Crepel, F. (1992) Postsynaptic calcium is necessary for the induction of LTP and LTD of monosynaptic EPSPs in prefrontal neurons: An in vitro study in the rat. *Synapse*, **10**, 173-175.

Hofer, S.B., Mrsic-Flogel, T.D., Bonhoeffer, T. & Hubener, M. (2009) Experience leaves a lasting structural trace in cortical circuits. *Nature*, **457**, 313-317.

Holst, B., Madsen, K.L., Jansen, A.M., Jin, C., Rickhag, M., Lund, V.K., Jensen, M., Bhatia, V., Sorensen, G., Madsen, A.N., Xue, Z., Moller, S.K., Worldbye, D., Qvortrup, K., Huganir, R., Stamou, D., Kjaerulff, O. & Gether, U. (2013) PICK1 Deficiency Impairs Secretory Vesicle Biogenesis and Leads to Growth Retardation and Decreased Glucose Tolerance. *PLoS*, **11**, e1001542.

Holthoff, K., Tsay, D. & Yuste, R. (2002) Calcium Dynamics of Spines Depend on Their Dendritic Location. *Neuron*, **33**, 425-437.

Hunt, D.L. & Castillo, P.E. (2012) Synaptic plasticity of NMDA receptors: mechanisms and functional implications. *Current Opinion in Neurobiology*, **22**, 496-508.

Isas, J.M., Ambroso, M.R., Hedge, P.B., Langen, J. & Langen, R. (2015) Tubulation by amphiphysin requires concentration-dependent switching from wedging to scaffolding. *Structure*, **23**, 873-881.

Itoh, T., Erdmann, K.S., Roux, A., Habermann, B., Werner, H. & De Camilli, P. (2005) Dynamin and the Actin Cytoskeleton Cooperatively Regulate Plasma Membrane Invagination by BAR and F-BAR Proteins. *Developmental Cell*, **9**, 791-804.

Iwakura, Y., Nagano, T., Kawamura, M., Horikawa, H., Ibaraki, K., Takei, N. & Nawa, H. (2001) N-Methyl-D-aspartate-induced α-Amino-3-hydroxy-5-methyl-4-isoxazoleproprionic Acid (AMPA) Receptor Down-regulation Involves Interaction of the Carboxyl Terminus of GluR2/3 with Pick1. *Journal of Biological Chemistry*, **276**, 40025-40032.

Jaafari, N., Henley, J.M. & Hanley, J.G. (2012) PICK1 Mediates Transient Synaptic Expression of GluA2-Lacking AMPA Receptors during Glycine-Induced AMPA Receptor Trafficking. *Journal of Neuroscience*, **32**, 11618-11630.

Jin, W., Ge, W.-P., Xu, J., Cao, M., Peng, L., Yung, W., Liao, D., Duan, S., Zhang, M. & Xia, J. (2006) Lipid Binding Regulates Synaptic Targeting of PICK1, AMPA Receptor Trafficking, and Synaptic Plasticity. *Journal of Neuroscience*, **26**, 2380-2390.

Jin, Y.-H., Wu, X.-S., Shi, B., Zhang, Z., Guo, X., Gan, L., Chen, Z. & Wu, L.-G. (2019) Protein Kinase C and Calmodulin Serve As Calcium Sensors for Calcium-Stimulated Endocytosis at Synapses. *Journal of Neuroscience*, **39**, 9478-9490.

Josselyn, S.A. & Tonegawa, S. (2020) Memory engrams: Recalling the past and imagining the future. *Science*, **367**, eaaw4325.

Kaksonen, M. & Roux, A. (2018) Mechanisms of clathrin-mediated endocytosis. *Nature Reviews Mollecular Cell Biology*, **19**, 313-326.

Kanwisher, N. (2010) Functional specificity in the human brain: A window into the functional architecture of the mind. *PNAS*, **107**, 11163-11170.

Karlsen, M.L., Thorsen, T.S., Johner, N., Ammendrup-Johnsen, I., Erlendsson, S., Tian, X., Simonsen, J.B., Hoiberg-Nielsen, R., Christensen, N.M., Khelashvili, G., Streicher, W., Teilum, K., Vestergaard, B., Weinstein, H., Gether, U., Arleth, L. & Madsen, K.L. (2015) Structure of dimeric and tetrameric complexes of the BAR domain protein PICK1 determined by small-angle X-ray scattering. *Structure*, **23**, 1258-1270.

Kastning, K., Kukhtina, V., Kittler, J.T., Chen, G., Pechstein, A., Enders, S., Lee, S.H., Sheng, M., Yan, Z. & Haucke, V. (2007) Molecular determinants for the interaction between AMPA receptors and the clathrin adaptor complex AP-2. *PNAS*, **104**, 2991-2996.

Kato, A.S., Gill, M.B., Ho, M.T., Yu, H., Tu, Y., Siuda, E.R., Wang, H., Qian, Y.-W., Nisenbaum, E.S., Tomita, S. & Bredt, D.S. (2010) Hippocampal AMPA Receptor Gating Controlled by Both TARP and Cornichon Proteins. *Neuron*, **68**, 1082-1096.

Kemp, A. & Manahan-Vaughan, D. (2004) Hippocampal long-term depression and long-term potentiation encode different aspects of novelty acquisition. *PNAS*, **101**, 8192-8197.

Kim, C.-H., Chung, H.J., Lee, H.-K. & Huganir, R.L. (2001) Interaction of the AMPA receptor subunit GluR2/3 with PDZ domains regulates hippocampal long-term depression. *PNAS*, **98**, 11725-11730.

Kim, E. & Sheng, M. (2004) PDZ domain proteins of synapses. *Nature Reviews Neuroscience*, **5**, 771-781.

Kirchhausen, T., Owen, D. & Harrison, S.C. (2014) Molecular Structure, Function, and Dynamics of Clathrin-Mediated Membrane Traffic. *Cold Spring Harbor Perspectives in Biology*, **6**, a016725.

Kittler, J.T., Delmas, P., Jovanovic, J.N., Brown, D.A., Smart, T.G. & Moss, S.J. (2000) Constitutive Endocytosis of GABAA Receptors by an Association with the Adaptin AP2 Complex Modulates Inhibitory Synaptic Currents in Hippocampal Neurons. *Journal of Neuroscience*, **20**, 7972-7977.

Kvainickas, A., Jimenez-Orgaz, A., Nagele, H., Hu, Z., Dengjel, J. & Steinberg, F. (2017) Cargo-selective SNX-BAR proteins mediate retromer trimer independent retrograde transport. *Journal of Cell Biology*, **216**, 3677-3693.

Laviv, T., Scholl, B., Parra-Bueno, P., Foote, B., Zhang, C., Yan, L., Hayano, Y., Chu, J. & Yasuda, R. (2020) In Vivo Imaging of the Coupling between Neuronal and CREB Activity in the Mouse Brain. *Neuron*, **105**, 799-812.

Lee, H.-J. & Zheng, J.J. (2010) PDZ domains and their binding partners: structure, specificity, and modification. *Cell Communication and Signaling*, **8**, 8.

Lee, S.-J.R., Escobedo-Lozoya, Y., Szatmari, E.M. & Yasuda, R. (2009) Activation of CaMKII in single dendritic spines during long-term potentiation. *Nature*, **458**, 299-304.

Lee, S.H., Liu, L., Wang, Y.T. & Sheng, M. (2002) Clathrin Adaptor AP2 and NSF Interact with Overlapping Sites of GluR2 and Play Distinct Roles in AMPA Receptor Trafficking and Hippocampal LTD. *Neuron*, **36**, 661-674.

Li, Y.-H., Zhang, N., Wang, Y.-N., Shen, Y. & Wang, Y. (2016) Multiple faces of protein interacting with C kinase 1 (PICK1): Structure, function, and diseases. *Neurochemistry International*, **98**, 115-121.

Lin, D.-T. & Huganir, R.L. (2007) PICK1 and phosphorylation of the glutamate receptor 2 (GluR2) AMPA receptor subunit regulates GluR2 recycling after NMDA receptor-induced internalization. *Journal of Neuroscience*, **27**, 13903-13908.

Lin, E.Y.S., Silvian, L.F., Marcotte, D.J., Banos, C.C., Jow, F., Chan, T.R., Arduini, R.M., Qian, F., Baker, D.P., Bergeron, C., Hession, C., A,, Huganir, R.L., Borenstein, C.F., Enyedy, I., Zou, J., Rohde, E., Wittmann, M., Kumaravel, G., Rhodes, K.J., Scannevin, R.H., Dunah, A.W. & Guckian, K.M. (2018) Potent PDZ-Domain PICK1 Inhibitors that Modulate Amyloid Beta-Mediated Synaptic Dysfunction. *Scientific Reports*, **8**, 13438.

Lisman, J., Cooper, K., Sehgal, M. & Silva, A.J. (2018) Memory formation depends on both synapse-specific modifications of synaptic strength and cell-specific increases in excitability. *Nature Neuroscience*, **21**, 309-314.

Liu, L., Wong, T.P., Pozza, M.F., Lingenhoehl, K., Wang, Y., Sheng, M., Auberson, Y.P. & Wang, Y.T. (2004) Role of NMDA Receptor Subtypes in Governing the Direction of Hippocampal Synaptic Plasticity. *Science*, **304**, 1021-1024.

Loebrich, S., Benoit, M.R., Konopka, J.A., Cottrell, J.R., Gibson, J. & Nedivi, E. (2016) CPG2 Recruits Endophilin B2 to the Cytoskeleton for Activity-Dependent Endocytosis of Synaptic Glutamate Receptors. *Current Biology*, **26**, 296-308.

Loebrich, S., Djukic, B., Tong, Z.J., Cottrell, J.R., Turrigiano, G.G. & Nedivi, E. (2013) Regulation of glutamate receptor internalization by the spine cytoskeleton is mediated by its PKA-dependent association with CPG2. *PNAS*, **110**, E4548-E4556.

Lu, W., Khatri, L. & Ziff, E.B. (2014) Trafficking of α-Amino-3-hydroxy-5-methyl-4-isoxazolepropionic Acid Receptor (AMPA) Receptor Subunit GluA2 from the Endoplasmic Reticulum Is Stimulated by a Complex Containing Ca2+/Calmodulin-activated Kinase II (CaMKII) and PICK1 Protein and by Release of Ca2+ from Internal Stores. *Journal of Biological Chemistry*, **289**, 19218-19230.

Lu, W. & Ziff, E.B. (2005) PICK1 Interacts with ABP/GRIP to Regulate AMPA Receptor Trafficking. *Neuron*, **47**, 407-421.

Luscher, C. & Malenka, R.C. (2012) NMDA Receptor-Dependent Long-Term Potentiation and Long-Term Depression (LTP/LTD). *Cold Spring Harbor Perspectives in Biology*, 4:a005710.

Ma, L., Jongbloets, B.C., Xiong, W.-H., Melander, J.B., Qin, M., Lameyer, T.J., Harrison, M.F., Zemelman, B.V., Mao, T. & Zhong, H. (2018) A Highly Sensitive A-Kinase Activity Reporter for Imaging Neuromodulatory Events in Awake Mice. *Neuron*, **99**, 665-679.e665.

Madasu, Y., Yang, C., Boczkowska, M., Bethoney, K.A., Zwolak, A., Rebowski, G., Svitkina, T. & Dominguez, R. (2015) PICK1 is implicated in organelle motility in an Arp2/3 complex–independent manner. *Molecular Biology of the Cell*, **26**, 1308-1322.

Madsen, K.L., Beuming, T., Niv, M.Y., Dev, K.K. & Weinstein, H. (2005) Molecular Determinants for the Complex Binding Specificity of the PDZ Domain in PICK1. *Journal of Biological Chemistry*, **280**, 20539-20548.

Madsen, K.L., Eriksen, J., Milan-Lobo, L., Han, D.S., Niv, M.Y., Ammendrup-Johnsen, I., Henriksen, U., Bhatia, V.K., Stamou, D., Sitte, H.H., McMahon, H.T., Weinstein, H. & Gether, U. (2008) Membrane Localization is Critical for Activation of the PICK1 BAR Domain. *Traffic*, **9**, 1327-1343.

Madsen, K.L., Thorsen, T.S., Rahbek-Clemmensen, T., Eriksen, J. & Gether, U. (2012) Protein Interacting with C Kinase 1 (PICK1) Reduces Reinsertion Rates of Interaction Partners Sorted to Rab11-dependent Slow Recycling Pathway. *Journal of Biological Chemistry*, **287**, 12293-12308.

Mahmood, M.I., Noguchi, H. & Okazaki, K.-I. (2019) Curvature induction and sensing of the F-BAR protein Pacsin1 on lipid membranes via molecular dynamics simulations. *Scientific Reports*, **9**, 14557.

Man, H.-Y., Lin, J.W., Ju, W.H., Ahmadian, G., Liu, L., Becker, L.E., Sheng, M. & Wang, Y.T. (2000) Regulation of AMPA Receptor–Mediated Synaptic Transmission by Clathrin-Dependent Receptor Internalization. *Neuron*, **25**, 649-662.

Martin, K.J., McGhee, E.J., Schwarz, J.P., Drysdale, M., Brachmann, S.M., Stucke, V., Sansom, O.J. & Anderson, K.I. (2018) Accepting from the best donor; analysis of long-lifetime donor fluorescent protein pairings to optimise dynamic FLIM-based FRET experiments. *PLoS One*, **13**, e0183585.

Masuda, M., Takeda, S., Sone, M., Ohki, T., Mori, H., Kamioka, Y. & Mochizuki, N. (2006) Endophilin BAR domain drives membrane curvature by two newly identified structure-based mechanisms. *EMBO Journal*, **25**, 2889-2897.

Matsuda, S., Kakegawa, W., Budisantoso, T., Nomura, T., Kohda, K. & Yazuki, M. (2013) Stargazin regulates AMPA receptor trafficking through adaptor protein complexes during long-term depression. *Nature Communications*, **4**, 2579.

Matsuda, S., Mikawa, S. & Hirai, H. (1999) Phosphorylation of Serine-880 in GluR2 by Protein Kinase C Prevents Its C Terminus from Binding with Glutamate Receptor-Interacting Protein. *Journal of Neurochemistry*, **73**, 1765-1768.

Matsuzawa, D., Hashimoto, K., Miyatake, R., Shirayama, Y., Shimizu, E., Maeda, K., Suzuki, Y., Mashimo, Y., Sekine, Y., Inada, T., Ozaki, N., Iwata, N., Harano, M., Komiyama, T., Yamada, M., Sora, I., Ujike, H., Hata, A., Sawa, A. & Iyo, M. (2007) Identification of Functional Polymorphisms in the Promoter Region of the Human PICK1 Gene and Their Association With Methamphetamine Psychosis. *American Journal of Psychiatry*, **164**, 1105-1114.

MaxChelator https://somapp.ucdmc.ucdavis.edu/pharmacology/bers/maxchelator/webmaxc/webmaxcE.htm.

McMahon, H.T. & Gallop, J.L. (2005) Membrane curvature and mechanisms of dynamic cell membrane remodelling. *Nature*, **438**, 590-596.

Meinecke, M., Boucrot, E., Camdere, G., Hon, W.-C., Mittal, R. & McMahon, H.T. (2013) Cooperative Recruitment of Dynamin and BIN/Amphiphysin/Rvs (BAR) Domain-containing Proteins Leads to GTP-dependent Membrane Scission. *Journal of Biological Chemistry*, **288**, 6651-6661.

Miguez-Cabello, F., Sanchez-Fernandez, N., Yefimenko, N., Gasull, X., Gratacos-Batlle, E. & Soto, D. (2020) AMPAR/TARP stoichiometry differentially modulates channel properties. *eLife*, **9**, e53946.

Mim, C., Cui, H., Gawronski-Salerno, J.A., Frost, A., Lyman, E., Voth, G.A. & Unger, V.M. (2012) Structural Basis of Membrane Bending by the N-BAR Protein Endophilin. *Cell*, **149**, 137-145.

Miyata, M., Finch, E.A., Khiroug, L., Hashimoto, K., Hayasaka, S., Oda, S.-I., Inouye, M., Takagishi, Y., Augustine, G.J. & Kano, M. (2000) Local Calcium Release in Dendritic Spines Required for Long-Term Synaptic Depression. *Neuron*, **28**, 233-244.

Mizuno, N., Jao, C.C., Langen, R. & Steven, A.C. (2010) Multiple Modes of Endophilin-mediated Conversion of Lipid Vesicles into Coated Tubes. *Journal of Biological Chemistry*, **285**.

Mondin, M., Labrousse, V., Hosy, E., Heine, M., Tessier, B., Levet, F., Poujol, C., Blanchet, C., Choquet, D. & Thoumine, O. (2011) Neurexin-neuroligin adhesions capture surface-diffusing AMPA receptors through PSD-95 scaffolds. *Journal of Neuroscience*, **31**, 13500-13515.

Moretto, E. & Passafaro, M. (2018) Recent Findings on AMPA Receptor Recycling. *Frontiers in Cellular Neuroscience*, **12**, 286.

Murakoshi, H., Lee, S.-J. & Yasuda, R. (2008) Highly sensitive and quantitative FRET-FLIM imaging in single dendritic spines using improved non-radiative YFP. *Brain Cell Biology*, **36**, 31-42.

Murakoshi, H. & Shibata, A.C.E. (2017) ShadowY: a dark yellow fluorescent protein for FLIM-based FRET measurement. *Scientific Reports*, **7**, 6791.

Nabavi, S., Fox, R., Proulx, C.D., Lin, J.Y., Tsien, R.Y. & Malinow, R. (2014) Engineering a memory with LTD and LTP. *Nature*, **348-352**.

Nair, D., Hosy, E., Peterson, J.D., Constals, A., Giannone, G., Choquet, D. & Sibarita, J.-B. (2013) Super-resolution imaging reveals that AMPA receptors inside synapses are dynamically organized in nanodomains regulated by PSD95. *Journal of Neuroscience*, **7**, 13204-13224.

Nakamura, Y., Wood, C.L., Patton, A.P., Jaafari, N., Henley, J.M., Mellor, J.R. & Hanley, J.G. (2011) PICK1 inhibition of the Arp2/3 complex controls dendritic spine size and synaptic plasticity. *EMBO Journal*, **30**, 719-730.

Neveu, D. & Zucker, R.S. (1996) Postsynaptic Levels of [Ca2+]i Needed to Trigger LTD and LTP. *Neuron*, **16**, 619-629.

Nevian, T. & Saksmann, B. (2006) Spine Ca2+ Signaling in Spike-Timing-Dependent Plasticity. *Journal of Neuroscience*, **26**, 11001-11013.

Nishimura, T., Morone, N. & Suetsugu, S. (2018) Membrane re-modelling by BAR domain superfamily proteins via molecular and non-molecular factors *Biochemical Society Transactions*, **46**, 379-389.

Osten, P., Khatri, L., Perez, J.L., Kohr, G., Giese, G., Daly, C., Schulz, T.W., Wensky, A., Lee, L.M. & Ziff, E.B. (2000) Mutagenesis reveals a role for ABP/GRIP binding to GluR2 in synaptic surface accumulation of the AMPA receptor. *Neuron*, **27**, 313-325.

Pan, L., Wu, H., Shen, C., Shi, Y., Jin, W., Xia, J. & Zhang, M. (2007) Clustering and synaptic targeting of PICK1 requires direct interaction between the PDZ domain and lipid membranes. *EMBO Journal*, **26**, 4576-4587.

Pant, S., Sharma, M., Patel, K., Caplan, S., Carr, C.M. & Grant, B.D. (2009) AMPH-1/Amphiphysin/Bin1 functions with RME-1/Ehd1 in endocytic recycling. *Nature Cell Biology*, **11**, 1399-1410.

Paoletti, P., Bellone, C. & Zhou, Q. (2013) NMDA receptor subunit diversity: impact on receptor properties, synaptic plasticity and disease. *Nature Reviews Neuroscience*, **14**, 383-400.

Parkinson, G.T. (2018) Mechanisms of AMPA Receptor Endosomal Sorting. *Frontiers in Molecular Neuroscience*, **11**, 440.

Perez, J.L., Khatri, L., Chang, C., Srivastava, S., Osten, P. & Ziff, E.B. (2001) PICK1 Targets Activated Protein Kinase Cα to AMPA Receptor Clusters in Spines of Hippocampal Neurons and Reduces Surface Levels of the AMPA-Type Glutamate Receptor Subunit 2. *Journal of Neuroscience*, **21**, 5417-5428.

Peter, B.J., Kent, H.M., Mills, I.G., Vallis, Y., Butler, P.J.G., Evans, P.R. & McMahon, H.T. (2004) BAR Domains as Sensors of Membrane Curvature: The Amphiphysin BAR Structure. *Science*, **303**, 495-499.

Petrini, E.M., Lu, J., Cognet, L., Lounis, B., Ehlers, M.D. & Choquet, D. (2009) Endocytic Trafficking and Recycling Maintain a Pool of Mobile Surface AMPA Receptors Required for Synaptic Potentiation. *Neuron*, **63**, 92-105.

Pinheiro, P.S., Jansen, A.M., de Wit, H., Tawfik, B., Madsen, K.L., Verhauge, M., Gether, U. & Sorensen, J.B. (2014) The BAR Domain Protein PICK1 Controls Vesicle Number and Size in Adrenal Chromaffin Cells. *Journal of Neuroscience*, **34**, 10688-10700.

Poudel, K.R., Dong, Y., Yu, H., Su, A., Ho, T., Liu, Y., Schulten, K. & Bai, J. (2016) A time course of orchestrated endophilin action in sensing, bending, and stabilizing curved membranes. *Molecular Biology of the Cell*, **27**, 2119-2132.

Presman, D.M., Ogara, M.F., Stortz, M., Alvarez, L.D., Pooley, J.R., Schiltz, R.L., Grontved, L., Johnson, T.A., Mittelstadt, P.R., Ashwell, J.D., Ganesan, S., Burton, G., Levi, V., Hager, G.L. & Pecci, A. (2014) Live Cell Imaging Unveils Multiple Domain Requirements for In Vivo Dimerization of the Glucocorticoid Receptor. *PloS Biology*, **12**, e1001813.

Qualmann, B., Koch, D. & Kessels, M.M. (2011) Let's go bananas: revisiting the endocytic BAR code. *EMBO Journal*, **30**, 3501-3515.

Racz, B., Blanpied, T.A., Ehlers, M.D. & Weinberg, J. (2004) Lateral organization of endocytic machinery in dendritic spines. *Nature Neuroscience*, **7**, 917-918.

Rajgor, D., Fiuza, M., Parkinson, G.T. & Hanley, J.G. (2017) The PICK1 Ca2+ sensor modulates N-methyl-D-aspartate (NMDA) receptor-dependent microRNA-mediated translational repression in neurons. *Journal of Biological Chemistry*, **292**, 9774-9786.

Ramjaun, A.R., Philie, J., de Heuvel, E. & McPherson, P.S. (1999) The N Terminus of Amphiphysin II Mediates Dimerization and Plasma Membrane Targeting. *Journal of Biological Chemistry*, **274**, 19785-19791.

Ringstad, N., Nemoto, Y. & De Camilli, P. (2001) Differential Expression of Endophilin 1 and 2 Dimers at Central Nervous System Synapses. *Journal of Biological Chemistry*, **276**, 40424-40430.

Rocca, D.L. & Hanley, J.G. (2015) PICK1 links AMPA receptor stimulation to Cdc42. *Neuroscience Letters*, **585**, 155-159.

Rocca, D.L., Martin, S., Jenkins, E.L. & Hanley, J.G. (2008) Inhibition of Arp2/3-mediated actin polymerisation by PICK1 regulates neuronal morphology and AMPA receptor endocytosis. *Nature Cell Biology*, **10**, 259-271.

Ross, J.A., Chen, Y., Muller, J., Barylko, B., Wang, L., Banks, H.B., Albanesi, J.P. & Jameson, D.M. (2011) Dimeric endophilin A2 stimulates assembly and GTPase activity of dynamin 2. *Biophysical Journal*, **100**, 729-737.

Rossy, J., Ma, Y. & Gaus, K. (2014) The organisation of the cell membrane: do proteins rule lipids? *Current Opinion in Chemical Biology*, **20**, 54-59.

Sabatini, B.L., Oertner, T.G. & Svoboda, K. (2002) The Life Cycle of Ca2+ Ions in Dendritic Spines. *Neuron*, **33**, 439-452.

Salzer, U., Kostan, J. & Djinovic-Carugo, K. (2017) Deciphering the BAR code of membrane modulators. *Cellular and Molecular Life Sciences*, **74**, 2413-2438.

Schwenk, J., Baehrens, D., Haupt, A., Bildl, W., Boudkkazi, S., Roeper, J., Fakler, B. & Schulte, U. (2014) Regional Diversity and Developmental Dynamics of the AMPA-Receptor Proteome in the Mammalian Brain. *Neuron*, **84**, 41-54.

Schwenk, J., Harmel, N., Brechet, A., Zolles, G., Berkenfeld, H., Muller, C.S., Bildl, W., Baehrens, D., Huber, B., Kulik, A., Klocker, N., Schulte, U. & Fakler, B. (2012) High-Resolution Proteomics Unravel Architecture and Molecular Diversity of Native AMPA Receptor Complexes. *Neuron*, **74**, 621-633.

Scoville, W.B. & Milner, B. (1957) Loss of recent memory after bilateral hippocampal lesions. *Journal of Neurology, Neurosurgery and Psychiatry*, **20**, 11-21.

Shanks, N.F., Cais, O., Maruo, T., Savas, J.N., Zaika, E.I., Azumaya, C.M., Yates, J.R., Greger, I. & Nakagawa, T. (2014) Molecular Dissection of the Interaction between the AMPA Receptor and Cornichon Homolog-3. *Journal of Neuroscience*, **34**, 12104-12120.

Shepherd, J.D. & Huganir, R.L. (2007) The Cell Biology of Synaptic Plasticity: AMPA Receptor Trafficking. *Annual Review of Cell and Developmental Biology*, **23**, 613-643.

Shewan, A., Eastburn, D.J. & Mostov, K. (2011) Phosphoinositides in Cell Architecture. *Cold Spring Harbor Perspectives in Biology*, **3**, a004796.

Shonesy, B.C., Jalan-Sakrikar, N., Cavener, V.S. & Colbran, R.J. (2014) CaMKII: A Molecular Substrate for Synaptic Plasticity and Memory. *Progess in Molecular Biology and Translational Science*, **122**, 61-87.

Simonetti, B., Danson, C.M., Heesom, K.J. & Cullen, P.J. (2017) Sequence-dependent cargo recognition by SNX-BARs mediates retromer-independent transport of CI-MPR. *Journal of Cell Biology*, **216**, 3695-3712.

Simunovic, M., Evergren, E., Golushko, I., Prevost, C., Renard, H.-F., Johannes, L., McMahon, H.T., Lorman, V., Voth, G.A. & Bassereau, P. (2016) How curvature-generating proteins build scaffolds on membrane nanotubes. *PNAS*, **113**, 11226-11231.

Simunovic, M., Voth, G.A., Callan-Jones, A. & Bassereau, P. (2015) When Physics Takes Over: BAR Proteins and Membrane Curvature. *Trends in Cell Biology*, **25**, 780-792.

Slepnev, V.I., Ochoa, G.-C., Butler, M.H. & De Camilli, P. (2000) Tandem Arrangement of the Clathrin and AP-2 Binding Domains in Amphiphysin 1 and Disruption of Clathrin Coat Function by Amphiphysin Fragments Comprising These Sites*. *Journal of Biological Chemistry*, **275**, 17583-17589.

Snead, W.T., Zeno, W.F., Kago, G., Perkins, R.W., Richter, J.B., Zhao, C., Lafer, E.M. & Stachowiak, J.C. (2019) BAR scaffolds drive membrane fission by crowding disordered domains. *Journal of Cell Biology*, **218**, 664-682.

Sobczyk, A., Scheuss, V. & Svoboda, K. (2005) NMDA Receptor Subunit-Dependent [Ca2+] Signaling in Individual Hippocampal Dendritic Spines. *Journal of Neuroscience*, **25**, 6037-6046.

Sossa, K.G., Court, B.L. & Carroll, R.C. (2006) NMDA receptors mediate calcium-dependent, bidirectional changes in dendritic PICK1 clustering. *Molecular Cell Neuroscience*, **31**, 574-585.

Srivastava, S., Osten, P., Vilim, F.S., Khatri, L., Inman, G., States, B., Daly, C., DeSouza, S., Abagyan, R., Valtschanoff, J.G., Weinberg, R.J. & Ziff, E.B. (1998) Novel anchorage of GluR2/3 to the postsynaptic density by the AMPA receptor-binding protein ABP. *Neuron*, **21**, 581-591.

Staudinger, J., Lu, J. & Olson, E.N. (1997) Specific Interaction of the PDZ Domain Protein PICK1 with the COOH Terminus of Protein Kinase C-α. *Journal of Biological Chemistry*, **272**, 32019-32024.

Staudinger, J., Zhou, J., Burgess, R., Elledge, S.J. & Olson, E.N. (1995) PICK1: a perinuclear binding protein and substrate for protein kinase C isolated by the yeast two-hybrid system. *Journal of Cell Biology*, **128**, 263-271.

Stefan, C.J., Trimble, W.S., Grinstein, S., Drin, G., Reinisch, K., De Camilli, P., Cohen, S., Valm, A.M., Lippincott-Schwartz, J., Levine, T.P., Iaea, D.B., Maxfield, F.R., Futter, C.E., Eden, E.R., Judith, D., van Vliet, A.R., Agostinis, P., Tooze, S.A., Sugiura, A. & McBride, H.M. (2017) Membrane dynamics and organelle biogenesis—lipid pipelines and vesicular carriers. *BMC Biology*, **15**, 102.

Stein, E.L.A. & Chetkovich, D.M. (2010) Regulation of stargazin synaptic trafficking by C-terminal PDZ ligand phosphorylation in bidirectional synaptic plasticity. *Journal of Neurochemistry*, **113**, 42-53.

Steinberg, F., Huganir, R.L. & Linden, D.J. (2004) N-ethylmaleimide-sensitive factor is required for the synaptic incorporation and removal of AMPA receptors during cerebellar long-term depression. *PNAS*, **101**, 18212-18216.

Steinberg, J.P., Takamiya, K., Shen, Y., Xia, J., Rubio, M.E., Yu, S., Jin, W., Thomas, G.M., Linden, D.J. & Huganir, R.L. (2006) Targeted In Vivo Mutations of the AMPA Receptor Subunit GluR2 and Its Interacting Protein PICK1 Eliminate Cerebellar Long-Term Depression. *Neuron*, **49**, 845-860.

Sun, Y., Rombola, C., Jyothikumar, V. & Periasamy, A. (2013) Förster resonance energy transfer microscopy and spectroscopy for localizing protein-protein interactions in living cells. *Cytometry A*, **83**, 780-793.

Sundborger, A., Soderblom, C., Vorontsova, O., Evergren, E., Hinshaw, J.E. & Shupliakov, O. (2011) An endophilin–dynamin complex promotes budding of clathrin-coated vesicles during synaptic vesicle recycling. *Journal of Cell Science*, **124**, 133-143.

Takeuchi, T., Duszkiewicz, A.J. & Morris, R.G.M. (2014) The synaptic plasticity and memory hypothesis: encoding, storage and persistence. *Philos Trans R Soc Lond B Biol Sci*, **369**, 20130288.

Tang, Y.-P., Shimizu, E., Dube, G.R., Rampon, C., Kerchner, G.A., Zhou, M., Liu, G. & Tsien, J.Z. (1999) Genetic enhancement of learning and memory in mice. *Nature*, **401**, 63-69.

Taniike, N., Lu, Y.F., Tomizawa, K. & Matsui, H. (2008) Critical differences in magnitude and duration of N-methyl D-aspartate(NMDA) receptor activation between long-term potentiation (LTP) and long-term depression (LTD) induction. *Acta Medica Okayama*, **62**, 21-28.

Terashima, A., Cotton, L., Dev, K.K., Meyer, G., Zaman, S., Duprat, F., Henley, J.M., Collingridge, G.L. & Isaac, J.T.R. (2004) Regulation of Synaptic Strength and AMPA Receptor Subunit Composition by PICK1. *Journal of Neuroscience*, **24**, 5381-5390.

Terashima, A., Pelkey, K.A., Rah, J.-C., Suh, Y.H., Roche, K.W., Collingridge, G.L., McBain, C.J. & Isaac, J.T.R. (2008) An Essential Role for PICK1 in NMDA Receptor-Dependent Bidirectional Synaptic Plasticity. *Neuron*, **57**, 872-882.

Thiels, E., Xie, X., Yeckel, M.F., Barrionuevo, G. & Berger, T.W. (1996) NMDA Receptor-dependent LTD in different subfields of hippocampus in vivo and in vitro. *Hippocampus*, **6**, 43-51.

Tomita, S., Stein, V., Stocker, T.J., Nicoll, R.A. & Bredt, D.S. (2005) Bidirectional synaptic plasticity regulated by phosphorylation of stargazin-like TARPs. *Neuron*, **45**, 269-277.

Traynelis, S.F., Wollmuth, L.P., McBain, C.J., Menniti, F.S., Vance, K.M., Ogden, K.K., Hansen, K.B., Yuan, H., Myers, S.J. & Dingledine, R. (2010) Glutamate Receptor Ion Channels: Structure, Regulation, and Function. *Pharmacological Reviews*, **62**, 405-496.

Tsien, J.Z., Huerta, P.T. & Tonegawa, S. (1996) The Essential Role of Hippocampal CA1 NMDA Receptor–Dependent Synaptic Plasticity in Spatial Memory. *Cell*, **87**, 1327-1338.

Turner, C., De Luca, M., Wolfheimer, J., Hernandez, N., Madsen, K.L. & Schmidt, H.D. (2020) Administration of a novel high affinity PICK1 PDZ domain inhibitor attenuates cocaine seeking in rats. *Neuropharmacology*, **164**, 107901.

Twomey, E.C., Yelshanskaya, M.V., Grassucci, R.A., Frank, J. & Sobolevsky, A.I. (2018) Structural Bases of Desensitization in AMPA Receptor-Auxiliary Subunit Complexes. *Neuron*, **94**, 569-580.

Ueda, Y. & Hayashi, Y. (2013) PIP3 Regulates Spinule Formation in Dendritic Spines during Structural Long-Term Potentiation. *Journal of Neuroscience*, **33**, 11040-11047.

van Weering, J.R.T., Sessions, R.B., Traer, C.J., Kloer, D.P., Bhatia, V.K., Stamou, D., Carlsson, S.R., Hurley, J.H. & Cullen, P.J. (2012) Molecular basis for SNX-BAR-mediated assembly of distinct endosomal sorting tubules. *EMBO Journal*, **31**, 4466-4480.

Vieira, A.V., Lamaze, C. & Schmid, S.L. (1996) Control of EGF receptor signaling by clathrin-mediated endocytosis. *Science*, **274**, 2086-2089.

Volk, L., Kim, C.-H., Takamiya, K., Yu, Y. & Huganir, R.L. (2010) Developmental regulation of protein interacting with C kinase 1 (PICK1) function in hippocampal synaptic plasticity and learning. *PNAS*, **107**, 21784-21789.

von Engelhardt, J., Mack, V., Sprengel, R., Kavenstock, N., Li, K.W., Stern-Bach, Y., Smit, A.B., Seeburg, P.H. & Monyer, H. (2010) CKAMP44: a brain-specific protein attenuating short-term synaptic plasticity in the dentate gyrus. *Science*, **327**, 1518-1522.

Walker, A.S., Neves, G., Grillo, F., Jackson, R.E., Rigby, M., O'Donnell, C., Lowe, A.S., Vizcay-Barrena, G., Fleck, R.A. & Burrone, J. (2017) Distance-dependent gradient in NMDAR-driven spine calcium signals along tapering dendrites. *PNAS*, **114**, E1986–E1995.

Wang, Q., Navarro, M.V.A.S., Peng, G., Molinelli, E., Goh, S.L., Judson, B.L., Rajashankar, K.R. & Sondermann, H. (2009) Molecular mechanism of membrane constriction and tubulation mediated by the F-BAR protein Pacsin/Syndapin. *PNAS*, **106**, 12700-12705.

Wang, Y.T. & Linden, D.J. (2000) Expression of cerebellar long-term depression requires postsynaptic clathrin-mediated endocytosis. *Neuron*, **25**, 635-647.

Wang, Z., Wang, Y.-N., Sun, C.-L., Yang, D., Su, L.-D., Xie, Y.-J., Zhou, L., Wang, Y. & Shen, Y. (2013) C-Terminal Domain of ICA69 Interacts with PICK1 and Acts on Trafficking of PICK1-PKCα Complex and Cerebellar Plasticity. *PLoS One*, **8**, e83862.

Warren, S.C., Margineanu, A., Alibhai, D., Kelly, D.J., Talbot, C., Alexandrov, Y., Munro, I., Katan, M., Dunsby, C. & French, P.M.W. (2013) Rapid Global Fitting of Large Fluorescence Lifetime Imaging Microscopy Datasets. *PLoS One*, **8**, e70687.

Weissenhorn, W. (2005) Crystal structure of the endophilin-A1 BAR domain. *Journal of Molecular Biology*, **351**, 653-661.

Whitlock, J.R., Heynen, A.J., Shuler, M.G. & Bear, M.F. (2006) Learning Induces Long-Term Potentiation in the Hippocampus. *Science*, **25**.

Widagdo, J., Fang, H., Jang, S.E. & Anggono, V. (2016) PACSIN1 regulates the dynamics of AMPA receptor trafficking. *Scientific Reports*, **6**, 31070.

Wigge, P., Kohler, K., Vallis, Y., Doyle, C.A., Owen, D., Hunt, S.P. & McMahon, H.T. (1997) Amphiphysin Heterodimers: Potential Role in Clathrin-mediated Endocytosis. *Molecular Biology of the Cell*, **8**, 2003-2015.

Wong, T.P., Howland, J.G., Robillard, J.M., Ge, Y., Yu, W., Titterness, A.K., Brebner, K., Liu, L., Weinberg, J., Christie, B.R., Philips, A.G. & Wang, Y.T. (2007) Hippocampal long-term depression mediates acute stress-induced spatial memory retrieval impairment. *PNAS*, **104**, 11471-11476.

Wu, F., Mattson, M.P. & Yao, P.J. (2010) Neuronal Activity and the Expression of Clathrin Assembly Protein AP180. *Biochemical and Biophysical Research Communications*, **402**, 297-300.

Xia, J., Chung, H.J., Wihler, C., Huganir, R.L. & Linden, D.J. (2000) Cerebellar long-term depression requires PKC-regulated interactions between GluR2/3 and PDZ domain-containing proteins. *Neuron*, **28**, 499-510.

Xia, J., Zhang, X., Staudinger, J. & Huganir, R.L. (1999) Clustering of AMPA Receptors by the Synaptic PDZ Domain–Containing Protein PICK1. *Neuron*, **22**, 179-187.

Xu, J., Kam, C., Luo, J. & Xia, J. (2014) PICK1 Mediates Synaptic Recruitment of AMPA Receptors at Neurexin-Induced Postsynaptic Sites. *Journal of Neuroscience*, **34**, 15415-15424.

Xu, J., Wang, N., Luo, J. & Xia, J. (2016) Syntabulin regulates the trafficking of PICK1-containing vesicles in neurons. *Scientific Reports*, **6**, 20924.

Xu, J. & Xia, J. (2006) Structure and Function of PICK1 *Neurosignals*, **15**, 190-201.

Xu, L., Chen, Y., Shen, T., Lin, C. & Zhang, B. (2018) Genetic Analysis of PICK1 Gene in Alzheimer's Disease: A Study for Finding a New Gene Target. *Frontiers in Neurology*, **9**, 1169.

Yang, S.-N., Tang, Y.-G. & Zucker, R.S. (1999) Selective Induction of LTP and LTD by Postsynaptic [Ca2+]i Elevation. *Journal of Neurophysiology*, **81**, 781-787.

Yasuda, R., Harvey, C.D., Zhong, H., Sobczyk, A., van Aelst, L. & Svoboda, K. (2006) Supersensitive Ras activation in dendrites and spines revealed by two-photon fluorescence lifetime imaging. *Nature Neuroscience*, **9**, 283-291.

Zacharias, D.A., Violin, J.D., Newton, A.C. & Tsien, R.Y. (2002) Partitioning of Lipid-Modified Monomeric GFPs into Membrane Microdomains of Live Cells. *Science*, **296**, 913-916.

Zamora Chimal, C.G. & De Schutter, E. (2018) Ca2+ Requirements for Long-Term Depression Are Frequency Sensitive in Purkinje Cells. *Frontiers in Molecular Neuroscience*, **11**, 438.

Zeno, W.F., Baul, U., Snead, W.T., DeGroot, A.C.M., Wang, L., Lafer, E.M., Thirumalai, D. & Stachowiak, J.C. (2018) Synergy between intrinsically disordered domains and structured proteins amplifies membrane curvature sensing. *Nature Communications*, **9**, 4152.

Zeno, W.F., Snead, W.T., Thatte, A.S. & Stachowiak, J.C. (2019) Structured and intrinsically disordered domains within Amphiphysin1 work together to sense and drive membrane curvature. *Soft Matter*, **15**, 8706-8717.

Zhang, M., Abrams, C., Wang, L., Gizzi, A., He, L., Lin, R., Chen, Y., Loll, P.J., Pascal, J.M. & Zhang, J. (2012) Structural basis for calmodulin as a dynamic calcium sensor. *Structure*, **20**, 911-923.

Zheng, K., Bard, L., Reynolds, J.P., King, C., Jensen, T.P., Gourine, A.V. & Rusakov, D.A. (2015) Time-Resolved Imaging Reveals Heterogeneous Landscapes of Nanomolar Ca2+ in Neurons and Astroglia. *Neuron*, **88**, 277-288.

Zhou, Z., Liu, A., Xia, S., Leung, C., Qi, J., Meng, Y., Xie, W., Park, P., Collingridge, G.L. & Jia, Z. (2018) The C-terminal tails of endogenous GluA1 and GluA2 differentially contribute to hippocampal synaptic plasticity and learning. *Nature Neuroscience*, **21**, 50-62.

Zhu, C., Das, S.L. & Baumgart, T. (2012) Nonlinear Sorting, Curvature Generation, and Crowding of Endophilin N-BAR on Tubular Membranes. *Biophysical Journal*, **102**, 1837-1845.